# Stony Brook University

A Thesis Presented

by

**Elizabeth Anne Suter**

to

The Graduate School

in Partial Fulfillment of the

Requirements

for the Degree of

**Master of Science**

in

**Marine and Atmospheric Science**

Stony Brook University

**August 2011**

**Stony Brook University**
The Graduate School

**Elizabeth Anne Suter**

We, the thesis committee for the above candidate for the
Master of Science degree, hereby recommend
acceptance of this thesis.

**Gordon T. Taylor – Thesis Advisor**
**Professor, School of Marine and Atmospheric Sciences**

**Kamazima M.M. Lwiza – Second Reader**
**Associate Professor, School of Marine and Atmospheric Sciences**

**Christopher J. Gobler – Third Reader**
**Associate Professor, School of Marine and Atmospheric Sciences**

This thesis is accepted by the Graduate School

Lawrence Martin
Dean of the Graduate School

Abstract of the Thesis

**Plankton Dynamics, Nutrient Stoichiometry, and Oxygen Utilization in Western Long Island Sound**

by

**Elizabeth Anne Suter**

**Master of Science**

in

**Marine and Atmospheric Sciences**

Stony Brook University

**2011**

Long Island Sound (LIS) is a seasonally hypoxic estuary that receives sewage effluent and nonpoint source nutrient pollution from New York City, Long Island, and the Housatonic, Connecticut, and Thames Rivers in Connecticut. Data collected on 9 research cruises during the summers of 2009 and 2010 in western LIS revealed that organic matter associated with surface water phytoplankton production explained about half the variability ($p<0.01$) in total community respiration in surface waters. Phytoplankton biomass and particulate organic carbon concentrations explained 66% ($p < 0.001$) and 72% ($p<0.01$) of the variability in bacterial abundances, respectively, suggesting bacteria were associated with organic matter from

phytoplankton production. Bacterial net production (BNP) seemed to be controlled by temperature ($r = 0.49$, $p < 0.01$). However, BNP did not correlate with respiration, DO, or organic matter concentrations. Bacterial abundances explained a portion of bottom water oxygen demand in the <20-µm fraction ($r = 0.50$, $p < 0.01$). Furthermore, bottom water column respiration of particles < 20-µm accounted for 41% of the variability in bottom water dissolved oxygen (DO) concentrations ($r = -0.64$, $p = 0.06$).

Despite 20% reductions in nitrogen-loadings to LIS in the past 17 years, the extent, duration, and volume of hypoxia have not significantly declined. A retrospective analysis of 15 years of chemical, biological, and hydrographic monitoring data from 9 stations along the central axis of LIS produced by the Connecticut Department of Environmental Protection (CTDEP) suggested that policies targeting nutrient reductions from sewage effluent have introduced excess phosphate and induced nitrogen-limitation for phytoplankton communities, particularly in western LIS. However, rather than an overall decrease in phytoplanktonic biomass, these changes in nutrient stoichiometry have caused a long-term shift in community composition. In particular, although diatoms still make up the majority of phytoplankton biomass, they have decreased in abundance in favor of nondiatom species, mainly dinoflagellates. In addition, nutrient stoichiometry has changed due to increases in inorganic phosphorus and organic nitrogen and carbon compounds. Furthermore, an unexplained regime shift in phytoplankton biomass occurred between 2000 and 2002, during which time, overall planktonic biomass dramatically increased.

## Table of Contents

## List of Figures

## List of Tables

**Acknowledgements**

I would like to thank Dr. Gordon Taylor, my advisor, for his immense contribution to this work, his commitment to my academic career, and for always pushing me to exceed my own expectations; Dr. Kamazima Lwiza, my mentor, for constantly challenging me and always having an open door for me to come with all types of concerns; and Dr. Chris Gobler, for his enthusiasm for this work which is a huge inspiration.

I also need to thank New York Sea Grant. Without their support, I would not have had the opportunity to take part in this learning experience that has pushed me to further pursue marine science as a career path. In addition, Dr. Julie Rose served as an excellent resource and role model for me as a young scientist and I am very grateful for her input and assistance in this project.

Of course, I would not have come this far without the support and guidance of my family. In particular, I need to thank my father for teaching me modesty and hard work; my mother for teaching me how to be compassionate and independent; my sister, who always reminds me of the importance of humor and friendship; my grandparents who have never doubted me and supported me through all steps of my life; and Jonathan for being my backbone throughout this process and through all of the small and large struggles I have faced.

There have been countless professors, officemates, roommates, co-workers and friends who have made my experience at SoMAS enjoyable and worthwhile. I am very grateful for their friendship and hope that I have contributed as much to their experiences as they have to mine.

## Introduction

Long Island Sound (LIS) is an estuary located between Long Island, New York, and the south shore of Connecticut. Seasonal hypoxia regularly occurs in LIS, and recurs every summer in the western basin (CTDEP, 2008). It may have started earlier but was first reported in the 1970s and became more severe in the 1980s (Parker and O'Reilly, 1991). Hypoxia is typically most severe in the Narrows and western LIS due to the proximity to New York City and long retention times of water (Buck et al., 2005). Low oxygen conditions are unfavorable for many estuarine species, including finfish and lobsters (CTDEP, 2009). In addition, the diversity and abundance of benthic macrofauna has been shown to decline at oxygen concentrations of 3 mg $L^{-1}$ and less. (Ritter and Montagna, 1999) Therefore, 3 mg $L^{-1}$ is the threshold for hypoxia used in several ecosystems, including LIS. Typically, hypoxia begins in late spring to early summer when seasonal stratification curtails ventilation of bottom waters and biological oxygen demand (BOD) exceeds the rate of supply of oxygen. BOD is driven by vertical export of biogenic organic matter form surface to bottom waters, usually due to phytoplankton blooms (Diaz and Rosenburg, 2008). This organic matter becomes the fuel for microbial respiration. Hypoxic conditions are reversed in late summer to early fall when stratification breaks down due to cooling of surface waters and increased wind mixing.

Water quality in western LIS has historically reflected the growth of human populations in the surrounding area. Some of the earliest monitoring data from the East River in the 1920s and 1930s revealed rapid declines in water quality as populations grew in New York City (Parker and O'Reilly, 1991). Hypoxia, first studied in western LIS in the 1970s, continues to be a significant problem despite recent advances made in wastewater treatment. Several other eutrophic estuaries in the United States, such as the Cheseapeake Bay, and the Delaware Bay

Estuary also suffer from seasonal hypoxia due to anthropogenic nutrient loading. A comparison of these estuaries has shown that nutrient loadings, and eventually abatement of these loadings, have had differential effects in each estuary depending on other characteristics of the ecosystem (Cloern, 2001). LIS is unique in that wastewater treatment plant (WWTP) upgrades have not improved upon the problem of eutrophication or hypoxia. The reason for this has been heavily studied but is still contested among stakeholders, managers, and researchers. This study aims to identify changes in nutrient microbial dynamics, stoichiometry and phytoplankton community structure that have occurred since the TMDLs were implemented in the 1990s.

In western LIS, dissolved oxygen (DO) in bottom water has been shown to oscillate in and out of hypoxic conditions with a frequency of approximately one week throughout the summer (Anderson and Taylor, 2001). Many of these fluctuations are caused vertical mixing due to wind stress (O'Donnell, 2008). However, it has been shown that some fluctuations do not always coincide with weakening of stratification. Furthermore, although stratification sets up the conditions for hypoxia to develop in early summer, the variability in bottom DO throughout summer exhibits a strong relationship with variability in stratification only at certain stations (A4, 09, 15, and H2) (Lee and Lwiza, 2008). Lee and Lwiza (2008) also showed that the timing of DO recovery at the end of the summer did not always coincide with overturn of stratification. Therefore, additional factors must be contributing to the fluctuations in bottom water hypoxia in western LIS.

In 1985, a partnership between the Environmental Protection Agency (EPA) and the states of New York and Connecticut formed what is called the Long Island Sound Study (LISS) with the goal of managing hypoxia and nitrogen-loadings. As part of this study, the Connecticut Department of Environmental Protection (CT DEP) started a water quality-monitoring program

in 1991 in which >40 stations are sampled for biological, chemical, and hydrographic parameters on a monthly basis (for map and station IDs, see Figure 1). In order to mitigate eutrophication, the LISS proposed a Total Maximum Daily Load (TMDL) program with the goal of reducing anthropogenic nitrogen loadings to LIS by 58% between 1994 and 2014 (EPA, 1998). Since 1994, point-source nitrogen loading into LIS has decreased by 20% (CTDEP, 2008). The main focus of the TMDLs is on nitrogen because it has historically been viewed as the primary limiting macronutrient for phytoplankton in marine and estuarine systems (Howarth and Marino, 2006). By limiting nitrogen, the LISS and managers hope to decrease the frequency and intensity of phytoplankton blooms, the subsequent sinking and delivery of organic matter to depth, and hypoxia. However, hypoxia has not decreased in intensity, frequency, or duration since the TMDLs were implemented (LISS, 2011). Despite reductions in external nitrogen loadings, no decreases in concentrations of nitrogen have been observed in LIS (LISS, 2011). Furthermore, increasing chlorophyll *a* concentrations, a proxy for phytoplankton biomass, have been observed in western LIS since 1994 (LISS, 2011).

While extremely useful, the CT DEP dataset is limited in that it contains only measurements of standing stock. Few studies have actually made rate measurements related to hypoxia and plankton dynamics in LIS (Welsh and Eller, 1991; Anderson and Taylor, 2001; Gobler et al., 2006; Goebel et al., 2006; Goebel and Kremer, 2007). In order to model and predict hypoxic conditions more accurately, realistic measurements of rates of plankton production, respiration, and transport are needed. For example, the Environmental Fluids Dynamic Code (EFDC) is a model used frequently by the EPA in estuaries, rivers, and lakes for the development of TMDLs (EPA, 2002). The input variables to this model include dissolved, particulate, organic, and inorganic carbon, nitrogen, phosphorus, and silica concentrations, and

phytoplankton stocks by major groups (cyanobacteria, diatoms, or green algae) (EPA, 2006). In this model, the major processes affecting bottom DO are algal photosynthesis and respiration, nitrification, heterotrophic respiration, oxidation of chemical species, ventilation from the surface, sediment oxygen demand, and external oxygen loads. However, the functional responses of these processes are poorly known and may vary among systems. The current model used by the EPA in LIS, the System-Wide Eutrophication Model (SWEM) is similar and fails at making accurate predictions of hypoxic dynamics (O'Donnell et al., 2010). Therefore, refinements in parameterization of the processes contributing to hypoxia are required in order to accurately model conditions in LIS.

In LIS, bottom water BOD has been shown to be controlled by export of organic matter from surface water, and this organic matter is typically associated with phytoplankton blooms that are stimulated by pulses in $NH_4^+$ loadings after precipitation events (Anderson and Taylor, 2001). Despite these findings, understanding of processes linking nitrogen pollution to hypoxia is still rudimentary. Hypoxia does not slowly develop and persist through the summer but instead, oscillates on the order of days (O'Donnell et al., 2008). The nonlinear ineraction between stratification, physical transport, physical ventilation, nutrient uptake, and metabolism and production of both phytoplankton and bacteria complicate modeling onset and recovery of hypoxia based solely on nitrogen loadings. Furthermore, nitrogen-consuming processes in bottom-water, such as nitrification, are not considered major sinks of nitrogen or oxygen in these models. However, these processes have not been investigated in western LIS or other urbanized estuaries.

In 2008, the LISS also identified the need to examine nutrient ratios (stoichiometry) in the past and how they have changed since TMDLs have been implemented, with the goal of

identifying any changes that have occurred in phytoplankton community composition and the effects of these changes on productivity and the food web (LISS, 2008). Nutrient ratios can potentially alter microalgal physiology, thereby imposing selective pressures on phytoplankton populations and altering community structure (Arrigo, 2005).

If nitrogen is considered to be the limiting nutrient of a phytoplankton community, then reduced N-loadings theoretically should decrease overall phytoplankton biomass, as measured by chlorophyll *a* (Chl*a*) or particulate organic carbon (POC). In addition, N-abatement can potentially change cellular C,N,P content of planktonic biomass. Experiments have shown that N-limitation can decrease the organic nitrogen content of diatoms, decreasing the organic nitrogen: phosphorus (N:P) ratio and increasing the organic carbon: nitrogen ratio (C:N) (Perry, 1976; Harrison et al., 1977; Williams, 1995; Kahler and Koeve, 2001; Gobler and Sanudo-Wilhelmy, 2003). N-limitation has also been shown to cause decreases in the Chl*a* –content of many diatoms (Holm-Hansen et al., 1968; Harrison et al., 1977).

In addition to changing the physiology of individual phytoplankton cells, N-limitation can exert selective pressures on phytoplankton community composition. Large phytoplankton cells generally become limited by low nitrogen availability before smaller cells because as cell volume increases, the cell's ability to satisfy resource requirements decreases (Sunda and Hardison, 2007). Therefore, larger cells are less able to compete for nutrients at low concentrations. In addition, N-limitation can select for diazotrophic groups of phytoplankton, such as cyanobacteria, which fix atmospheric $N_2$ and are generally smaller in size than diatoms (Paerl et al., 2007). This implies that N-limitation should select for smaller phytoplankton species such as crytophytes, chrysophytes, and cyanobacteria as opposed to diatoms. In addition,

at low concentrations of inorganic N, many dinoflagellates can switch to heterotrophy in order to supplement their diets (Stoeker, 1999).

Despite decreases in nitrogen loadings, hypoxia has not decreased in area or duration (LISS, 2011). Therefore, it may be expected that long-term N-abatement has not had any effects on phytoplankton dynamics. However, effects of nutrient abatement can also be assessed by examining nutrient ratios, specifically carbon: nitrogen: phosphorus: silica (C:N:P:Si) ratios (Justic et al., 1995). The global average N:P ratio of marine planktonic biomass is 16:1 (the Redfield ratio). Across ecosystems, N:P ratios of phytoplankton communities vary widely, from <5.0 to >100, depending on the species composition and environmental variability (Klausmeier et al., 2008). Assessing the *in situ* inorganic nutrient ratios and the organic nutrient ratios of planktonic biomass in an ecosystem can give valuable information about the status of a phytoplankton community, which is important in assessing the amount of sinking biomass that can potentially contribute to hypoxia.

In LIS, nutrient ratios have been reported by a handful of studies. Anderson and Taylor (2001) reported an average inorganic N:P ratio of 12.6 for station A4, in western LIS, during the summers of 1992 and 1993. In 1993 and 1994, Capriulo et al. (2002) reported year-round inorganic N:P ratios between 5.6 and 7.1 at Stamford (close to station C2 in this study). Gobler et. al (2006) found an average inorganic N:P ratio of 0.88 in discrete samples from western LIS (between stations A4 and B3) in summer 2000. Therefore, at least in summer, it seems that TMDLs have possibly changed ratio of N:P since 1992, but not yet mitigated hypoxia. An aim of this study is to determine the degree of change of nutrient concentrations and ratios in LIS and the effects of these changes on the phytoplankton community.

By examining in situ rates of production and respiration by the planktonic community, it should be possible to improve upon the current model used by the EPA (SWEM) with realistic rates of oxygen uptake and production. Therefore, this study aims to both refine the understanding of microbial processes related to hypoxia and to identify the effectiveness of TMDLs on water quality in LIS over the previous 15 years.

**Objectives**

1- To assess the relationships between nutrient loadings, phytoplankton blooms, planktonic biomass, bottom water microbial respiration, and physical circulation during hypoxic condition in western LIS.

2- To quantify rates of microbial activity in bottom waters during summer hypoxia in western LIS in order to improve upon current attempts to forecast hypoxia.

3- To assess the changes imposed by the TMDLs by examining changes in nutrient concentrations, nutrient stoichiometry, planktonic biomass, and phytoplankton community composition between 1994 and 2009.

**Hypotheses**

$H_1$: The majority of bottom water biological oxygen demand (BOD) is associated with bacterial respiration of large planktonic biomass >20-μm in size.

$H_2$: Microbial respiration in bottom water reaches maximum rates leading up to and during hypoxia, and then decreases at the end of summer due to cooling of bottom water temperatures.

$H_3$: Reductions in nitrogen loadings from wastewater treatment plants (WWTPs) have changed the nutrient stoichiometry in LIS, which has consequently favored non-diatom species over diatoms.

## Methods

*Field Sampling*

Samples and hydrographic data were collected aboard the R/V Seawolf (operated by Stony Brook University) at station A4 on 9 days during the summers of 2009 and 2010 (Fig. 1). Station A4 is not representative of the entire LIS however it was chosen because of the frequency of hypoxia in this location and the proximity to nutrient pollution from NYC. Hydrographic profiles of temperature, salinity, density, dissolved oxygen, photosynthetically active radiation (PAR), and fluorescence were taken with a conductivity temperature depth (CTD) sensor (Seabird Inc.). Discrete samples were collected with Niskin bottles at 4 depths: 2m from the surface (surface), 2 samples within the pycnocline (upper and lower pycnocline), and 2m above the bottom (bottom). For analysis of inorganic nutrients ($NH_4^+$, $NO_3^-$, $NO_2^-$, and $PO_4^{3-}$), 125-ml of seawater were filtered through Whatman GF/F filters. Filtrate was stored frozen in polyethylene bottles until analysis. Samples were analyzed at the SoMAS Analytical Laboratory using a Lachat Instruments QuickChem FIA5000 autoanalyzer and standard colorimeteric techniques, as described by Parsons et al. (1984). For particulate organic carbon (POC) and nitrogen (PON), 25-ml of seawater was captured on precombusted Whatman GF/F filters and stored frozen until analysis. POC and PON analyses were performed by the SoMAS Analytical Laboratory on a Carlo-Erba 1100 CHNS-O analyzer according to Sharp et al. (1993). For DOC analysis, 30-ml samples were filtered through Whatman G/F filters. Filtrate was stored in acid-washed glass vials with Teflon-lined lids at 5˚C until analysis. Samples were analyzed in a Shimadzu-500 TOC-analyzer in the Stony Brook Chemistry Department, according to Sharp et al. (1995). The analyzers were flushed with deionized water before analysis and all concentrations were corrected with appropriate blanks.

Samples for bacterial abundance were preserved in the field with 2% formaldehyde, filtered onto 0.2-µm black polycarbonate membranes, and stained with acridine orange (0.01% final concentration) according to Hobbie et al. (1977). Cell abundances were then enumerated using epifluorescent microscopy under a 100x objective lens and blue excitation. Bacterial abundances were converted to bacterial biomass using an average of 37.0 femtograms C/cell. This value was calculated for bacteria in western LIS during a previous study (Taylor, unpublished data).

Water from each depth was sequentially filtered from an $N_2$-pressurized fiberglass canister through a series of Nitex mesh sieves or polycarbonate filters in order to determine production and activity in the <20-µm and <2-µm fractions compared to whole water (WW). After 14 July 2009, we used a 5-µm mesh instead of the 2-µm polycarbonate membrane for the smallest fraction due to time constraints while filtering. Each of the size fractions was analyzed for Chl*a* content, $O_2$-respiration rates, bacterial net production (BNP), adenosine triphosphate (ATP) content, and rates of light and dark carbon fixation. Filtration occasionally increased rates of BNP and almost always increased rates of respiration in the <2 or 5-µm fraction. It is possible bacterial activity in this fraction was enhanced due to the release of DOC from cells during filtration. Therefore, it is important to note that the rates of BNP and respiration in <2 or 5-µm size fraction are potential rates and not *in situ* rates. Size-fraction was performed pre-incubation because oxygen drawdown could not be measured without first separating the community by size fraction. For all other rate measurements, filtration was performed pre-incubation for consistency.

For Chl*a* quantification, 100-ml of seawater were filtered onto Whatman GF/F filters in triplicate, immersed in 10-ml of 90% acetone, and stored at -20˚C. All Chl*a* samples were analyzed within 2 days using standard fluorometric techniques on a calibrated Turner Designs

Fluorometer. Phaeopigments were quantified after addition of 10% HCl and total Chl*a* was corrected by subtracting phaeopigments, according to Parsons et al. (1984).

$O_2$-respiration rates were determined in a continuous-flow automated respirometer, as described in Taylor et al. (2003). Samples were dispensed into 2-L gas-impermeable Tedlar sampling bags, after eliminating gas bubbles, and placed in a darkened water bath at *in situ* temperatures. Subsamples were then withdrawn from each sample bag approximately hourly through a solenoid valve into a manifold, passed by a flow-through $O_2$-microelectrode (Lazar Laboratories), through a peristaltic pump, and then discharged. The electrode potential was recorded electronically and compared to an $O_2$-saturated dd-$H_2O$ standard to determine $O_2$ concentration over a 3-4 day period. Chemical oxygen demand (COD) was also determined from a formaldehyde-preserved sample (final concentration 2%). $O_2$-respiration rates were then estimated from the maximum slope of oxygen depletion over time, and corrected for COD. The maximum slope was taken because oxygen drawdown often did not immediately begin until several hours into the incubation. For a better description of the method and its advantages, see Taylor et al. (2003).

In order to estimate primary productivity in light samples from the surface, water from each size fraction was incubated with $^{14}$C-bicarbonate (final concentration, 0.025 μCi $ml^{-1}$) according to Taylor et al. (2003). The tracer was prepared in an alkaline brine so that it sank to the bottom of the bottle immediately after injection. The samples were then gently homogenized. Each bottle was covered with a screen in order to filter light to 56.7, 37.5, or 2.5% of the incoming irradiance ($I_o$). These light levels mimic light at specific depths within the photic zone. The depth of 1% $I_o$ was measured by the PAR sensor on the CTD. Using this, the depth-dependent light attenuation coefficient (k) was calculated according to:

$$-kz = \ln(I_z/I_o)$$

where z is the depth of 1% $I_o$ and $I_z/I_o$ is 0.01. The depths of 56.7, 37.5, and 2.5% $I_o$ were then back-calculated using this value of k in the equation above and by changing the ratio of $I_z/I_o$ for each percentage of $I_o$. This resulted in depths of approximately 0.5, 1.0, and 3.5m respectively. After calculating the depths at each light intensity, integrated photic zone primary productivity was calculated using trapezoidal integration, assuming rates were zero at 1% $I_o$ and were equal to the rate measured at 56.7% $I_o$ at a depth of 0 m. The assumption that rates at 0m were equal to those at an approximate depth of 0.5m led to a conservative calculation of primary productivity. After 24-hours (1 diel cycle), particles were collected on 0.2-µm cellulosic filters in duplicate, rinsed twice with sterile seawater, and purged of unassimilated $^{14}C$ by exposure to an HCl atmosphere for one hour. The filters were dried and then suspended in Hionic-Fluor scintillation cocktail and radioassayed in a Packard Tri-Carb Liquid Scintillation Counter. Results were adjusted for isotopic discrimination (x1.06). Rates were normalized to units of µM C $d^{-1}$ by calculating the specific activity of the tracer based on the assumption of conservative mixing of DIC with salinity (Parsons et al., 1984). The DIC from the $^{14}C$-bicarbonate tracer in each bottle was 1.5µM, and was negligible compared to in situ concentrations of DIC, which ranged between 1000 and 2200 µM.

Nitrification, a chemoautrophic process performed by particular groups of prokaryotes, consumes oxygen and ammonium in a 2:1 molar ratio (Wezernak and Gannon, 1967). All known nitrifying microbes are chemoautotrophs and fix carbon using the oxidation of ammonia to nitrate or nitrate to nitrite (Wezernak and Gannon, 1967). Concentrations of ammonia are high in

LIS and therefore nitrification may be a significant portion of biological oxygen demand in bottom waters. In order to estimate dark DIC assimilation (DDA), WW samples from each of the 4 depths were incubated with $^{14}$C-bicarbonate, similar to the samples for primary productivity. In addition, parallel samples were incubated with the ammonia-oxidation inhibitor, Nitrapyrin (dissolved in 100% ethanol, final concentration 10 μM) in order to determine the percentage of DDA attributable to ammonia-oxidation (Dore and Karl, 1996). In some instances the addition of Nitrapyrin increased rates of carbon-fixation above those measured in WW. Therefore, starting on 1 October 2009, a third treatment was added in which the ammonia-oxidation inhibitor, allylthiourea (ATU) was used (final concentration, 86 μM) in combination with the nitrite-oxidation inhibitor, sodium azide (final concentration, 24 μM). In combination, these two inhibitors should stop the entire nitrification process (Ginestat et al., 1998). Nitrapyrin has been shown to inhibit metabolic processes other than ammonia-oxidation. For example, Nitrapyrin needs to dissolve in a solvent, and ethanol can further inhibit or enhance other processes in the sample (Dore and Karl, 1996). Therefore, the DDA rates measured with the Nitrapyrin inhibitor were not considered realistic, and are presented in Appendix C. After 24 hours of incubation in the dark at *in situ* temperatures, particles were collected on 0.2-μm cellulosic filters in duplicate, and radioassayed similar to samples for light carbon-fixation. DDA rates in the ATU treatments were subtracted from uninhibited rates in order to estimate dark-carbon fixation by the nitrifying community.

Bacterial net production (BNP) was measured using incorporation of $^{3}$H-leucine into protein biomass, according to Kirchman (1993). Triplicate samples were spiked with the leucine tracer (0.04 μCi ml$^{-1}$, 10nM leucine, final concentration). Samples were incubated on deck for 3 hours in the dark at ambient temperatures, then fixed with TCA (5% final concentrations). Time-

zero blanks ($T_o$) were preserved at the time of collection by immediate fixation with TCA, and then spiked with $^3$H-leucine. Samples were then heated to 80˚C for 15 minutes, cooled to room temperature, collected on 0.2-µm cellulosic filters, rinsed twice with 3-ml of 5% TCA, twice with 2-ml of 80% ethanol, and once with 1-ml of 80% ethanol. Filters were dissolved with 0.5-ml of 100% ethyl acetate, suspended in Hionic-Fluor scintillation cocktail and radioassayed in a Packard Tri-Carb Liquid Scintillation Counter. BNP was estimated using a conversion factor of 3.1 kg C $mol^{-1}$ leucine (Kirchman, 1993).

Samples for ATP quantification were collected from each depth in each size fraction. 200-ml of seawater were filtered onto GF/F filters in triplicate, immediately transferred into glass vacutainer tubes with 3-ml of 0.5M $H_3PO_4$, and stored frozen (Karl, 1993). Immediately before analysis, ATP standards ranging 0 to 100 ng $ml^{-1}$ were prepared using a fresh bottle of purified ATP as disodium salt, free of vanadium (Sigma-Aldrich). For the standard curve, 0.2-ml of each standard solution was put into a Turner Luminometer with automatic injector and injected with 1-ml of buffered firefly lantern extract (FLE, Sigma-Alrich). The corresponding peak light emission was recorded. Once thawed, samples were treated similarly and the peak light emission was recorded and compared to the standard curve in order to back-calculate the ATP concentration. On many occasions, measured ATP concentrations were equal to or less than the analytical blanks, and therefore results from the ATP extraction were not used in the analysis and are presented in appendix C. There are several possible explanations for this. First, errors may have occurred while preparing the solutions or carrying out the protocols. Secondly, western LIS is a eutrophic estuary with high concentrations of organic matter and inorganic nutrients. Organic and inorganic ions can cause the loss of ATP through chelation or decrease the activity of the luciferase enzyme in the FLE (Karl, 1993).

During several field dates, incubations were performed with the BacLight™ RedoxSensor™ Green Vitality Kit (Invitrogen). The RedoxSensor Green (RSG) reagent produces a green signal when activated by bacterial reductase activity, and therefore stains only those cells that have an active electron transport chain (Invitrogen, 2005). For this measurement, 5-ml of seawater from the <20-µm fraction from each depth were stained with the kit according to protocols given by the manufacturer (Invitrogen, 2005), and incubated in the dark at ambient temperatures. 1-ml from each sample was fixed with formaldehyde (2% final concentration) at regular time intervals after the start of the incubations (0, 2, 4, and 8 hours). Once fixed, samples were stored refrigerated at 4˚C until analysis. The kit includes a counterstain, propidium iodide (PI), which dyes all cells with intact membranes red. For negative controls, the kit includes sodium azide, and carbonyl cyanide 3-chlorophenyllhydrazone (CCCP), which kill all cells before incubation with RSG or PI. The kit indicates the fraction of the community that has intact membranes and is actively respiring. Green and red cells were quantified on a flow cytometer (FACScalibur) based on fluorescence intensity (excitation 488nm, emission for green fluorescence 530 nm, emission for red fluorescence 610 nm). 20,000 events were counted per sample. Data analysis was performed on the WinMDI software package, v.2.8 (http://facs.scripps.edu/software.html).

Although the protocol from Invitrogen states that the Baclight RSG kit is compatible with fixation by formaldehyde, this is strictly for short-term experiments. This dye was designed for laboratories in which only sterile solutions can be put in the flow cytometer and therefore, fixation should happen immediately before counting on the flow cytometer. Once the cells are fixed, the RSG dye does not remain within the cells because it is not covalently attached to any component of the cell, and therefore the dye mixes within the fluid that cells are suspended in

(Invitrogen, personal communication). In this analysis, the samples were counted on the flow cytometer 2-4 months after fixation. Therefore, rates of change in the fraction of respiring community were near zero and these data are not presented.

*Fifteen-Year Time Series*

Nutrients, chlorophyll *a*, and hydrographic data were obtained from the CT DEP database (available at http://lisicos.uconn.edu/). For this analysis, data from 2 depths (surface and bottom) at 9 stations along Long Island Sound's primary axis were tabulated between December 1994 and May 2009. The stations included A4, B3, C2, D3, E1, H4, I2, J2, and M3 (Figure 1). Each survey included continuous depth profiles of density, temperature, salinity, and dissolved oxygen. Discrete Niskin bottle samples were analyzed for concentrations of particulate biogenic silica (BioSi), chlorophyll a (Chl a), orthophosphate (or dissolved inorganic phosphorus, DIP), dissolved organic carbon (DOC), ammonium ($NH_4^+$), nitrate + nitrite ($NO_x$), particulate carbon (PC), particulate nitrogen (PN), particulate phosphorus (PP), dissolved silica (Dsi), total dissolved nitrogen (TDN), total dissolved phosphorus (TDP), and total suspended solids (TSS). Collection and analytical methods used by CTDEP are available on the website (http://lisicos.uconn.edu/). PC and PN samples taken by the CTDEP are different than POC and POC measured in my field samples because the CTDEP did not acidify their samples, and therefore only measured C and N content irrespective of the source (organic or inorganic). Dissolved inorganic nitrogen (DIN) was calculated by summing $NH_4^+$ and $NO_x$ for each sample. The dissolved organic fractions of nitrogen (DON) and phosphorus (DOP) were calculated by

subtracting the inorganic fractions from the total dissolved fractions. Atomic ratios of carbon to nitrogen (C:N) and nitrogen to phosphorus (N:P) were calculated for the particulate and dissolved inorganic fractions.

When calculating nutrient ratios, DIP concentrations below detection would result in infinite DIN:DIP ratios. To handle this situation, an excess DIN index (DINxs) was used, where:

$$DINxs = DIN - 16*DIP$$

DINxs was originally developed to estimate the relative contribution of nitrogen fixation and denitrification to the nitrogen budget in open ocean ecosystems by estimating the deviation of the N:P ratio from the Redfield ratio of 16:1 (Hansell et al., 2004). For LIS, additional factors affect the nitrogen budget, specifically anthropogenic nitrogen loading, and potentially nitrification, so I use the DINxs parameter solely as a 'Redfieldian' index of DIN concentrations relative to DIP concentrations.

The CT DEP also monitors phytoplankton community composition by pigment analysis, reported as percent contribution to total Chl*a*. Pigment concentrations were measured using High Performance Liquid Chromatography (HPLC) (CTDEP, 2005). Ratios of pigments were compared to known photopigment ratios of communities from LIS and analyzed on Chemtax in order to estimate the contribution by each group (CTDEP, 2005). This monitoring program began in April 2002 and data used for this study included monthly data between April, 2002 and May, 2010 from stations A4, B3, C1, D3, E1, F2, H4, I2, J2, and K2. All samples were taken from a depth of 2m. Analyzed taxonomical groups of phytoplankton included Bacillariophyceae (diatoms), Dinophyceae (dinoflagellates), cyanobacteria, Prasinophyceae, Chlorophyceae,

Cryptophyceae, Prymnesiophyceae A & B, Raphidophyceae, Eustigmatophyceae, Chrysophyceae, and Euglenophyceae. The percent contribution of each group was multiplied by total Chl*a*. The diatom group frequently overwhelmed the total Chl*a*-contribution and so the Chl*a* from all non-diatom groups was summed and considered as an additional variable.

Meterological data were also compared with nutrients and phytoplankton data. Monthly precipitation totals from La Guardia Airport (Fig. 1) were downloaded from NOAA (lwf.ncdc.noaa.gov/oa/ncdc.html). Cloud cover (reported as percent cloud cover) and wind speed at the Flushing weather station (Fig. 1) were downloaded from Weather Underground (wunderground.com). Wind speed was converted to wind energy by taking the square of the speed in m/s. Monthly freshwater discharge from the Connecticut River was downloaded from USGS (http://waterdata.usgs.gov/nwis). The Connecticut River contributes >70% of the riverine freshwater being discharged into Long Island Sound, and thus served as a conservative estimate of freshwater input (Lee and Lwiza 2005).

In order to have concurrent datasets, all of the monthly to biweekly datasets were linearly interpolated and resampled on approximately the 15th day of each month, at an evenly spaced gap of 30.5 days. This method was used in order to have a realistic estimation of conditions at exactly the time at all stations for all variables. Nutrients, chlorophyll *a*, and the meterological data were interpolated between 15 December, 1994 and 15 May, 2009. The phytoplankton abundance datasets were shorter, and therefore interpolated between 15 April, 2002 and 15 May, 2010. All variables displayed strong annual cycles. To remove the effect of seasonality, the average annual cycle was calculated for each variable at each station and subtracted from the respective interpolated observation. The generated anomalies were then used for all statistics and spatial or temporal comparisons.

Once the annual cycle was removed, long-term trends of nutrients, chlorophyll *a*, and the phytoplankton clades were calculated over time using the Theil-Sen (T-S) estimator, a robust regression method which improves upon the least squares estimator of a regression by taking into account the possibility of heteroscedastic data (Wilcox, 2005). The T-S estimator derives a trend by taking the median of all possible slopes and y-intercepts. Confidence intervals (CI) were estimated by bootstrapping 599 estimates of the median trend and taking the middle 95% of these estimates, according to Wilcox (2005). To analyze relationships between variables, Pearson-product moment correlation coefficients were calculated.

In order to determine relationships between summertime hypoxia and all possible variables, the summertime hydrographic characteristics, nutrients, nutrient ratios, chlorophyll *a*, precipitation, river discharge, cloud cover, wind speed, and phytoplankton community analyses were compared to summertime hypoxic volume over the entire LIS. Summer was defined as July, August, and September between 1995 and 2008 because hypoxia only occurred during these months. The relationships were determined using Pearson-product moment correlation analysis.

## Results

*Field Sampling*

The biological, physical, and chemical variables from station A4 from the 9 field dates are presented in Tables 1-4. These measurements will be used in the development of a biogeochemical model of hypoxia in LIS. Before the modeling process began, biomass stocks, nutrient concentrations, and productivity rates needed to be examined in order to elucidate relationships between these variables in space and time. These relationships are explored below.

Depth profiles of the hydrographic variables are presented in Figs. 2a-i. On 11 August, 28 August, and 15 September 2009, a shallow pycnocline was present in the water column at depths of 6m and above. On 9 June, 23 June and 14 July 2009, deeper, gradual pycnoclines formed and the bottom layers started at depths of 9m and deeper. On 1 October 2009, 16 August, and 10 September 2010, no clear pycnoclines had formed. Prior to the 10 September 2010 sampling, a tropical storm had passed through, accounting for the well-mixed water column (as seen in the density profile) and the high concentrations of bottom water DO observed on that day (Fig. 2i). Bottom-water hypoxia, defined as DO concentrations <3 mg $L^{-1}$, occurred on 23 June, 14 July, 11 August, and 28 August 2009 at station A4. In addition, on 15 September 2009 and 16 August 2010, bottom water DO concentrations reached 3 mg $L^{-1}$, the cutoff concentration for hypoxia. Fluorescence profiles suggested that Chl*a* in the surface layer was well-mixed and, was controlled by density mixing below the pycnocline. PAR profiles were similar on all cruises and decreased exponentially with depth. The depths of 1% $I_o$ are presented in each figure above the PAR profiles. PAR and fluorescence were not measured on 14 July 2009 and the average depth of the photic zone on all other days was used for calculations. The photic zone was shallowest (1.1m) on 28 August 2009, and deepest (14.6m) on 15 September 2009.

Surface water Chl*a* ranged between 0.9 and 37.5 μg $L^{-1}$ during the summer of 2009 and between 0.7 and 4.8 μg $L^{-1}$ during the summer of 2010. In order to calculate the Chl*a* in each size range, the Chl*a* in the smaller fractions were subtracted from that larger fracitons. On average, the 2 or 5-μm to 20-μm size fraction made up the largest portion of Chl*a* (42%, ±10%). Between 9 June 2009 and 28 August 2009, 60% (± 7%) of Chl*a* was in 2 or 5-μm to 20-μm size fraction (Fig. 3). During the later cruises of 2009 and the August and September cruises of 2010, total Chl*a* declined and the majority (60% ± 4.8) was in the <5-μm size fraction. Therefore, the majority of phytoplankton biomass was between 2 or 5-μm and 20-μm for the majority of the summer of 2009, and was <5-μm in late summer 2009 in the summer of 2010.

Photic zone-integrated primary productivity covaried with surface Chl*a* in the WW fraction ($r = 0.78$, $p = 0.01$) and <20-μm fraction ($r = 0.76$, p 0.01). Primary productivity was highest between 9 June 2009 and 28 August 2009 (Fig. 4). Furthermore, the majority of primary productivity occurred in the 2 or 5-μm to 20-μm size fraction on all dates (52%, ± 9%). Even when total primary productivity was relatively low, after 28 August 2009, the <2 or 5-μm to 20-μm fraction still accounted for the majority of total primary productivity. Therefore, total phytoplankton production and biomass seemed to be dominated by the mid-size range, between 2 or 5-μm and 20-μm.

Chl*a* samples taken during the summers of 2009 and 2010 from surface water were significantly negatively correlated with total DIN ($NH_4^+ + NO_3^- + NO_2^-$) concentrations ($r = -0.74$, $p < 0.001$), with $NO_3^-$+$NO_2^-$ concentrations ($r = -0.61$, $p = 0.01$), and with $PO_4^{3-}$ concentrations ($r = -0.53$, $p = 0.04$). However, there was no significant relationship between Chl*a* and $NH_4^+$ concentrations. These relationships indicate that phytoplankton are closely coupled with DIN, $NO_x$, and DIP concentrations during the summer. Phytoplankton have been shown to be

nitrogen-limited in summer in western LIS, and therefore this relationship is probably due to nutrient-limitation (Capriulo et al, 2002; Gobler et al., 2006). Many species of phytoplankton actually prefer $NH_4^+$ as a nitrogen resource. However, additional processes such as remineralization, nitrification, and anthropogenic loading may account for the variance in $NH_4^+$ concentrations.

In order to determine the contribution of phytoplankton biomass to total particulate carbon in surface waters, I compared Chl*a* and POC from all surface samples from the summers of 2009 and 2010 (Fig. 5). Chl*a* explained 94% of the variability in surface POC ($p < 0.001$), suggesting that POC was largely composed of phytoplankton biomass during these times. The C:Chl*a* ratio of these samples was 42.8 g C $g^{-1}$ Chl*a*. C:Chl*a* ratios of marine phytoplankton can vary from 20 to >160 g C $g^{-1}$ Chl*a*, depending on nutrient variability, grazing, and species composition (Taylor et al., 1997). Using the conversion factor described in the methods, bacterial abundances were converted to carbon biomass and were compared to total POC taken from the same samples. Bacterial biomass ranged between 2.2 and 12.8% of total POC for the summers of 2009 and 2010 at station A4. In addition, bacterial abundances strongly covaried with Chl*a* in surface waters ($r = 0.81$, $p < 0.001$) and with POC at all depths ($r = 0.85$, $p<0.01$). Therefore, while the majority of POC in surface water is phytoplankton-derived, bacteria are also strongly associated with this phytoplankton biomass. This association likely occurred because phytoplankton are a source of organic matter for heterotrophic microbes.

BNP varied between 0.3 and 8.8 µgC $L^{-1}$ $d^{-1}$ in the WW fraction (Table 3). The BNP measured in the <20-µm and <2 or 5-µm fractions may have been stimulated by release of DOC during filtration or release from grazing pressure because the BNP rates measured in these smaller fractions were greater than in the WW fraction in 11 of 32 samples. On average, rates in

the >20-µm, 2 or 5 to 20-µm and <2 or 5-µm fractions were -8% (± 15%), 56% (± 9%), and 46(± 8%) total BNP, respectively. A negative percentage indicated that the BNP measured in the <20-µm fraction was sometimes greater than that measured in WW, and therefore the rate of BNP in the >20-µm fraction about zero on average. Therefore, about half of bacterial activity was associated with particles between 2 or 5 and 20-µm in size, and about half was free-living or associated with particles <2 or 5-µm in size. In general, surface water BNP rates were greater than bottom water BNP rates (Figs. 6a-b). Throughout the summer of 2009, BNP varied between dates but with no clear temporal pattern. Maximum BNP rates in WW were observed on 16 August 2010 in surface and bottom water and minimum rates were measured on 10 September 2010 in surface water and on 28 August 2009 in bottom water. Therefore, maximum bottom water BNP rates did not necessarily coincide with hypoxic conditions. Furthermore, there were significant positive relationships between temperature and BNP in the WW fraction ($r = 0.49$, $p < 0.01$), the <20-µm fraction ($r = 0.57$, $p < 0.01$), and the <2 or 5-µm fraction ($r = 0.50$, $p < 0.01$), suggesting that BNP was temperature-dependent for both free-living and particle-attached bacteria.

Respiration rates from all depths and all fractions are presented in Table 4 and Figs. 7a-b. In bottom water and lower pycnocline samples, respiration rates ranged between 3.4 and 210.6 µM $d^{-1}$ (0.1 and 6.6 mg $L^{-1}$ $d^{-1}$). By dividing the respiration rates by total DO concentrations at the beginning of the incubation, I calculated DO turnover rates to be between 8 and 80% $d^{-1}$. Therefore, if bottom waters were initially saturated, BOD would deplete DO in 1.2 to 12.3 days. On most dates, respiration rates in the WW fraction were similar in surface and bottom waters. The only exceptions were on 28 August and 15 September 2009, when bottom water respiration rates were higher than on any other dates. During these times, *in situ* DO concentrations were

also low and hypoxia occurred. On almost all occasions, respiration rates in the <2 or 5-µm fraction surpassed those in the WW and <20-µm fraction and therefore, subtracting the <2 or 5-µm fraction from the larger fractions resulted in negative rates. On average, rates in the >20-µm, 2 or 5 to 20-µm and <2 or 5-µm fractions were 11% (± 8%), -337% (± 85%) and 426% (± 88%) of total community respiration, respectively. For the BNP experiments, rates in the <20-µm fraction and <2 or 5-µm fraction exceeded those in WW 8 and 3 times, respectively. For respiration experiments, rates in the <20-µm fraction and <2 or 5-µm fraction exceeded those in WW 10 and 25 times respectively. Both BNP and respiration would be enhanced by release from grazing pressure or addition of DOC during filtration. Therefore, it is unclear why only one of these processes was stimulated by filtration to <2 or 5-µm.

Phytoplankton can contribute to total community respiration when their oxygen demand exceeds the rate of photosynthesis, which happens under low light conditions, or when growing heterotrophically (Jensen et al., 1990). Respiration rates in surface samples were significantly correlated with Chl*a* concentrations in WW samples ($r = 0.70$, $p<0.01$) and the <20-µm fraction ($r = 0.68$, $p< 0.01$). Furthermore, respiration in the <20-µm fraction was significantly correlated with $NH_4^+$ concentrations ($r = -0.48$, $p = 0.01$) and total DIN concentrations ($r = -0.61$, $p <0.01$). In surface and upper pycnocline samples, respiration in the WW samples was also correlated with $NH_4^+$ concentrations ($r =-0.49$, $p = 0.05$), and total DIN concentrations ($r = -0.58$, $p = 0.01$). These relationships did not hold true for bottom water and lower pycnocline samples. These imply that approximately half of surface water respiration is algal respiration, driven by the remineralization of algal-derived organic matter and by the endogenous respiration by phytoplankton themselves. The relationship between respiration and inorganic nutrients in surface water was probably driven by the covariation between inorganic nutrients and Chl*a*.

Below the photic zone, the main process controlling DO concentrations are physical mixing and BOD. However, in bottom water and the lower pycnocline samples, there was no significant relationship between respiration in WW and DO concentrations. Despite this, there was a relationship between respiration in the <20-µm fraction and DO in bottom and lower pycnocline samples, significant at the 90%-level ($r = -0.64$, $p = 0.06$). There was also a significant positive relationship between bacterial abundances and respiration rates in the <20-µm fraction ($r = 0.50$, $p < 0.001$) for all depths. These results seem to indicate that oxygen drawdown in bottom waters and bacterial activity at all depths were associated with particles <20-µm in size.

Total DDA and nitrification rates are presented in Table 4. On 9 June 2009, DDA was not detected at any depth. On all other dates, DDA ranged between <1 and 229 µgC $L^{-1}$ $d^{-1}$. Rates were highest in the surface on 11 August 2009 and in the bottom on 14 July, 2009 (Figs. 8a-b). Generally, DDA rates decreased with depth, except on 14 July 2009 when they increased with depth. In surface samples, DDA rates were significantly positively correlated with Chl*a* in the <2 or 5-µm fraction ($r = 0.78$, $p = 0.01$) and with photic-zone integrated primary productivity in the <20-µm fraction ($r = 0.77$, $p = 0.03$). Therefore, in surface samples, phytoplankton production by the smaller size fractions could explain about 60% of the variability in DDA, suggesting that anaplerotic reactions were responsible for the majority of dark DIC assimilation in surface waters. Anaplerotic reactions are reactions used by all organisms (heterotrophic and autotrophic) to replenish the intermediates of the TCA cycle by fixing $CO_2$. Anaplerotic reactions can range between 2 and 8% of an organisms carbon metabolism (Li, 1982). By conservatively estimating that anaplerotic reactions were equivalent to 10% of average BNP below the photic zone, these reactions accounted for an average of 0.2 (± 0.05) µg C $L^{-1}$ $d^{-1}$ of dark carbon fixation. This is

2% of average DDA in the aphotic zone, suggesting that 98% of measured DDA below the photic zone was driven by chemoautotrophic processes.

The nitrification-inhibition ATU-treatment was performed on 3 cruise dates, 1 October 2009, 16 August 2010, and 10 September 2010. Carbon-fixation by nitrifiers contributed between 2 and 82% of total DDA. Nitrification rates were constant with depth on 1 October 2009 and 16 August 2010, but decreased with depth on 10 September 2010 (Figs. 9a-c). Nitrification rates did not correlate with respiration rates or DO concentrations. Unfortunately, I do not have measurements of nitrification on days that hypoxia occurred. However, the highest rates of DDA in bottom water occurred on dates that coincided with hypoxic conditions (23 June, 14 July, 11 August, and 28 August 2009). Furthermore, total DDA rates were statistically compared to DO concentrations in order to examine the possibility that nitrification was contributing to oxygen drawdown. In bottom water and upper pycnocline samples, there was a significant negative relationship between dark carbon-fixation and DO concentrations ($r = -0.78$, $p < 0.001$). However, there were no significant relationships between DDA and respiration rates or $NH_4^+$, $NO_3^-$, or $NO_2^-$ concentrations. This is therefore some evidence that nitrification may contribute to variations in bottom water DO concentrations, but further evidence is needed.

*Time Series Analyses*

Nutrient concentrations from the field samples showed that western LIS waters were strongly nitrogen-limited during July, August, and September of 2009 and 2010, with an average DINxs value of -14.0 (± 01.9) (Table 1). This was different than for a previous study in western LIS in which conditions were only slightly nitrogen-limited in in the summers of 1992 and 1993,

with a DIN:DIP ratio of 12.6 (± 3.8) (Anderson and Taylor, 2001). This comparison prompted an exploration of the historic data provided by the CTDEP in order to determine if the TMDLs on nitrogen had changed the degree of nitrogen-limitation for phytoplankton production between these two studies.

Considerable seasonal variability was evident at station A4 in the dissolved nitrogen inventories as a consequence of variations in loadings, hydraulic residence times, and productivity (Fig. 10a). However, statistical removal of the annual cycle revealed significant interannual trends in the anomalies of this variable (Fig. 10b). All biological, physical, and chemical parameters from the CTDEP database were treated this way and interannual trends are presented by station in tables 5-8. The variables with the most dramatic changes were plotted as hovmoller diagrams through time and space in Figs. 11-24.

The dissolved nitrogen species have significantly changed at all stations in LIS. TDN concentrations, which include DIN and DON, have increased significantly between 1995 and 2009 at most stations in surface and bottom waters (Table 5). The largest increases were observed in western LIS. DON concentrations have significantly increased at all stations in surface and bottom waters (Fig. 11, Table 7). DIN concentrations, which include $NH_4^+$ and $NO_x$, have decreased significantly at most stations, except A4, where they increased (Fig. 12, Table 5). The modest decreases in DIN concentrations at most stations were largely driven by decreases in concentrations of $NO_x$ (Fig. 13, Table 5). There were no major trends in $NH_4^+$ concentrations, except at A4 where they significantly increased in surface and bottom waters (Fig. 14, Table 5). In general, the inorganic dissolved nitrogen species have decreased Sound-wide in favor of increases in the dissolved organic form. The only exception is A4, where both the inorganic and organic dissolved nitrogen species have increased.

Dissolved phosphorus also showed long-term changes in this dataset. TDP concentrations have significantly increased at all stations in surface and bottom waters (Table 5). The largest increases were observed in western LIS. No measureable changes in DOP concentrations were observed at any station in this dataset (not shown). DIP concentrations have also significantly increased at all stations in surface and bottom waters, with the largest changes also observed in western LIS (Fig. 15, Table 5). Increases in TDP concentrations were therefore driven by increases in the inorganic fraction at all stations, particularly in western LIS.

Significant changes in the silica species were also evident in LIS between 1995 and 2009. DSi concentrations significantly increased at all stations in surface and bottom waters (Fig. 16, Table 5). Despite increases in the availability of inorganic silica, BioSi significantly decreased at all stations in surface and bottom waters (Fig. 17, Table 6). The largest changes were in western LIS. Decreases in BioSi concentrations indicate decreases in the abundances of diatoms. This happened despite the increased availability of DSi to diatom cells. Increases in DSi were generally larger than decreases in BioSi, and therefore total Si significantly increased at most stations (Table 7). Therefore, silica loadings into LIS have probably increased in magnitude during this time.

Given that interannual trends among dissolved inorganic nutrients varied, changing nutrient stoichiometry was expected. In fact, the DINxs index significantly decreased at all stations in surface and bottom waters (Fig. 18, Table 5). The largest changes were observed in western LIS. Negative trends in DINxs likely indicate increasing nitrogen-limitation of the phytoplankton community through time. Increasing nitrogen-limitation was driven by modest decreases in DIN concentrations at some stations and large increases in DIP at all stations. There were no measurable changes in the DIN:DSi ratio through time at any station (data not shown).

Changes in Chl*a*, TSS, PC, and PN concentrations can all theoretically be used to estimate changes in planktonic biomass. Chl*a*, a specific proxy for phytoplankton biomass, significantly increased at all 9 stations in surface and bottom water between 1995 and 2009 (Fig. 19, Table 6). In contrast, TSS which represents all suspended matter in the water column, significantly decreased at all stations, and consistent spatial patterns were not evident (Table 6). Furthermore, particulate carbon and nitrogen (PC, PN) concentrations, which include both living and detrital carbon or nitrogen, significantly decreased at all stations in surface and bottom waters, particularly in the west (Figs. 20-21, Table 6). Measurable changes in PP were not apparent at any of the stations (data not shown). From these trends, it seems that phytoplankton biomass has increased and, in turn, detrital and non-photosynthetic planktonic biomass have decreased. The relative changes could also be caused by changes in phytoplanktonic community structure if, for instance, populations with more Chl*a* per cellular C and N were flourishing in the evolving nutrient regime.

Particulate nutrient ratios can be used to tease out changes that may be occurring in phytoplankton community structure. The ratio of particulate carbon: nitrogen concentrations (PC:PN) increased modestly, but significantly at most stations in surface and bottom water (Table 6). While the stocks of PC and PN have both decreased, this change in ratio was due to more dramatic declines in PN concentrations than for PC. The ratio of particulate nitrogen to phosphorus concentrations (PN:PP) has significantly decreased at all stations in surface and bottom water, but with no clear spatial trend (Table 6). This was driven principally by declines in PN concentrations because long-term PP concentrations remained stable throughout this dataset. There were no measurable changes in the PN:BioSi ratio at any station (data not shown). This is due to the fact that both PN and BioSi have declined at similar rates. The changes in the PC:PN

and PN:PP ratio indicate that the planktonic community has become increasingly depleted in N relative to C or P.

Despite decreases in PC concentrations, DOC concentrations have increased at a faster rate, causing total organic C (TOC) to significantly increase at all stations in surface and bottom waters (Table 7). Total N (inorganic and organic) has significantly decreased at most stations (Table 7). This was driven by decreases in the concentration of PN and $NO_x$. Concentrations of total P (inorganic and organic) have increased slightly at all stations, likely driven by the increases in DIP (Table 7). The source of organic carbon to estuaries is typically fixation of atmospheric $CO_2$ by phytoplankton, river loadings, and effluent from WWTPs. Therefore, increases in TOC (and DOC) might have been due to increased rates of carbon fixation by phytoplankton or by increases in organic C loadings from rivers and sewage plants. Decreases in total N are likely due to the decreases in N-loadings. It is not immediately clear why total P (mostly as DIP) has increased throughout the Sound.

Trends in temperature, salinity, and DO are shown in Figures 22-24 and Table 8. While these properties varied over the 15-year time series, robust, long-term trends were not apparent, with one exception. Slight, yet statistically significant decreases in DO concentrations were observed in bottom waters in western LIS.

*Phytoplankton Community Analyses*

By far, the phytoplankton group that exhibited the most interannual change was the diatoms. From 2002 to 2010, diatom-Chl*a* decreased dramatically in western LIS, by up to 0.62 µg-Chl*a* $L^{-1}$ $yr^{-1}$, (decay constant, k = .15 halving per year) (Fig. 25, Table 6). Decreases in

diatoms were also observed in central and eastern LIS, but were less than 0.20 µg- Chl*a* $L^{-1}$ $yr^{-1}$ in magnitude. Increases in dinoflagellates were observed at most stations, mostly in western and eastern LIS (Fig. 26, Table 5). Cyanobacterial biomass decreased in central and eastern LIS (Fig. 27, Table 6). The biomasses of the Prymnesiophyceae A, Cryptophyceae, Raphidophyceae and Euglenophyceae groups significantly increased at stations in western and central LIS (Figs. 28-31, Table 6). For all other groups analyzed, changes were undetectable (data not shown). Total biomass of all non-diatom groups significantly increased at all stations. The largest changes were observed in western LIS (Fig. 32, Table 6).

Anomalies in the Chl*a* contribution of different phytoplankton groups in surface water were compared to anomalies of nutrient concentrations and Chl*a* in surface and bottom waters using linear correlation analyses between 2002 and 2009. This was only performed at station A4, in western LIS. Surface Chl*a* ($r = 0.70$, $p < 0.001$) and bottom Chl*a* ($r = 0.59$, $p < 0.001$) anomalies were significantly positively correlated with the anomalies in diatom biomass. However, there was no relationship between Chl*a* anomalies and the biomass of the non-diatom groups, indicating that diatoms contributed to the majority of variability in Chl*a*. This relationship seemed contradictory because diatom biomass decreased between 2002 and 2010, BioSi decreased between 1995 and 2009, and Chl*a* increased between 1995 and 2009. In 2002, diatoms accounted for between 48.3 and 81.5% of total *Chla* biomass. In 2009, they accounted for between 23.8 and 99.1% of total *Chla* biomass. Therefore, despite large decreases in diatom abundances at A4, diatoms were still controlling the majority of variability in Chl*a* by 2009. Similarly, surface TSS anomalies were significantly positively correlated with the anomalies in the biomass of diatoms ($r = 0.30$, $p = 0.01$), but not the biomass of the non-diatom group. Therefore, despite decreases in overall abundances of diatoms, diatoms still controlled the

variability in TSS and Chl*a* between 2002 and 2010 because they still made up the majority of Chl*a*.

Surface-water diatom biomass at A4 was also related to all of the inorganic nitrogen species in both surface and bottom waters. Diatoms were significantly negatively correlated with anomalies in the concentration of $NH_4^+$ (surface: $r = -0.47$, $p < 0.001$; bottom: $r = -0.22$, $p = 0.05$), $NO_x$ (surface: $r = -0.27$, $p = 0.01$; bottom: $r = -0.21$, $p = 0.05$), and DIN (surface: $r = -0.45$, $p < 0.001$; bottom: $r = -0.29$, $p = 0.01$). The non-diatom groups showed no relationship with $NH_4^+$, $NO_x$, or DIN. These results suggest that diatoms are influenced by the availability of inorganic nitrogen, and as the biomass of diatoms increases, inorganic nitrogen becomes depleted. However, the non-diatom groups do not have this strong coupling with inorganic nitrogen.

Diatom abundances were also negatively correlated with anomalies in DIP concentrations at A4 (surface: $r = -0.33$, $p < 0.001$; bottom: $r = -0.24$, $p = 0.03$). However, unlike DIN, DIP was also significantly negatively correlated with the biomass of the non-diatom groups in bottom water ($r = -0.30$, $p < 0.001$). This suggests that the non-diatom groups are able to deplete DIP during growth even though their depletion of DIN is not statistically detectable.

Not surprisingly, anomalies of DSi concentrations in the surface were significantly negatively correlated with the anomalies of the biomass of diatoms in the surface ($r = -0.40$, $p < 0.001$) and anomalies of the concentration of BioSi were significantly positively correlated with the anomalies in the biomass of diatoms in surface water ($r = 0.62$, $p < 0.001$). This is likely due to assimilation of DSi and transformation into BioSi by diatoms during growth. It also suggests that the use of BioSi as a proxy for trends in diatom abundances pre-2002 (when HPLC data was not available) is appropriate.

Interannual variations in diatom-Chl*a* were also strongly related to other proxies of total biomass at A4. For instance, diatom biomass was positively correlated with PC anomalies (surface: $r = 0.63$, $p < 0.001$; bottom: $r = 0.63$, $p < 0.001$), PN anomalies (surface: $r = 0.55$, $p < 0.001$; bottom: $r = 0.39$, $p < 0.001$), and PP anomalies (surface: $r = 0.41$, $p < 0.001$, bottom: no relationship). PC, PN, and PP include both the inorganic and organic particulate fractions. Therefore, these results suggest that diatoms drive the variability in total particulate C, N, or P from all sources. Variations in PC and PN did not relate to those of the non-diatom groups. PP anomalies were significantly positively correlated with the biomass of the non-diatom groups, but only explained about 6% of the variance (surface: $r = 0.24$, $p < 0.03$; bottom: $r = 0.24$, $p = 0.02$). This and the previous result showing that non-diatom groups were associated with the depletion of DIP both suggest that the non-diatom groups are more responsive to P as a limiting resource than to N while diatoms are likely limited by both N and P.

Many phytoplankton have been shown to use DON as an alternative to DIN in situations when DIN is a limiting resource (Anderson et al., 2008, Heisler et al., 2008). Therefore, I performed further statistical analysis on the relationships between DON concentrations and the different phytoplankton groups. In surface water samples, DON anomalies were not correlated with anomalies in the diatoms or the non-diatom aggregate. However, surface DON anomalies were significantly positively correlated with the anomalies in cyanobacteria ($r = 0.21$, $p = 0.05$), the Prasinophyceae group ($r = 0.35$, $p < 0.001$), and the Cryptophyceae group ($r = 0.31$, $p < 0.001$), but only explained 4 to 12% of their variance. Unlike the relationship between DIN and diatoms, the relationship between DON and these non-diatom groups is a positive one. This can still mean that DON stimulates growth by these groups, but the DON pool may be large enough to mask depletion.

The other chemical (DOC, total C, total N), physical (temperature, salinity, density, DO), and meteorological variables (cloud cover, wind energy, precipitation), and river discharge were not significantly correlated with interannual variation of any of the phytoplankton clades.

*Regime Shift Analysis*

Paradoxically, the above results suggest that while diatoms contributed to the majority of Chl*a* in LIS, Chl*a* increased while BioSi decreased between 1995 and 2009. Furthermore, total particulates (PC and PN) and TSS all decreased. A further examination of the time series of nutrients and phytoplankton data at A4 led me to assess the possibility of a regime shift in the phytoplankton community. For this analysis, the focus was on station A4 because it showed the most dramatic changes in Chl*a* and diatom abundances. Furthermore, A4 is the westernmost station in this analysis and, as a result, is the most influenced by sewage-derived nutrients from New York City WWTPs (Sweeney and Sanudo-Wilhelmy, 2004). The other 8 stations in this dataset showed a similar regime shift in Chl*a*, but changes were not as dramatic (see Fig. 19).

After the 15-year trends were calculated, the time series were further split into 3 periods based on actual observations of Chl*a* concentrations. Trends during each of these phases were calculated using the TS-estimator and the confidence intervals (CI) were calculated with bootstrapping. If the CI of the slope crossed zero, the trends were not considered significant (Wilcox, 2005). During the first phase, between December 1994 and January 2000, Chl*a* steadily declined. During the second phase, between February 2000 and March 2002, Chl*a* rapidly increased. During the third phase, between April 2002 and May 2009, Chl*a* slowly declined again. Therefore, the increases in Chl*a* observed in the 15-year analysis were largely driven by a

rapid, dramatic increase between 2000 and 2002, and did not occur consistently over the entire 15 years. The time series of Chl*a* at A4 and the computed trends are given in Fig. 33.

Following these observations in Chl*a*, a similar analysis was done for the other proxies of planktonic biomass: TSS, PC, PN, PP, and BioSi (Figs. 34-38). Similar to Chl*a*, all of these variables significantly decreased during the first phase of analysis, indicating decreases in total biomass, total phytoplankton biomass, total particulates, and diatoms. During the second phase of analysis, all of the above variables significantly increased in surface and bottom waters, indicating an increase in phytoplankton biomass, diatoms, total particulates, and total biomass. Then, during the third phase of analysis, these different variables began to become decoupled from Chl*a*. Chl*a* and TSS declined at rates much slower than during the first phase. PC, PN, and PP concentrations all decreased in surface and bottom water. These trends were not as dramatic as they were during the first phase, but steeper than for Chl*a* during the third phase. BioSi decreased in surface waters during the third phase at about the same rate as during the first phase. BioSi also declined in bottom waters, but this rate was about 25% of the rate of decline observed during the first phase of analysis. The above observations did not immediately reveal why Chl*a* had dramatically increased in 2000. However, they did reveal that, while variance in Chl*a* covaried with TSS, PC, PN, PP, and BioSi between1994 and 2002, the variables started to become decoupled after 2002 and diatom biomass declined at a faster rate than total phytoplankton biomass. This is consistent with the observations made for the phytoplankton clades using the HPLC data.

In order to determine possible drivers of a phytoplankton regime shift at A4 in western LIS, I performed a similar analysis on the chemical variables and meteorological data. In Figs. 39-45, trends in DIN, DIP, DINxs, wind energy, river discharge, cloud cover, and precipitation

are presented during each of the same 3 phases of time described above. During the first phase of analysis, DIN concentrations significantly decreased while DIP concentrations significantly increased. The resultant effect was a dramatic decline in the DINxs index, indicating increasing nitrogen-limitation for phytoplankton. Nitrogen-limitation could be one of the reasons for the dramatic declines in phytoplankton biomass, especially of diatoms, during this first phase. Furthermore, wind energy significantly decreased during this phase. These conditions would induce stratification and nitrogen-limitation, further limiting phytoplankton production. Decreases in river discharge could also have contributed to the declines in DIN. However, this does not explain why DIP concentrations increased. There were no trends observed in cloud cover and precipitation during this time.

During the second phase, between 2000 and 2002, while phytoplankton biomass seemed to dramatically increase, DIN concentrations continued to decrease while DIP concentrations continued to increase, driving DINxs downward. This means that both total phytoplankton biomass and diatom biomass were increasing despite apparent increasing nitrogen-limitation. It is unclear whether DIN was declining during this period due to rapid uptake by phytoplankton, decreases in nitrogen loadings, or both. During this period, wind energy also declined slightly, although it was not statistically significant. Decreases in wind energy would decrease vertical mixing, decreasing the availability of nutrients in surface water, which should have caused diatom biomass to decline. However, the opposite occurred. During this second phase, precipitation and river discharge also declined, which could have contributed to the decreases in DIN concentrations. Cloud cover also significantly decreased during this period, meaning that more light was reaching surface waters. Although this trend in cloud cover is dramatic compared to the trend during the first and third phases, the anomalies in cloud cover during this period

were not extreme compared to the rest of the dataset. Increases in incoming irradiance may have caused increases in phytoplankton production during the second phase. However, it is difficult to say whether these changes were enough to increase Chl*a* biomass so dramatically.

During the third phase, DIN, surface DINxs, wind energy, river discharge, cloud cover, and precipitation did not change significantly. DIP and bottom water DINxs were the only driver variables that changed during this period. DIP concentrations decreased while bottom water DINxs increased. Although this does not definitively explain why diatoms were declining in favor of non-diatom species during this period, the observed covariation between nondiatom species and DIP concentrations suggested that the non-diatom species were associated with depletion of DIP. Therefore, decreases in DIP concentrations may have resulted from uptake by non-diatom species, which were increasing in abundance during this period.

*Relationships with Hypoxia*

In order to determine how observed changes in nutrients and planktonic biomass might affect hypoxia, summertime average hypoxic volumes in bottom water during the months of July, August, and September were compared to summertime nutrient variables, phytoplankton abundance data, and the meterological data. Hypoxic volume varied between $3.4 \times 10^8$ $m^3$ and $3.6 \times 10^{10}$, except on occasions when hypoxic volume was zero (Fig. 46). Hypoxia only occurred during July, August, or September and typically reached its maximum extent during August. By applying the TS estimator, an increasing trend in maximum hypoxic volume over the entire LIS was revealed ($2.89 \times 10^8$ $m^3 yr^{-1}$, CI = $1.82 \times 10^8$, $4.77 \times 10^8$).

There were no relationships between hypoxic volume and any of the phytoplankton groups at any station. There were also no statistically significant relationships between hypoxic volume and river discharge, precipitation, cloud cover, or wind energy.

Summertime hypoxic volume was negatively correlated with summertime DINxs anomalies ($r = -0.30$, $p = 0.04$) and DIN:DSi anomalies ($r = -0.31$, $p = 0.05$ ) in bottom water at station A4. This relationship indicates that hypoxic volume is greatest when DIN is depleted relative to DIP or DSi in bottom water. Furthermore, DINxs at station A4 has decreased while hypoxic volume has increased. DIN becomes depleted due to several processes. Production by phytoplankton can deplete DIN, producing biomass that sinks to bottom waters and fuels respiration. However, only bottom and not surface anomalies of DINxs and DIN:DSi ratios covaried with hypoxic volume. Therefore, other bottom-water processes are more likely depleting DIN relative to DIP or DSi and, at the same time, depleting DO. One possible explanation is nitrification, a process that consumes both DIN (as $NH_4^+$) and DO (Herbert, 1999). An alternative explanation is that during hypoxia, denitrification is enhanced because it cannot occur under normoxic conditions. Denitrification converts $NO_x$ species into $N_2$ (Herbert 1999). This would account for the depletion of DIN in bottom waters during times that hypoxia is widespread, and for the decreasing trend in DINxs as hypoxic volume has increased between 1994 and 2009. There were no statistically significant relationships between $NH_4^+$ or $NO_x$ and hypoxic volume. Therefore, it is unclear which of these processes is causing DIN depletion in bottom water or if both nitrification and denitrification are occurring simultaneously as a coupled process. Furthermore, these processes could be occurring as a lagged response to DO depletions. Interrannual variations in hypoxic volume did not covary with DIN, DIP, or DSi at station A4.

The variable that repeatedly had a significant relationship with hypoxic volume was TSS. Summertime TSS was correlated with hypoxic volume at station B3, in the surface ($r = 0.36$, $p = 0.02$), C2 surface ($r = 0.37$, $p = 0.016$), C2 bottom ($r = 0.36$, $p = 0.02$), D3 bottom ($r = 0.33$, $p = 0.03$), E1 surface ($r = 0.32$, $p = 0.04$) and E1 bottom ($r = 0.33$, $p = 0.03$). Because TSS consistently appeared to be related to hypoxic volume, a correlation analysis was used to identify any relationships between TSS in surface and bottom waters, and the nutrient and meteorological variables at the stations at which hypoxia can occur (A4, B3, C2, D3, and E1). TSS anomalies were significantly positively related to PC, PN, PP, and BioSi anomalies at all 5 stations, in surface and bottom water (Table 10). Furthermore, TSS anomalies were significantly positively related to Chl*a* anomalies in surface water at stations B3 and E1 and in bottom water at stations A4 and C2. These results suggest that the variability in TSS can be explained by variability in phytoplankton biomass, especially diatom biomass, and particulate C and N matter in surface and bottom waters. At station A4, TSS was also significantly negatively correlated with DIP and DSi concentrations, suggesting that TSS was closely associated with uptake of these inorganic nutrients by phytoplankton, especially by diatoms. Surprisingly, TSS showed no relationship with DIN concentrations. Therefore, the reason for the correlation between TSS and hypoxic volume is probably due to the uptake and rapid growth by phytoplankton, which sink and contribute to BOD.

## Discussion

### *Microbial Dynamics*

Statistical analyses of results from my field sampling and the historical data support the idea that the majority of water column particulate organics in western LIS is phytoplankton-derived. In 1992 and 1993, Anderson and Taylor (2001) found that Chl*a* explained only 5% of the POC pool in western LIS. This calculation included samples at depth. A higher fraction of POC is detrital at depth due to the rapid remineralization of phytoplankton-derived organic matter as particles sink. Still, it seems that the ratio of Chl*a* and particulate carbon has changed since the early 1990s, probably due to decreases in particulate loads from WWTPS. In the current study, the majority of planktonic biomass was between 5 and 20-µm in size, particularly in summer when phytoplankton stocks were high. At the end of summer, when phytoplankton stocks declined and hypoxia abated, the <5-µm fraction made up the majority of phytoplankton biomass. This contradicts a previous study between 1993 and 1995 in which an average 70% of total Chl*a* was in the >20-µm fraction at stations in western LIS (Capriulo, 2002). However, the 1993-95 study made observations year-round and the summertime peaks in Chl*a* during July and August were primarily composed of Chl*a* in the 10-20-µm fraction. Therefore, the observation that the majority of Chl*a* in this study is <20-µm is probably only a summertime occurrence that happens due to the nutrient-limited conditions, selecting for smaller phytoplankton (Raven and Kubler, 2002).

The traditional model of the biological carbon pump indicates that production and sinking of large phytoplankton and zooplankton significantly contributes to the sinking organic matter flux, while picoplankton and nanoplankton contribute less (Michaels and Silver, 1988). In western LIS, diatoms dominate the phytoplankton community. However, at least in the summer,

these and other phytoplankton are not typically greater than 20-µm in size. Furthermore, recent studies have shown that plankton of this size can form aggregates and sink to bottom water, therefore contributing to bottom water carbon-loading as significantly as larger cells (Lomas and Moran, 2011). Interestingly, particles <20-µm seemed to contribute significantly to bacterial activity in this study, suggesting that surface water phytoplankton cells do not even need to aggregate in order to sink and contribute to bottom water BOD.

In this study, size-fractionation was performed in order to estimate the relative contribution of different components of the planktonic community to stocks and activity measurements. In the case of respiration, BNP, and primary productivity measurements, size-fractionation was performed pre-incubation and therefore the rates in each size-fraction were measured without the influence of the larger fractions. On 10 occasions, respiration rates in the <20-µm fraction were stimulated above those in WW samples. In these instances, filtering likely eliminated large grazers, such as copepods, leaving small phytoplankton, some protozoans, and bacteria. Bacterivory by protozoan grazers has been shown to create a positive feedback loop in which predation releases nutrients and substrates, thereby further enhancing bacterial growth (Caron, 2001; Sherr and Sherr, 2002). Therefore, respiration in the <20-µm fraction was likely stimulated by the removal of grazers of protozoans. In the <2 or 5-µm fraction, most bacterivores should be eliminated, and the positive feedback loop would be interrupted, therefore underestimating the contribution of bacteria to respiration (Caron, 2001). However, respiration rates in this size fraction were frequently greater than in WW samples. Therefore, it is likely that the filtration process lysed cells and released dissolved organic matter, thereby enhancing bacterial respiration.

Recent studies have shown that mixotrophic phytoplankton, particularly some coastal dinoflagellates, are able to use dissolved organic matter and can therefore affect the measurement of $^{3}$H-leucine uptake by bacteria. In particular, in the Gulf of Mexico, dinoflagellates in the >5-µm size-fraction contributed up to 95% of leucine and thymidine uptake in experiments in which bacteria were a small percent of total biomass (Mulholland et al., 2011). Dinoflagellates are common in the summer in western LIS and the analysis of historical data showed that they have likely become more abundant than seen in previous studies (Capriulo, 2002). Therefore, in the current study, it is possible that BNP measurements in WW and the <20-µm fraction were overestimates of bacterial heterotrophy. This would mask any stimulation of BNP in the <2 or 5-µm fraction due to release of dissolved organic matter during filtration, and would explain why the effect of filtration in this size fraction was only seen for respiration measurements.

In surface water, phytoplankton contribute to total community respiration because they either utilize DO by oxidizing their own cellular reserves, become prey of zooplankton, or exude organic material for respiration by bacteria (Cole, 1992). Therefore, a strong correlation between respiration rates and Chl*a* is not surprising. In the current study, Chl*a* accounted for half the variability in surface water respiration. This is consistent with a previous study in 2002 and 2003 that estimated the algal contribution to surface water community respiration to be approximately 50% of total, based on the statistical relationship between respiration and Chl*a* stocks (Goebel and Kremer, 2007).

In the 2002 and 2003 study, Goebel et al. (2006) also found total community respiration in surface waters ranged between -50 and 1660 mmol $O_2$ $m^2$ $d^{-1}$ for samples from western and central LIS, where negative respiration was due to production of $O_2$. In order to compare these values to this study, I integrated the surface water respiration rates 10m through the water

column. Surface water respiration rates in this study ranged between 125 and 872 mmol $O_2$ $m^2$ $d^{-1}$, similar to Goebel et al. (2006). Furthermore, the maximum rate of respiration in surface waters in 2009 (872 mmol $m^2$ $O_2$ $d^{-1}$) was similar to the maximum rate measured by Goebel et al. at the same station in summer 2002 (1120 mmol $m^2$ $d^{-1}$).

In the classical model of eutrophication, bacterial respiration in bottom waters is the primary driver of bottom water BOD. In this study, respiration in the <20-µm fraction in bottom water accounted for 41% of the variance in DO concentrations, suggesting that bacterial consumption of particles <20-µm in size was a significant, but minor contributor to BOD. While bottom water bacterial abundances correlated with respiration, bacterial activity could not be linked with bottom water respiration nor DO concentrations. Certainly, bacteria play a role in bottom water BOD, but additional factors control both total community respiration and bacterial activity. Algal respiration can continue to contribute to respiration in bottom waters due to vertical migration by some flagellated phytoplankton, sinking cells, and by transport via undigested fecal pellets (Dam et al., 1995; Olli, 1999). Bacterial activity in bottom water can be controlled by grazing, substrate availability and temperature (Shiah and Ducklow, 1994). It is difficult to determine the availability of substrates because it is difficult to measure the lability of particulate and dissolved organic matter. However, POC concentrations, much of which was composed of phytoplankton biomass, explained 72% of the variance in bacterial abundances at all depths, but were not related to BNP. Furthermore, PON and DOC concentrations were not related to BNP or bacterial abundances. Temperature has been shown to be an important control of estuarine bacteria, particularly as the seasons change from summer to fall (Shiah and Ducklow, 1994). In this study, we saw a strong relationship between temperature and BNP in which temperature explained 24% of the variance in BNP in WW samples.

In this study, bottom water respiration rates in WW samples ranged between 3 and 211μM $O_2$ $d^{-1}$ (or 0.1 to 8.8 mmol $O_2$ $m^{-3}$ $h^{-1}$). This range of respiration rates overlaps with the range (undetectable to 1.9 mmol $O_2$ $m^{-3}$ $h^{-1}$) measured by Goebel and Kremer (2007) using the Winkler titration method. During 2009, respiration rates in bottom water were highest on 28 August and 15 September (Fig. 7b). On all other dates, bottom water respiration ranged between 0.1 to 2.0 mmol $O_2$ $m^{-3}$ $h^{-1}$, equivalent to the range observed by Goebel and Kremer (2007) during the summers of 2002 and 2003. Furthermore, bottom water DO concentrations were hypoxic on 15 September, 2009 and anoxic on 28 August, 2009, suggesting that the high respiration rates measured on those dates were realistic.

Rates of DO turnover ranged between 8 and 82% $d^{-1}$. Furthermore, the maximum rate of respiration in the WW samples observed in this study is equivalent to 6.6 mg $O_2$ $L^{-1}$ $d^{-1}$. The maximum bottom water DO concentration observed during this study was 6.4 mg $L^{-1}$, observed on 9 June 2009. Therefore, at the maximum rate observed, water column respiration could completely deplete DO concentrations in less than a day. From this study and previous ones, it has been shown that bottom water DO concentrations oscillate throughout the summer. Because the water column is highly stratified during these times, DO is probably frequently replenished by mixing events and lateral transport of oxygenated water into the bottom layer (Torgersen et al., 1997; O'Donnell et al., 2008). Without physical mixing, water column BOD could potentially create completely anoxic conditions within hours.

*Long-Term Change in LIS*

At all stations in the western and central basins of LIS, there have been major changes in nutrient dynamics. Although the field-sampling portion of this study focused on station A4 because it is the most eutrophic and consistently experiences seasonal hypoxia, it should be noted that this station was not necessarily representative of the entire LIS. In general, DIN species at most stations have declined in favor of DON while DIP has increased at all stations. In addition, total nitrogen (the sum of all organic, inorganic, particulate, and dissolved fractions) has decreased at most stations while total phosphorus has increased at most stations. DSi concentrations have increased but diatom abundances have declined. Many of these changes seem counterintuitive at first. Decreases in total N have probably been driven by decreased anthropogenic loadings. But this does not explain why DON concentrations have increased. Diatoms are the only phytoplankton dependent on silica, and are usually limited by silica in the spring bloom (Gobler et al., 2006). If DSi availability has increased, diatom abundances should have increased. There is also no clear explanation for the increases in DIP.

DIP can be released from sediments under anoxic conditions (Kemp et al., 2005). However, in western LIS, this should be a seasonal effect and should not have contributed to long-term increases in the concentrations of $PO_4^{3-}$. Increases in bottom water temperatures can cause increased rates of remineralization in sediments, therefore increasing the rate of regeneration of DIP (Jensen and Andersen, 1992). The sediment reservoir can then become an increasingly important source of P to the water column. However, in this analysis, bottom water temperatures actually decreased at all stations except in eastern LIS (Table 8b). Alternatively, as the phytoplankton community has shifted to one which is more dependent on organic sources of nutrients, organic phosphorus may have become a more important source of P, decreasing the

assimilation rate of DIP and therefore causing it to accumulate in the water column. Another possibility is that the concentrations of $PO_4^{3-}$ in wastewater may have increased during this study. Previous studies have shown that the main source of $PO_4^{3-}$ into western LIS is sewage contamination from the East River (Sweeney and Sanudo-Wilhelmy, 2004). Phosphorus in sewage comes from human waste but has also recently been added to drinking water as a corrosion inhibitor in order to prevent the leaching of lead into drinking water. Starting in late 1992, New York City began adding ortho-phosphoric acid to all drinking water supplies (Maas et al., 2005). Changes in P-loadings from the East River and LIS cannot be determined from this dataset. Furthermore, increases in DIP concentrations were observed throughout the Sound while loadings from the East River mainly affect western LIS. Therefore, it is impossible to determine which of these possibilities was the likely cause for increased DIP concentrations in the water column between 1994 and 2009.

It is possible that as N-loadings into LIS have decreased, the dynamics of N-cycling have changed, therefore altering the ratio of DIN to DON. Secondary treatment of sewage does not completely eliminate DOC or DON from effluent, and therefore concentrations of these compounds are usually elevated in urban areas that have a lot of sewage influence (Sharp et al., 2009). However, it is unlikely that the majority of these organic compounds are labile because BOD in effluent significantly decreases in plants with secondary treatment (NRC 1993). Furthermore, WWTP upgrades between 1994 and 2009 should have decreased these concentrations over this time period. Therefore, it is possible that these organic nutrients have built up over time if they are relatively refractory.

An increasing ratio of dissolved organic nutrients relative to inorganic has likely favored the dominance of mixotrophic phytoplankton over time. This in turn, can potentially have an

impact on the planktonic food web. Specifically, the microbial loop dominates over the traditional food web when selective forces favor smaller phytoplankton over diatoms or dinoflagellates. While diatoms are consumed by larger crustacean zooplankton like copepods, small phytoplankton are consumed by heterotrophic protists. Copepods do not significantly graze phytoplankton biomass in surface waters (Lonsdale, 1996). However, copepods produce fecal pellets, which efficiently sink to bottom water and fuel BOD (Butler and Dam, 1994). On the other hand, protistan grazing can consume a substantial fraction of daily primary production, making it unavailable to sink to bottom water and fuel BOD (Calbet and Landry, 2004). Increased protistan grazing in surface waters would increase the recycling rate of C and N in surface water, making nutrients available for uptake by phytoplankton and bacteria, and continuing the cycling of resource within this loop. Increased retention of substrates in surface water would be favorable for reducing bottom water hypoxia. However, despite large decreases in diatom abundances, diatoms still dominate the phytoplankton community. It is possible that as inorganic nitrogen loads into LIS decrease, diatoms will continue to decline, the microbial food web will gain dominance, and hypoxia will eventually decline. However, more significant decreases in N-loadings are probably necessary.

It is still unclear what fraction of the dissolved organic compounds in LIS is labile. If concentrations of these compounds have increased due to increased sewage loadings, they are likely refractory in nature and are not contributing to BOD in natural waters. If these chemical species have increased due to shifts from a diatom-dominated phytoplankton community to one dominated by mixotrophic phytoplankton, which has in turn increased C and N recycling rates, then a fraction of the DOC and DON compounds are likely labile and therefore further contributing to production by mixotrophic phytoplankton and protistan zooplankton. Capriulo et

al. (2002) showed that DON concentrations account for 40% of the total nitrogen pool in LIS, whereas the global average is 64%. Therefore, it is likely that DON is rapidly regenerated and highly labile in this system.

In many estuaries, as the degree of eutrophication increases, diatom abundances decline because the N:Si ratio increases and diatoms become limited by silica (Cloern, 2001). However, in LIS, the opposite seems to be true. Over 15 years, diatom abundances (indicated by BioSi concentrations) decreased as the degree of eutrophication decreased (indicated by DINxs). This indicates that diatoms were probably not limited by silica at the peak of eutrophication in western LIS. Instead, nitrogen was likely the limiting macronutrient for diatom production. DIN concentrations have declined and diatom abundances have decreased despite increased availability of Si. In addition, the PN:BioSi ratio of plankton biomass has not changed, indicating that both PN and BioSi have declined at similar rates. Because I have shown that diatom biomass accounts for the majority of planktonic biomass (mean 60% ± 2% at station A4) between 2002 and 2010, diatom abundances were probably the major phytoplankton group controlling the variability in PN and BioSi concentrations and these have likely all declined due to DIN-limitation.

The evidence presented here also suggests that the planktonic community is shifting to one richer in C and P relative to N-compounds. This was likely driven by the changes in the ratio of incoming nutrients (DIN:DIP). In the northern Baltic Sea, it has been shown that diatoms respond to DIN-enrichments while dinoflagellates and Chrysophyceae respond positively to both DIN and DIP-enrichments (Lagus et al., 2004). In the Adriatic Sea, mesocosm experiments showed that nitrogen or silicon-deficient conditions favored the dominance of small flagellated phytoplankton (Carlsson and Graneli, 1999). In Tolo Harbor in Hong Kong, as N:P ratios

declined in both long-term and short-term experiments, non-siliceous phytoplankton increased in dominance while diatom abundances declined (Hodgkiss and Ho, 1997). Therefore, in a system in which DIP has become more available than DIN, it may be expected that diatom abundances would decrease in favor of dinoflagellates and other non-siliceous phytoplankton (Heisler et al., 2008). As DIN concentrations decline, species that can utilize alternate forms of nitrogen are at an advantage. Phytoplankton such as Prasinophyceae, Chrysophyceae, and cyanobacteria have been shown to be directly dependent on DON as a source of nitrogen (Berg et al., 1997, 2001). In particular, the Pelagophycean *Aureococcus anophagefferens*, a harmful algal bloom that is increasing in prevalence in bays in Long Island, has been shown to use heterotrophic metabolism in environments with large amounts of organic matter and low light in order to outcompete other phytoplankton (Gobler et al., 2011). In some ecosystems, diatoms have been shown to have the mechanisms for DON uptake but generally have a lower affinity for DON than for DIN (Berman and Bronk, 2003). In LIS, there have also been consistent increases in DOC concentrations, which may have contributed to increases in dinoflagellate abundances, due to the ability of some dinoflagellates to switch between heterotrophy and autotrophy (Jeong et al., 2010).

Phytoplankton production can be limited by various factors, including light, and therefore the relationship between N-loadings and phytoplankton biomass is not always straightforward (Cloern, 2001). In LIS, it seems that total phytoplankton stocks declined between 1994 and 2000, possibly driven by nitrogen-limitation due to upgrades to WWTPs (LISS, 2011). Between 2000 and 2002, a massive regime shift occurred in the phytoplankton community during which Chl*a* dramatically increased at all stations analyzed in this study. Changes such as this can be caused by increases in the abundance of phytoplankton or increases in the amount of Chl*a* per cell. In this case, these changes were caused by increases in total biomass, as indicated by simultaneous

increases in biogenic silica and particulate nitrogen and carbon concentrations. The reason for these increases is still unclear. After 2002, Chl*a* stocks declined again, but at a much slower rate than previous to 2000. During this time, the declines were driven more by shifts in community structure rather than changes in total planktonic biomass. It seems that the TMDLs were successful in limiting Chl*a* production before 2000. Since 2000, there have been no major changes to N-loadings or DIN concentrations in the water column (LISS, 2011).

Although DIN concentrations were not changing between 2002 and 2009, an analysis of the DINxs parameter revealed that N was extremely depleted relative to P, especially in the western basin (Figure 18). It is possible that during this time, changes in community structure were due to gradual adaptation to nutrient conditions. N and P-deficiency have been shown to decrease the *Chla* content across many species, including diatoms and dinoflagellates, although the effects are different for different species (Riemann et al., 1989; Henriksen et al., 2002). Furthermore, across ecosystems, cyanobacteria, dinoflagellates, and Prymnesiophyceae have been shown to have lower Chl*a*:carbon ratios than diatoms (Geider et al., 1997). Therefore, modest decreases in Chl*a* after 2002 were likely caused by declines in diatom abundances and decreases in Chl*a*-content due to N-deficiency. Concurrent decreases in PC and PN were not observed, therefore the declines in Chl*a* did not necessarily indicate declines in overall phytoplankton biomass.

*Implications for Hypoxia*

Generally, in LIS, diatoms are believed to contribute to bottom water organic matter loads because they are relatively large phytoplankton with siliceous tests that sink rapidly and because they support secondary production by copepods, which create fecal pellets that also sink rapidly (Michaels and Silver, 1988; Bulter and Dam, 1994). On the other hand, nanophytoplankton are considered to contribute less to bottom water organic matter loads because they sink more slowly and can use flagella to remain buoyant (Capriulo et al., 2002). There have been no major studies examining the make-up of sinking organic matter in LIS. However, recent studies in the open ocean have shown that even picoplankton can form aggregates with other plankton and significantly contribute to sinking biomass (Wilson and Steinberg, 2010). In this study, I have shown that about half of bottom water bacterial activity and respiration occurred on particles between 5 and 20-μm in size, indicating that particles in the size range of nanoplankton are an important organic carbon source to bottom water respiration. Therefore, decreases in surface water diatom abundances and increases in non-diatom species may not necessarily decrease the amount of sinking organic matter in bottom waters of LIS.

In some hypoxic ecosystems, there are concerns that persistent hypoxia inhibits nitrification, which decreases the rates of denitrification, and increases retention of N in the system (Kemp et al., 1990). This results in greater recycling rates of nitrogen. In this study, hypoxic conditions were associated with depletions in bottom water DIN concentrations, indicating that low-oxygen conditions enhance rates of denitrification. Although I have shown water column nitrification is likely occurring in western LIS, it is impossible to tell from this dataset if the rate of coupled nitrification-denitrification has decreased over the years as hypoxia has persisted. While total DIN stocks have declined since 1994, excess DIN concentrations in

bottom waters in western LIS, particularly at A4 (Figs. 18 and 41) have increased since 2002, possibly indicating that DIN stocks have built up in bottom waters due to decreased rates of coupled nitrification-denitrification. Furthermore, these processes do not necessarily affect the DON pool, which is becoming larger and more important in western LIS. These observations indicate that the recycling and retention of nitrogen in LIS waters has increased. A further assessment of these processes is necessary in order to determine how the N pool is being affected and if the TMDLs are enough to reduce total N concentrations.

Hypoxia in LIS has been extensively studied since the start of the LISS. In 1991, and again in 2000, two studies showed that hypoxic events were highly correlated with density stratification, and in particular temperature rather than salinity stratification (Welsh and Eller, 1991; O'Shea and Brosnan, 2000). This is different than the Chesapeake Bay and Gulf of Mexico, where salinity controls density stratification more than temperature (Welsh and Eller 1991). Because of this, the water column in western LIS resists tidal mixing throughout most of the summer. The average rate of westward bottom flow (5 cm/s) is not high enough to replenish the western basin with oxygenated waters from the central and eastern basins. In fact, seasonal hypoxia development propagates eastward, against this flow (Parker and O'Reilly 1991; Anderson and Taylor 2001). Approximately 80% of ventilation of oxygenated waters in the bottom layer during hypoxia was shown to be due to vertical mixing, brought on by wind stress in the along-sound direction (O'Donnell et al., 2008).

Wind mixing has been shown to be important in controlling summer stratification and thus hypoxic conditions throughout the summer (Wilson et al., 2008). Because of this, western LIS does not remain hypoxic over the entire summer, but instead oscillates in and out of hypoxic conditions with wind-mixing events (Anderson and Taylor, 2001). In this study, we were unable

to elucidate any relationship between hypoxia and wind speed. However, Wilson et al. (2008) showed that directional constancy of winds blowing from the southwest (203˚T) favored stratification and increased the rate of hypoxia development in western LIS. In addition, winds of this direction increased surface DO saturation, suggesting that phytoplankton production increased due to this stratification. Increases in stratification are typically unfavorable for phytoplankton because this creates a barrier to the advection of nutrients from bottom to surface waters. However, in western LIS, nutrient-replete water from wastewater treatment plants are buoyant because this water is fresher than ambient water. This is a mechanism for nutrient-replete water to reach the surface despite strong density stratification. In this study, although we saw no relationship with winds, TSS in surface and bottom water were frequently correlated with hypoxia. Furthermore, TSS were shown to be composed of mostly phytoplankton organic matter. Therefore, it seems possible that winds blowing from the southwest favor hypoxia in 2 ways: by setting up a physical barrier to vertical mixing and by favoring conditions for planktonic production, which increases the amount of organic matter in bottom water fueling BOD.

Even though wind is responsible for short-term variation in hypoxia, nitrogen loadings are ultimately responsible for the long-term degradation in water quality. This is why the TMDLs are expressed as allowable annual loads of nitrogen (NYSDEC, 2000). Evidence from this study and previous studies has shown that inorganic nitrogen concentrations in surface waters are tightly coupled with phytoplankton production (Anderson and Taylor, 2001; Gobler et al., 2006). Furthermore, in one study, 92% of the variability in hypoxic volume was explained in a multiple linear regression using spring Chl*a*, summer wind speed, spring river discharge, and spring total nitrogen as the independent variables (Lee and Lwiza, 2008). However, of the 4 variables, total nitrogen was the weakest. Furthermore, in this study, there was no direct

correlation between any of the nitrogen species and DO concentrations or hypoxic volume. Many processes control *in situ* nitrogen concentrations. Uptake by phytoplankton, discharge from WWTPs, nonpoint discharge during precipitation events, recycling within the food web, and coupled nitrification-denitrification all effect the nitrogen budget. In this study, at station A4, total nitrogen ranged between 16.9 and 81.1 μmol $kg^{-1}$ and total phosphorus ranged between 0.95 and 6.33 μmol $kg^{-1}$. This is a 4-fold range in N-concentrations and 6-fold range in P-concentrations. Therefore, the effects of a 20% decrease in N-loadings over 15 years may be undetectable compared to the large, natural fluctuations of total nitrogen in the water column. Furthermore, increased N-recycling rates can buffer the decreases in N-loadings so that they have negligible overall effects on the nitrogen consuming processes in the water column.

*Summary of Major Findings*

1. The majority of the organic matter in the water column in LIS is phytoplankton-derived and tightly coupled to the availability of inorganic nitrogen. Phytoplankton respiration contributes about half of total community respiration in surface water. In addition, high concentrations of this autochthonous organic matter are present in the water column during hypoxia, suggesting a link between surface water phytoplankton loading and bottom water oxygen drawdown.
2. The TMDLs, combined with increased DIP concentrations, have induced DIN-limitation of the phytoplankton community, which in turn has likely caused the decreases in diatom abundances in favor of nondiatom species.
3. The observed changes in nutrient conditions and phytoplankton community in western LIS may indicate a regime shift away from the classical food web to one that is becoming increasingly dominated by the microbial loop. These changes could potentially decrease bottom BOD due to decreases in sinking organic matter and the efficiency of protistan grazing on phytoplankton biomass. However, smaller particles still contribute substantially to bottom water BOD and therefore changes in bottom water hypoxia have not been observed.

*Future Work*

Nitrification is often overlooked as an oxygen-consuming process in estuaries. The current model used by the EPA to predict hypoxia in LIS (System-Wide Eutrophication Model, SWEM) often fails at accurately predicting hypoxia because it underestimates respiration, which leads to an overestimation of summertime DO concentrations (O'Donnell et al., 2010). The respiration term in this model includes algal respiration, nitrification, and organic carbon oxidation. However, nitrification is modeled as an insignificant portion of the total respiration (O'Donnell et al., 2010). In addition, nitrification rates in the model are estimated simply based on functional responses to temperature and oxygen concentration (Hydroqual, 1996). In reality, nitrification is controlled by a variety of environmental variables. Ammonium concentration, pH, and labile organic carbon concentrations have been shown to be more important than temperature in controlling nitrification rates (Strauss et al. 2002).

The experiments in this study showed that nitrification can occur in the water column in western LIS and can contribute up to 82% of total DDA at times. However, in this study, nitrification rates were in units of carbon-fixation. Ammonia oxidation is a thermodynamically marginal reaction (Madigan et al. 2009). Ammonia-oxidizers can turn over large amounts of nitrogen and oxygen without comprising a large fraction of the total carbon biomass. Therefore, further work should examine the effect of nitrification on the nitrogen and oxygen pools and determine what environmental variables are controlling this process.

Total stock measurements of carbon, nitrogen, phosphorus, and silica pools are useful but they do not give information about utilization rates. In estuaries, a large portion of the DOC and DON pools are refractory, unable to be used by heterotrophic or mixotrophic organisms. However, this study highlighted the changing dynamics within these pools of nutrients and that

they may have become increasingly important. In order to accurately predict the relationship between substrate pools and uptake dynamics, the labile fraction of these pools must be determined.

The above analyses revealed evidence of a dramatic regime shift in Chl*a* and phytoplankton abundances in LIS between 2000 and 2002 during which phytoplankton stocks dramatically increased. There were no major changes in light availability, precipitation, or river discharge. Furthermore, an analysis of the wind direction and directional constancy did not indicate any notable anomalies during this period (Wilson et al., 2008). Dramatic regime shifts in phytoplankton abundances and community structure have also been observed in Narrragansett Bay (Karentz and Smayda, 1998). These shifts have been attributed to large-scale climatological oscillations in light and temperature regimes due to the interannual variability in the North Atlantic Oscillation (NAO) and the north wall of the Gulf Stream (GSNW) (Borkman and Smayda, 2009). Therefore, a further analysis of climatological drivers in LIS may reveal the reasons for this apparent regime shift. However, climatological cycles oscillate with long periods of several years. The LIS historical dataset only contains 15 years of observations and may not be long enough to do such an analysis.

**References**


Anderson, D. M., P. M. Glibert, J.M. Burkholder. (2002). Harmful algal blooms and eutrophication: Nutrient sources, composition, and consequences. Estuaries 25(4B): 704-726.

Anderson, T. H. and G. T. Taylor (2001). Nutrient pulses, plankton blooms, and seasonal hypoxia in western Long Island Sound. Estuaries 24(2): 228-243.

Arrigo, K.R. (2005). Marine microorganisms and global nutrient cycles. Nature 437: 349- 355.

Berg, G. M., P. M. Glibert, N.O.G. Jorgensen, M. Balode, I. Purina. (2001). Variability in inorganic and organic nitrogen uptake associated with riverine nutrient input in the Gulf of Riga, Baltic Sea. Estuaries 24(2): 204-214.

Berg, G. M., P. M. Glibert, M.W. Lomas, M.A. Burford. (1997). Organic nitrogen uptake and growth by the chrysophyte *Aureococcus anophagefferens* during a brown tide event. Marine Biology 129(2): 377-387.

Berman, T. and D. A. Bronk (2003). Dissolved organic nitrogen: a dynamic participant in aquatic ecosystems. Aquatic Microbial Ecology 31(3): 279-305.

Bronk, D. A., J. H. See, P. Bradley, L. Killberg. (2007). DON as a source of bioavailable nitrogen for phytoplankton. Biogeosciences 4(3): 283-296.

Buck, N. J., C. J. Gobler, S.A. Sanudo-Wilhelmy. (2005). Dissolved trace element concentrations in the East River-Long Island Sound system: Relative importance of autochthonous versus allochthonous Sources." Environ. Sci. Technol. 39: 3528-3537.

Butler, M. and H. G. Dam (1994). Production rates and characteristics of fecal pellets of the copepod *Acartia tonsa* under simulated phytoplankton bloom conditions: implications for vertical fluxes. Marine Ecology-Progress Series 114: 81-91.

Calbet, A., M.R. Landry. (2004). Phytoplankton growth, microzooplankton grazing, and carbon cycling in marine ecosystems. Limnol. Oceaogr. 49(1): 51-57.

Capriulo, G. M., G. Smith, R. Troy, G.H. Wikfors, J. Pellet, C. Yarish. (2002). The planktonic food web structure of a temperate zone estuary, and its alteration due to eutrophication. Hydrobiologia 475(1): 263-333.

Carlsson, P. and E. Graneli (1999). Effects of N : P : Si ratios and zooplankton grazing on phytoplankton communities in the northern Adriatic Sea. II. Phytoplankton species composition. Aquatic Microbial Ecology 18(1): 55-65.

Caron, D.A. (2001). Protistan Herbivory and Bacterivory. Methods in Microbiology 30: 289-315.

Cloern, J. E. (2001). Our evolving conceptual model of the coastal eutrophication problem. Marine Ecology-Progress Series 210: 223-253.

Cole, J.J., N.F. Caraco, B.J. Peierls. (1992). Can phytoplankton maintain a positive carbon balance in a turbid, freshwater estuary? Limnol. Oceanogr. 37(8) 1608-1617.

CTDEP. (2005). Monitoring Phytoplankton Community Composition in Long Island Sound With HPLC Photopigment Profiles. Connecticut Department of Environmental Protection, Fact Sheet. March, 2005.

CTDEP. (2008). Water Quality Measures, Sound Health 2008 Environmental Indicators. Long Island Sound Study.

CTDEP. (2009). 2009 Long Island Sound Hypoxia Season Review. Connecticut Department of Environmental Protection.

Dam, H. G., M. R. Roman, et al. (1995). Downward export of respiratory carbon and dissolved inorganic nitrogen by diel-migrant mesozooplankton at the JGOFS Bermuda time-series station. Deep Sea Research Part I: Oceanographic Research Papers 42(7): 1187-1197.

Diaz, R.J., R. Rosenburg. (2008). Spreading dead zones and consequences for marine ecosystems. Science 321: 926-929.

Dore, J.E., D.M. Karl. (1996). Nitrification in the euphotic zone as a source for nitrite, nitrate, and nitrous Oxide at Station ALOHA. Limnol. and Oceanogr. 41(8): 1619-1628.

EPA. (1998). Phase III actions for hypoxia management. Long Island Sound Study, EPA-902-R-97-003.

EPA. (2002). Environmental fluid dynamics code (EFDC). Ecosystems Research Division, United States Environmental Protection Agency.

EPA. (2006). Updated model report for Christina River Basin, Pennsylvania, Delaware, and Maryland. High-flow nutrient and DO TMDL development. Philadelphia, PA., U.S. Environmental Protection Agency.

Fenchel, T. B.J. Finlay (1983). Respiration rates in heterotrophic, free-living protozoa. Microbial Ecology 9:99-122.

Geider, R. J., H. L. MacIntyre, T.M. Kana. (1997). Dynamic model of phytoplankton growth and acclimation: Responses of the balanced growth rate and the chlorophyll *a*: carbon ratio to light, nutrient-limitation and temperature. Marine Ecology-Progress Series 148(1-3): 187-200.

Ginestat, P., J.M. Audic, V. Urbain, J.C. Block. (1998). Estimation of nitrifying bacterial activities by measuring oxygen uptake in the presence of the metabolic inhibitors Allylthiourea and Azide. Applied and Environmental Microbiology 64(6): 2266-2268.

Gobler, C. J., D. L. Berry, Dyhrman, S. T., S. W. Wilhelm, A. Salamov, A. V. Lobanov, Y. Zhang, J. L. Collier, L. L. Wurch, A. B. Kustka, B. D. Dill, M. Shah, N. C. VerBerkmoes, A. Kuo, A. Terry, J. Pangilinan, E. A. Lindquist, S. Lucas, I. T. Paulsen, T. K. Hattenrath - Lehmann, S. C. Talmage, E. A. Walker, F. Koch, A. M. Burson, M. A. Marcoval, Y. Z. Tang, G. R. LeCleir, K. J. Coyne, G. M. Berg, E. M. Bertrand, M. A. Saito, V. N. Gladyshev, I. V. Grigoriev. (2011). Niche of harmful alga *Aureococcus anophagefferens* revealed through ecogenomics. Proceedings of the National Academy of Sciences of the United States of America 108(11): 4352-4357.

Gobler, C. J., N. J. Buck, M.E. Sieracki, S.A. Sanudo-Wilhelmy. (2006). Nitrogen and silicon limitation of phytoplankton communities across an urban estuary: The East River-Long Island Sound system. Estuarine Coastal and Shelf Science 68(1-2): 127-138.

Gobler, C.J. and S.A. Sanudo-Wilhelmy. (2003). Cycling of colloidal organic carbon and nitrogen during as estuarine phytoplankton bloom. Limnol. and Oceanogr. 48(6): 2314-2320.

Goebel, N.L., J.N. Kremer, C.A. Edwards. (2006). Primary production in Long Island Sound. Estuaries and Coasts 29(2): 232-245.

Goebel, N.L., J.N. Kremer. (2007) Temporal and spatial variability of photosynthetic parameters and community respiration in Long Island Sound. Marine Ecology Progress Series 329: 23-42.

Hansell, D. A., N. R. Bates, D.B. Olson. (2004). Excess nitrate and nitrogen fixation in the North Atlantic Ocean. Marine Chemistry 84(3-4): 243-265.

Harrison, P. J., H. L. Conway, R.W. Holmes, C.O. Davis. (1977). Marine diatoms grown in chemostats under silicate or ammonium limitation. 3. Cellular chemical composition and

morphology of *Chaetoceros-Debilis*, *Skeletonema-Costatum*, and *Thalassiosira-Gravida*. Marine Biology 43(1): 19-31.

Heisler, J., P.M. Gilbert, J.M. Burkholder, D.M. Anderson, W. Cochlan, W.C. Dennison, Q. Dortch, C.J. Gobler, C.A. Heil, E. Humphries, A. Lewitus, R. Magnien, H.G. Marchall, K. Sellner, D.A. Stockwell, D.K. Stoeker, M. Suddleson. (2008). Eutrophication and harmful algal blooms: A scientific consensus. Harmful Algae 8:3-13.

Henriksen, P., B. Riemann, H. Kaas, H.M. Sorenson, H.L. Sorenson. (2002). Effects of nutrient-limitation and irradiance on marine phytoplankton pigments. Journal of Plankton Research 24(9): 835-858.

Herbert, R. A. (1999). Nitrogen cycling in coastal marine ecosystems. FEMS Microbiology Reviews 23(5): 563-590.

Hobbie, J. E., R. J. Daley, S. Jasper. (1977). Use of Nucleopore filters for counting bacteria by fluorescence microscopy. Applied and Environmental Microbiology 33(5): 1225-1228.

Hodgkiss, I.J., K.C. Ho. (1997). Are changes in N:P ratios in coastal water the key to increased red tide blooms? Hydrobiologia 352: 141-147

Holm-Hansen, O., W. H. Sutcliff, J. Sharp. (1968). Measurement of Deoxyribonucleic Acid in Ocean and Its Ecological Significance. Limnology and Oceanography 13(3): 507-&.

Howarth, R. W. and R. Marino (2006). Nitrogen as the limiting nutrient for eutrophication in coastal marine ecosystems: Evolving views over three decades. Limnol. and Oceanogr. 51(1): 364-376.

Hydroqual. 1996. Water quality modeling analysis of hypoxia in Long Island Sound using LIS3.0. Management Committee Long Island Sound Estuary Study and New England Interstate Water Pollution Control Commission. Job Number NENG0035.

Invitrogen (2005). Baclight™ RedoxSensor™ Green Vitality Kit. Molecular Probes™ Invitrogen Detection Technologies, Product Information. MP 34954.

Jensen, L.M., K. Sand-Jensen, S. Marcher, M. Hansen. (1990). Plankton community respiration along a nutrient gradient in a shallow Danish estuary. Marine Ecology Progress Series 61: 75-85

Jensen, H.S., F.O. Andersen. (1992). Importance of temperature, nitrate, and pH for phosphate release from aerobic sediments of four shallow, eutrophic lakes. Limnol and Oceanogr. 37(3): 577-589.

Jeong, H. J., Y. D. Yoo, J.S. Kim, K.A. Seong, N.S. Kang, T.H. Kim. (2010). Growth, feeding and ecological roles of the mixotrophic and heterotrophic dinoflagellates in marine planktonic food webs. Ocean Science Journal 45(2): 65-91.

Justic, D., N. N. Rabalais, R. E. Turner. (1995). Stoichiometric Nutrient Balance and Origin of Coastal Eutrophication. Marine Pollution Bulletin 30(1): 41-46.

Kahler, P. and W. Koeve. (2001). Marine dissolved organic matter: can its C:N ratio explain carbon overconsumption? Deep-Sea Research Part 1 48: 49-62.

Karl, D. M. (1993). Total microbial biomass estimation derived from the measurement of particulate adenosine-5'-triphosphate. Handbook of methods in aquatic microbial ecology. P. F. Kemp, B. E. Sherr, E. B. Sherr and J. J. Cole**:** 359-368.

Kemp, W. M., W. R. Boynton, , J. E. Adolf, D. F. Boesch, W. C. Boicourt, G. Brush, J. C. Cornwell, T. R. Fisher, P. M. Glibert, J. D. Hagy, L. W. Harding, E. D. Houde, D. G. Kimmel, W. D. Miller, R. I. E. Newell, M. R. Roman, E. M. Smith, J.C. Stevenson. (2005). Eutrophication of Chesapeake Bay: historical trends and ecological interactions. Marine Ecology-Progress Series 303: 1-29.

Kemp, W. M., P. Sampou, J. Caffrey, M. Mayer, K. Henriksen, W.R. Boynton. (1990). Ammonium recycling versus denitrification in Chesapeake Bay sediments. Limnology and Oceanography 35(7): 1545-1563.

Kirchman, D. L. (1993). Leucine incorporation as a measure of biomass production by heterotrophic bacteria. Handbook of methods in aquatic microbial ecology. P. F. Kemp, B. E. Sherr, E. B. Shern and J. J. Cole, Lewis: 509-512.

Klausmeier, C. A., E. Litchman, T. Daufresne, S.A. Levin. (2008). Phytoplankton physiology. Stoichiometry in Ecology 23: 479-485.

Lagus, A., J. Suomela, G. Weithoff, K. Heikkila, H. Helminen, J. Sipura . (2004). Species-specific differences in phytoplankton responses to N and P enrichments and the N : P ratio in the Archipelago Sea, northern Baltic Sea. Journal of Plankton Research 26(7): 779-798.

Lee, Y. J. and K. M. M. Lwiza (2005). Interannual variability of temperature and salinity in shallow water: Long Island Sound, New York. Journal of Geophysical Research 110(C09022).

Lee, Y. J. and K. M. M. Lwiza (2008). Characteristics of bottom dissolved oxygen in Long Island Sound, New York. Estuarine Coastal and Shelf Science 76(2): 187-200.

Li, W.K. (1982). Estimating heterotrophic bacterial productivity by inorganic radiocarbon uptake: Importance of establishing time course uptake. Marine Ecology Progess Series 8: 167-172.

LISS (2008). 2009 Monitoring Assessment, and Research Needs to Support Attainment of LISS Goals and Targets. The Long Island Sound Study.

LISS. (2011). Status and Trends: LISS Environmental Indicators. Long Island Sound Study, from http://longislandsoundstudy.net/category/status-and-trends/.

Lomas, M.L., S.B. Moran (2011). Evidence for aggregation and export of cyanobacteria and nano-eukaryotes from the Sargasso Sea euphotic zone. Biogeosciences 8:203-216.

Maas, R.P., S.C. Patch, D.M. Morgan, T.J. Pandolfo. (2005). Reducing lead exposure from drinking water: Recent history and current status. Public Health Reports 120: 316-321.

Madigan, M. T., J. M. Martino, P. V. Dunlap, and D. P. Clark. (2009). Metabolic diversity: Phototrophy, autotrophy, chemolithotrophy, and nitrogen fixation. Brock Biology of Microorganisms, 12th Ed. Pearson Benjamin Cummings.

Michaels, A.F., M.W. Silver. (1988). "Primary production, sinking fluxes and the microbial food web." Deep Sea Research Part A 35(4) 473-490.

Moran, M. A., W. M. Sheldon, J.E. Sheldon. (1999). Biodegradation of riverine dissolved organic carbon in five estuaries of the southeastern United States. Estuaries 22(1): 55-64.

Mulholland, M.R., A.M. Rocha, G.E. Boneillo. (2011). Incorporation of Leucine and Thymidine by Estuarine Phytoplankton: Implications for Bacterial Productivity. Estuaries and Coasts 34: 310-325

NYSDEC (2000). A Total Maximum Daily Load analysis to achieve water quality standards for dissolved oxygen in Long Island Sound, NY. State Department of Environmental Conservation, Connecticut Department of Environmental Protection.

O'Donnell, J.H., H.G. Dam, W.F. Bohlen, W. Fitzgerald, P.S. Gay, A.E. Houk, D.C. Cohen, M.M. Howard- Strobel. (2008). Intermittent ventilation in the hypoxic zone of western Long Island Sound during the summer of 2004. Journal of Geophysical Research 113: C09025.

O'Donnell, J., H. Dam, G. McCardell, T. Fake. (2010). Simulation of Long Island Sound with

the System-Wide Eutrophication Model (SWEM): Inter-annual variability and vensitivity. Long Island Sound Study EPA Assistance Award Final Report. EPA, University of Connecticut.
O'Shea, M. L. and T. M. Brosnan (2000). Trends in indicators of eutrophication in western Long Island Sound and the Hudson-Raritan Estuary. Estuaries 23(6): 877-901.
Olli, K. (1999). Diel vertical migration of phytoplankton and heterotrophic flagellates in the Gulf of Riga. Journal of Marine Systems 23(1-3): 145-163.
Paerl, H.W., L.M. Valdes-Weaver, A.R. Joyner, V. Winkelman. (2007). Phytoplankton indicators of ecological changes in the eutrophying Pamlico Sound System, North Carolina. Ecological Applications Supplement 17(5): S88-S101.
Parker, C. A. and J. E. O'Reilly (1991). Oxygen depletion in Long-Island Sound: A historical perspective. Estuaries 14(3): 248-264.
Parsons, T. R., Y. Maita, C.M. Lalli. (1984). A manual of chemical and biological methods for seawater analysis. New York, Pergamon Press.
Perry, M. J. (1976). Phosphate utilization by an oceanic diatom in phosphorus-limited chemostat culture and in oligotrophic waters of Central North-Pacific. Limnol, and Oceanogr. 21(1): 88-107.
Raven, J.A., J.E. Kubler. (2002). New light on the scaling of metabolic rate with the size of algae. Journal of Phycology 38: 11-16.
Riemann, B., P. Simonsen, L. Stensgaard. (1989). The carbon and chlorophyll content of phytoplankton from various nutrient regimes. Journal of Plankton Research 11(5): 1037-1045.
Ritter, C., P.A. Montagna. (1999). Seasonal hypoxia and models of benthic responses in a Texas bay. Estuaries 22(1): 7-20.
Sharp, J. H., R. Benner, L. Bennet, C.A. Carlson, S.E. Fitzwater, E.T. Peltzer, L.M. Tupas. (1995). Analyses of dissolved organic-carbon in seawater - the JGOFS EQPAC methods comparison. Marine Chemistry 48(2): 91-108.
Sharp, J. H., E. T. Peltzer, M.J. Alperin, G. Cauwet, J.W. Farrington, B. Fry, D.M. Karl, J.H. Martin, A. Spitzy, S. Tugrul, C.A. Carlson. (1993). Measurement of dissolved organic-carbon and nitrogen in natural-waters - Procedures subgroup report. Marine Chemistry 41(1-3): 37-49.
Sharp, J. H., K. Yoshiyama, A.E. Parker, M.C. Schwartz, S.E. Curless, A.Y. Beauregard, J.E. Ossolinkski, A.R. Davis. (2009). A biogeochemical view of estuarine eutrophication: Seasonal and spatial trends and correlations in the Delaware Estuary. Estuaries and Coasts 32(6): 1023-1043.
Sherr, E.B., B.F. Sherr. (2002). Significance of predation by protists in aquatic microbial food webs. Antonie van Leeuwenhoek 81: 293-308.
Shiah, F.-K. and H. W. Ducklow (1994). Temperature regulation of heterotrophic bacterioplankton abundance, production, and specific growth rate in Chesapeake Bay. Limnol. and Oceanogr. 39(6): 1243-1258.
Stoeker, D.K. (1999), Mixotrophy among Dinoflagellates. Journal of Eukaryotic Microbiology 46(4) 397-401.
Strauss, E. A., N. L. Mitchell, and G. A. Lamberti. 2002. Factors regulating nitrification in aquatic sediments: effects of organic carbon, nitrogen availability, and pH. Canadian Journal of Fisheries and Aquatic Sciences 59: 554-563.

Sunda, W. G. and D. R. Hardison (2007). Ammonium uptake and growth limitation in marine phytoplankton. Limnol. and Oceanogr. 52(6): 2496-2506.
Swaney, D. P., D. Scavia, R.W. Howarth, R.M. Marino. (2008). Estuarine classification and response to nitrogen loading: Insights from simple ecological models. Estuarine Coastal and Shelf Science 77(2): 253-263.
Sweeney, A. and S. A. Sanudo-Wilhelmy (2004). Dissolved metal contamination in the East River-Long Island sound system: potential biological effects. Marine Pollution Bulletin 48(7-8): 663-670.
Taylor, A.H., R.J. Geider, F.J.H. Gilbert. (1997) Seasonal and latitudinal dependencies of phytoplankton carbon-to-chlorophyll *a* ratios: results of a modeling study. Marine Ecology Progess Series 152: 51-66.
Taylor, G. T., M. Iabichella, T.Y. Ho, M.I. Scranton, R.C. Thunell, F. Muller-Karger, R. Varela. (2001). Chemoautotrophy in the redox transition zone of the Cariaco Basin: A significant midwater source of organic carbon production. Limnol. and Oceanogr. 46(1): 148-163.
Taylor, G. T., J. Way, M.I. Scranton. (2003). Planktonic carbon cycling and transport in surface waters of the highly urbanized Hudson River estuary. Limn. and Oceanogr. 48(5): 1779-1795.
Welsh, B. L. and F. C. Eller (1991). Mechanisms controlling summertime oxygen depletion in western Long-Island Sound. Estuaries 14(3): 265-278.
Wezernak, C. T. and J. J. Gannon (1967). Oxygen-nitrogen relationships in autotrophic nitrification. Applied Microbiology 15(5): 1211-&.
Wilcox, R. R. (2005). Regression and correlation. Introduction to robust estimation and hypothesis testing. San Diego, CA, Academic Press.
Williams, P.J. leB. (1995). Evidence for the seasonal accumulation of carbon-rich dissolved organic material, its scale in comparison with changes in particulate material and the consequential effect on net C/N assimilation ratios. Marine Chemistry 51: 17-29.
Wilson, R. E., R. L. Swanson, H.A. Crowley. (2008). Perspectives on long-term variations in hypoxic conditions in western Long Island Sound. Journal of Geophysical Research 113(C12011): 1-13.
Wilson, S. E. and D. K. Steinberg (2010). Autotrophic picoplankton in mesozooplankton guts: evidence of aggregate feeding in the mesopelagic zone and export of small phytoplankton. Marine Ecology-Progress Series 412: 11-27.

**Appendix A: Figures**

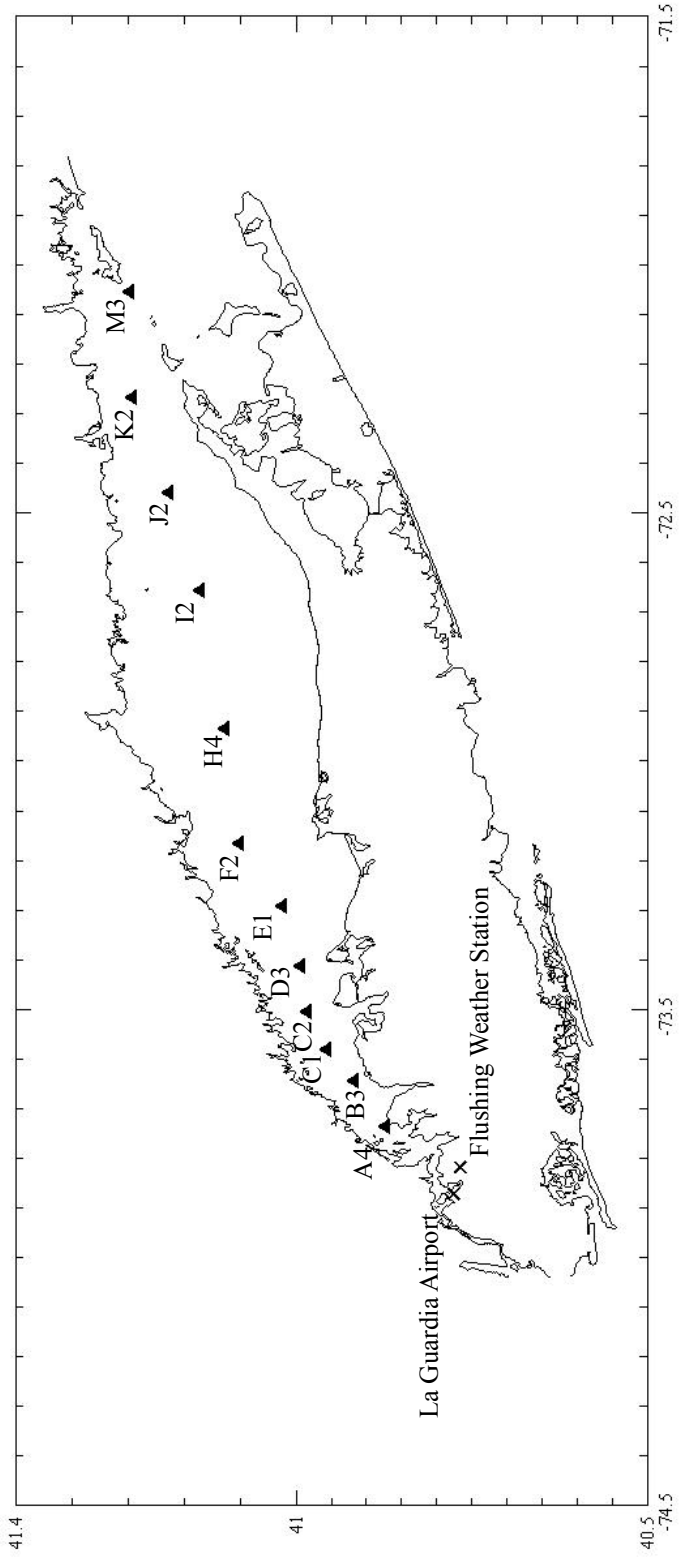


Figure 1: Map of LIS and the relevant Connecticut Department of Environmental Protection stations (triangles). Meteorological data were taken from La Guardia airport (circle) and the Flushing weather stations (x).

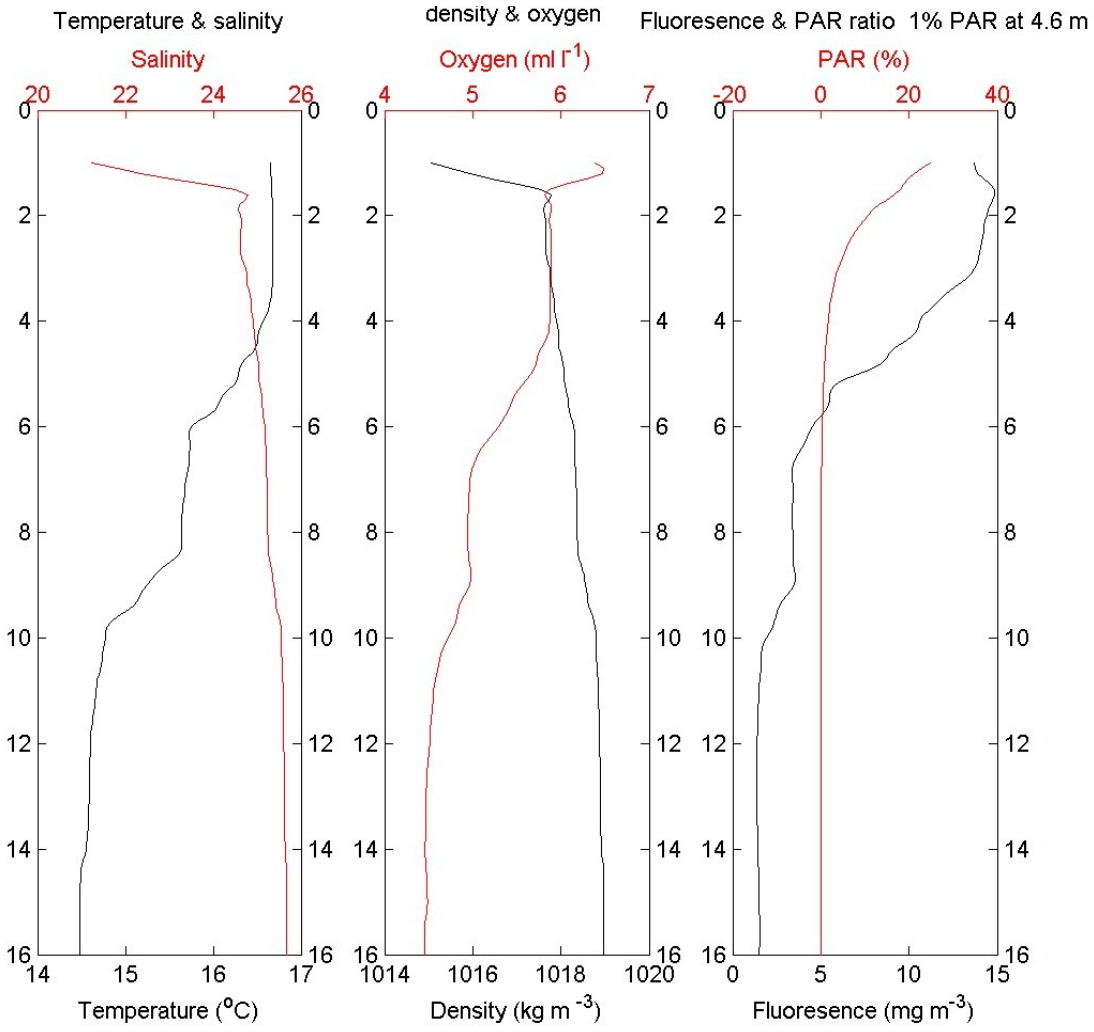


Figure 2a: Water column properties, with depth, measured by the CTD at station A4 on 9 June 2009.

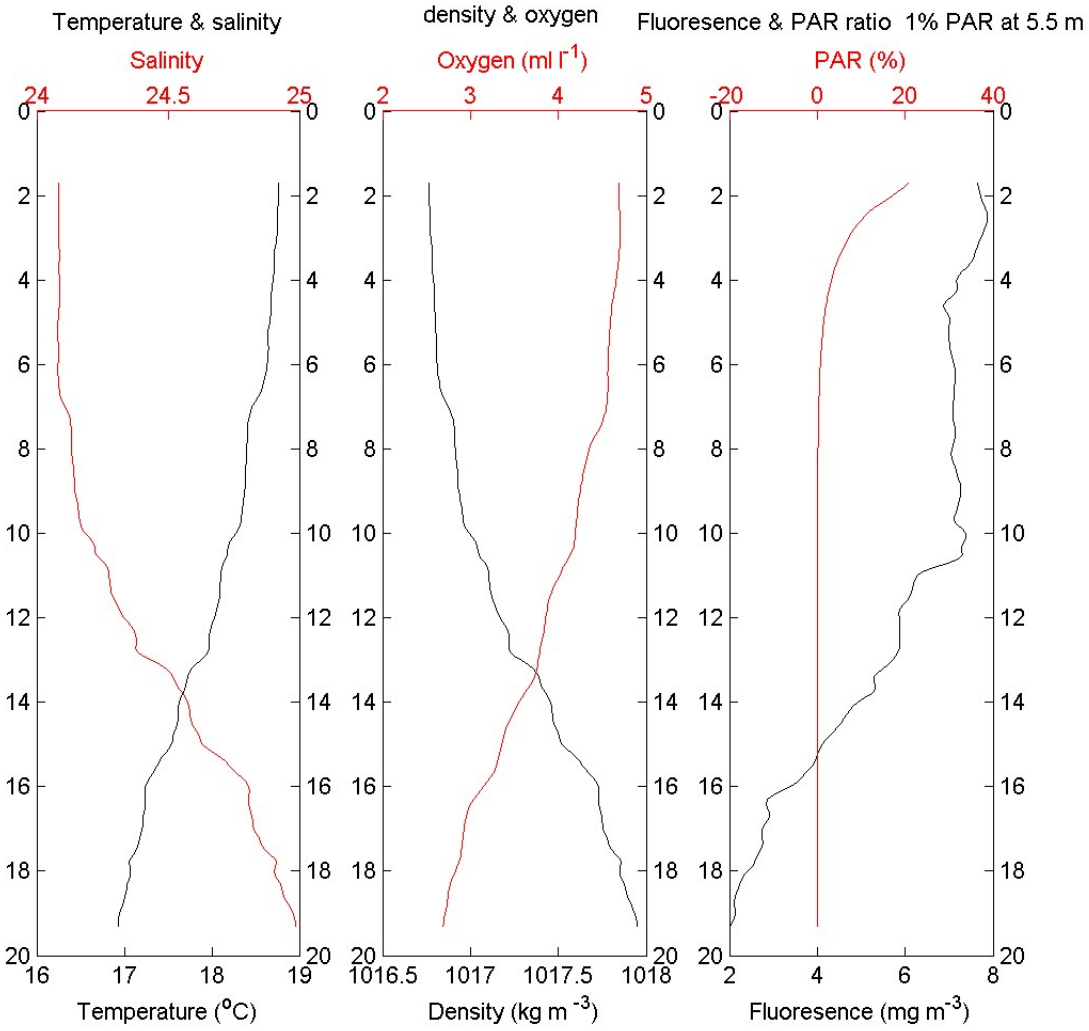


Figure 2b: Water column properties, with depth, measured by the CTD at station A4 on 23 June 2009.

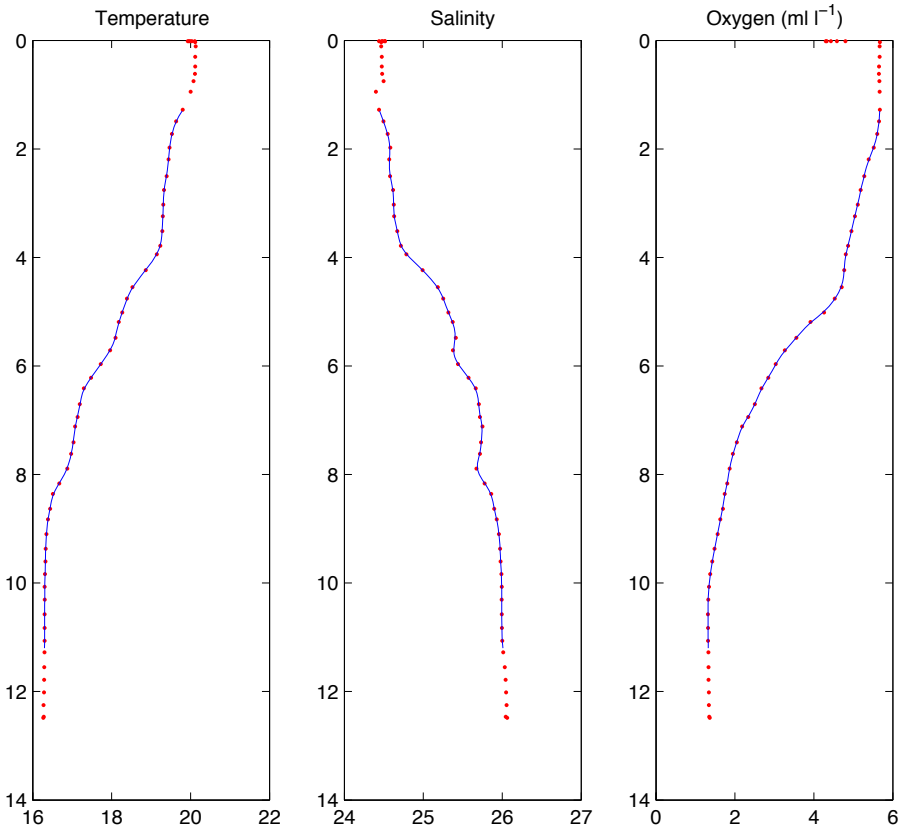


Figure 2c: Water column properties, with depth, measured by the CTD at station A4 on 14 July 2009. During this cruise, a different CTD and different software was used to take the measurements. Therefore, density, fluorescence, and PAR were not measured.

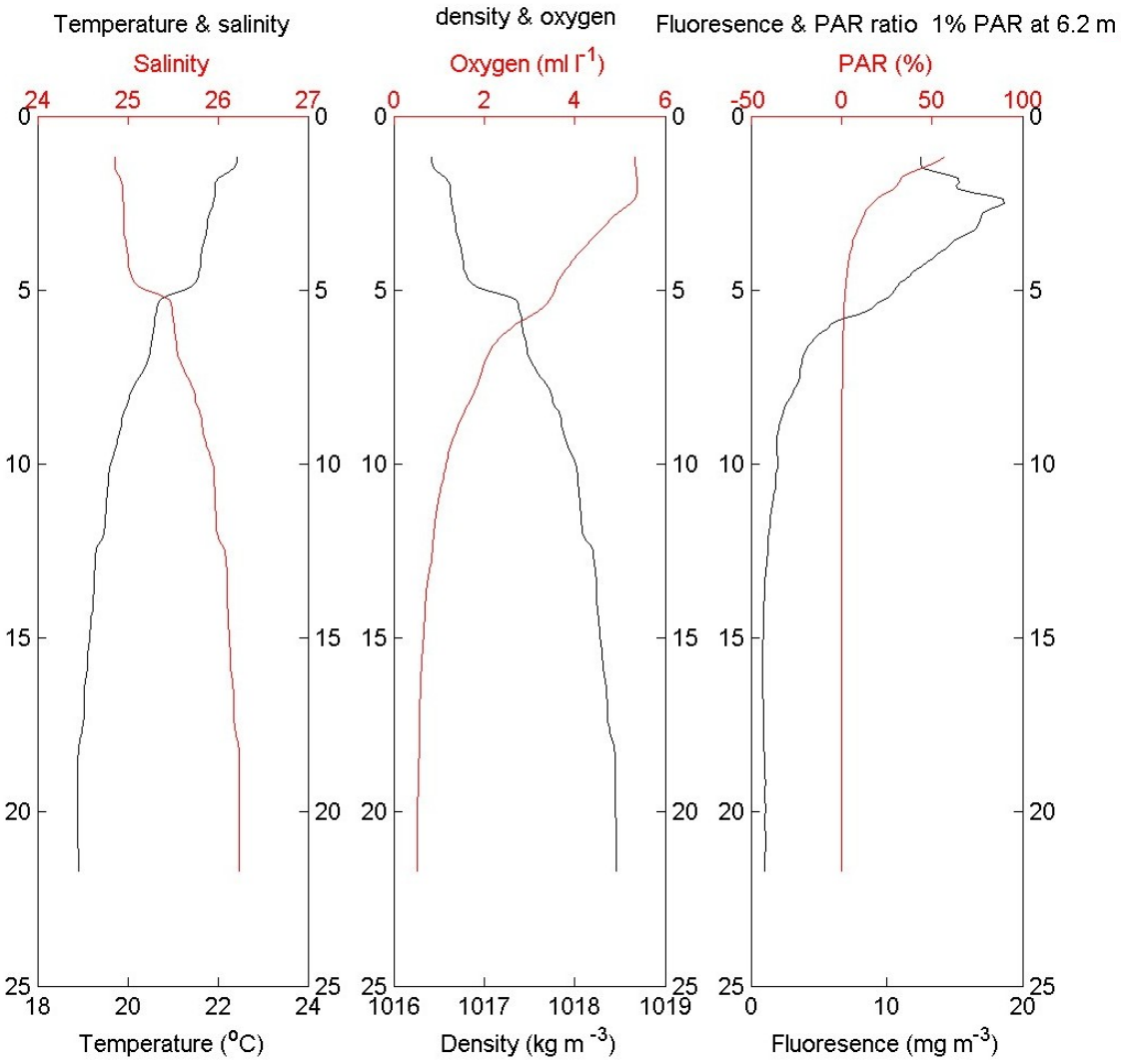


Figure 2d: Water column properties, with depth, measured by the CTD at station A4 on 11 August 2009.

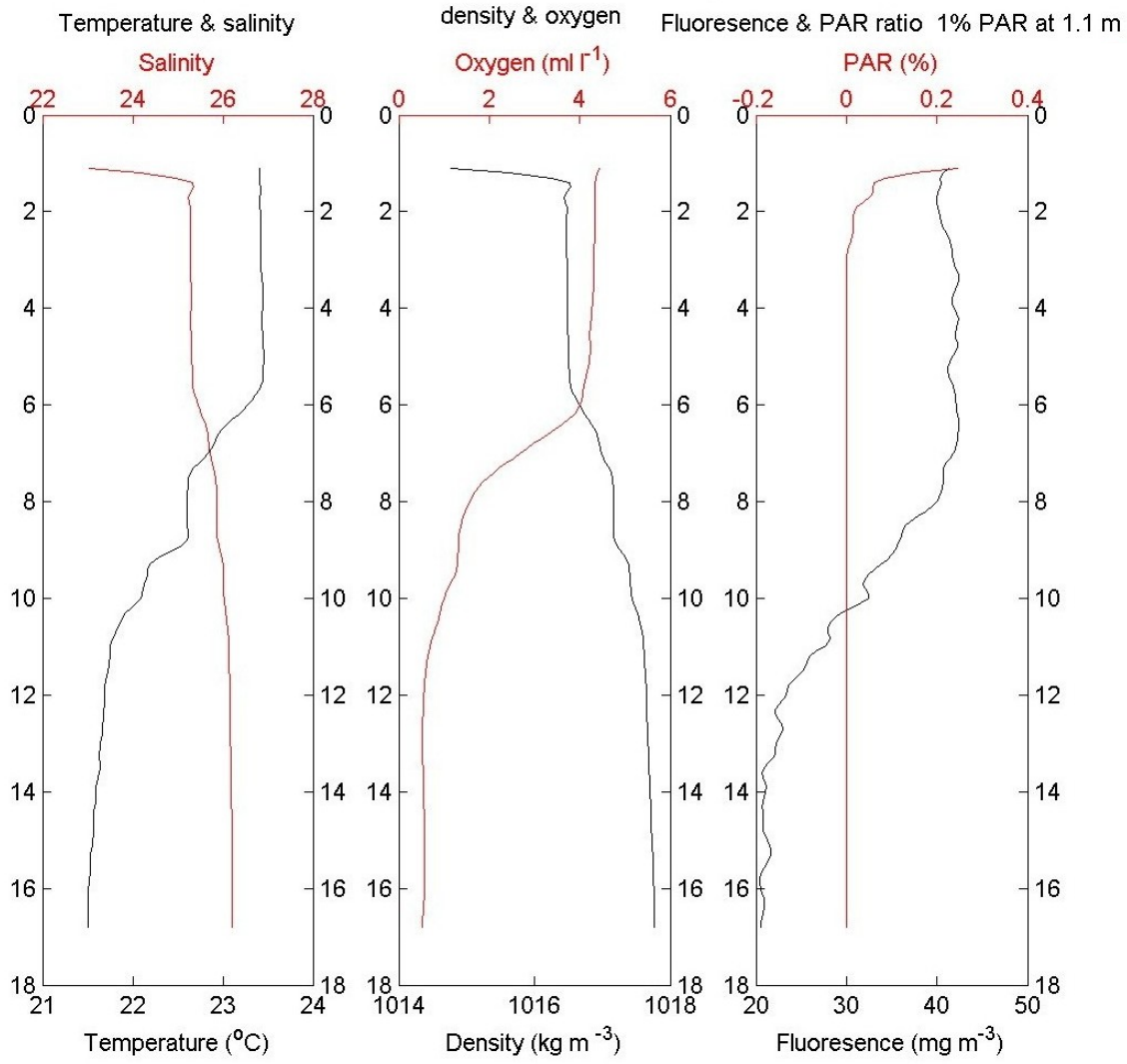


Figure 2e: Water column properties, with depth, measured by the CTD at station A4 on 28 August 2009.

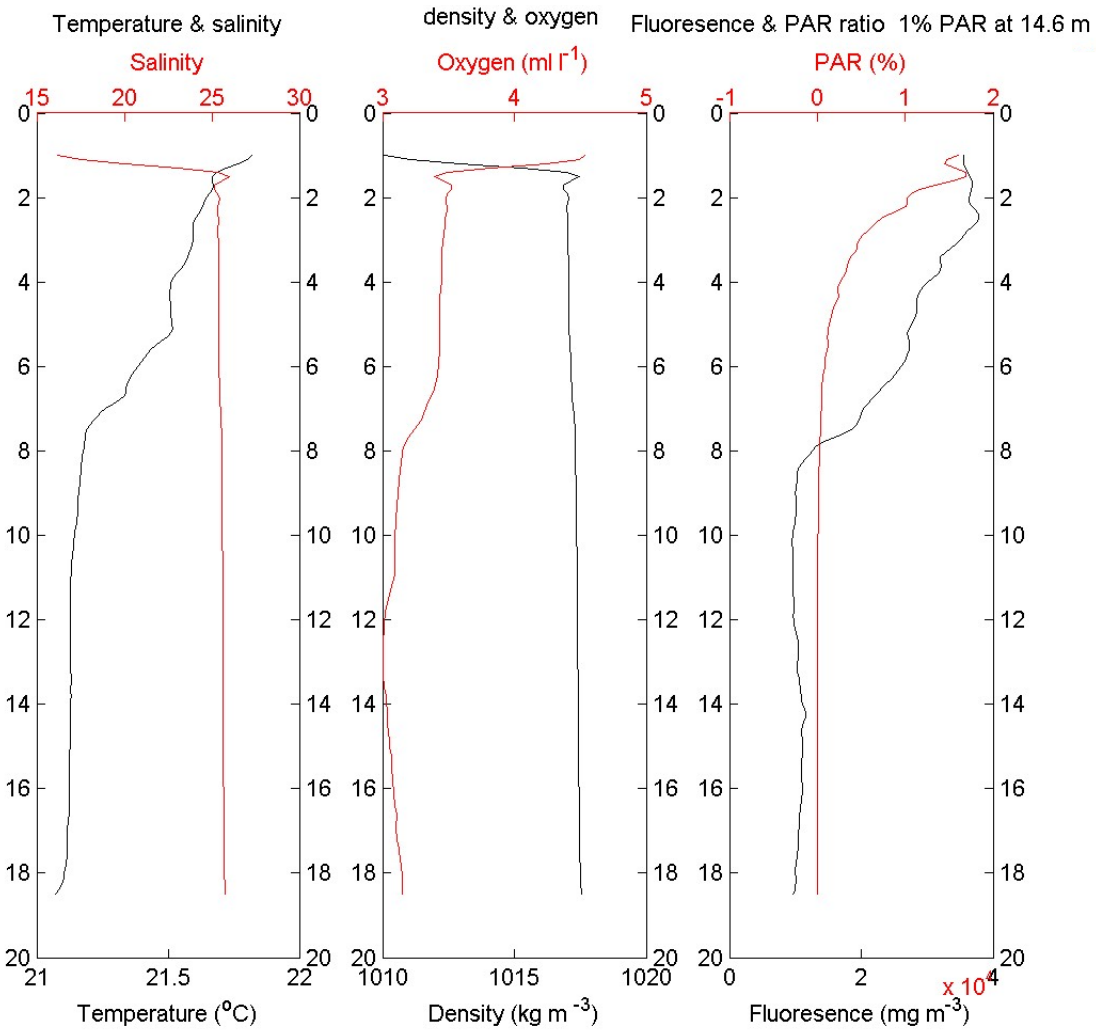


Figure 2f: Water column properties, with depth, measured by the CTD at station A4 on 15 September 2009.

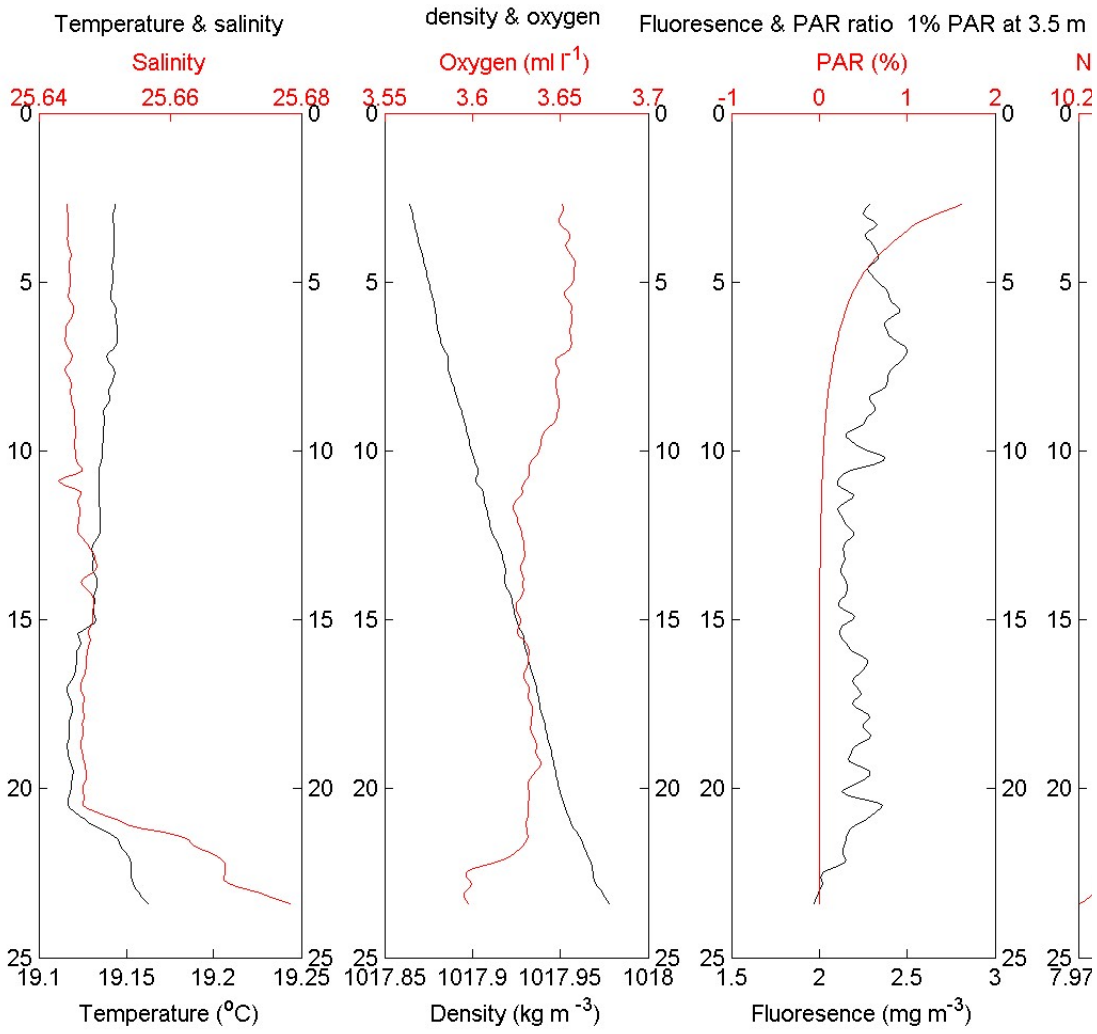


Figure 2g: Water column properties, with depth, measured by the CTD at station A4 on 1 October 2009.

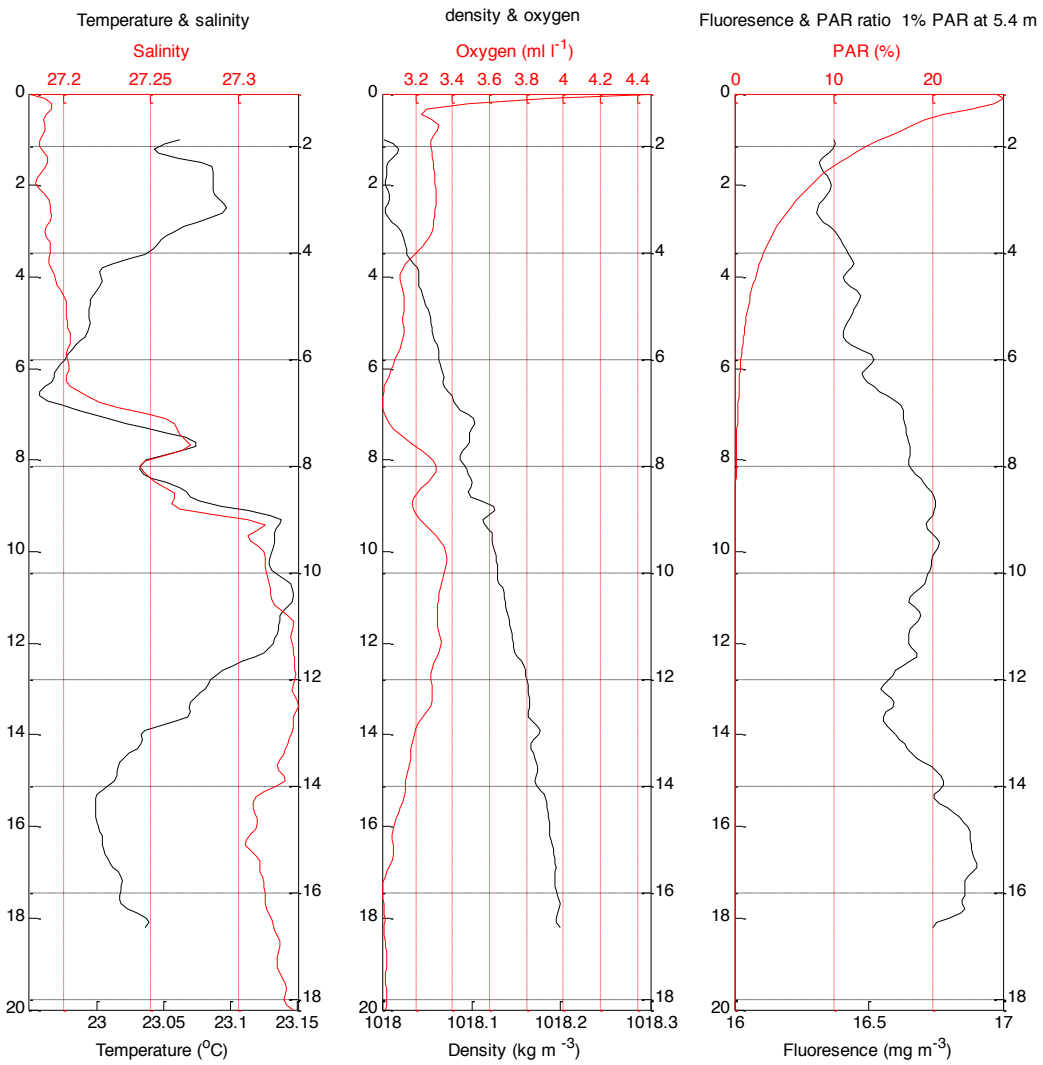


Figure 2h: Water column properties, with depth, measured by the CTD at station A4 on 16 August 2010.

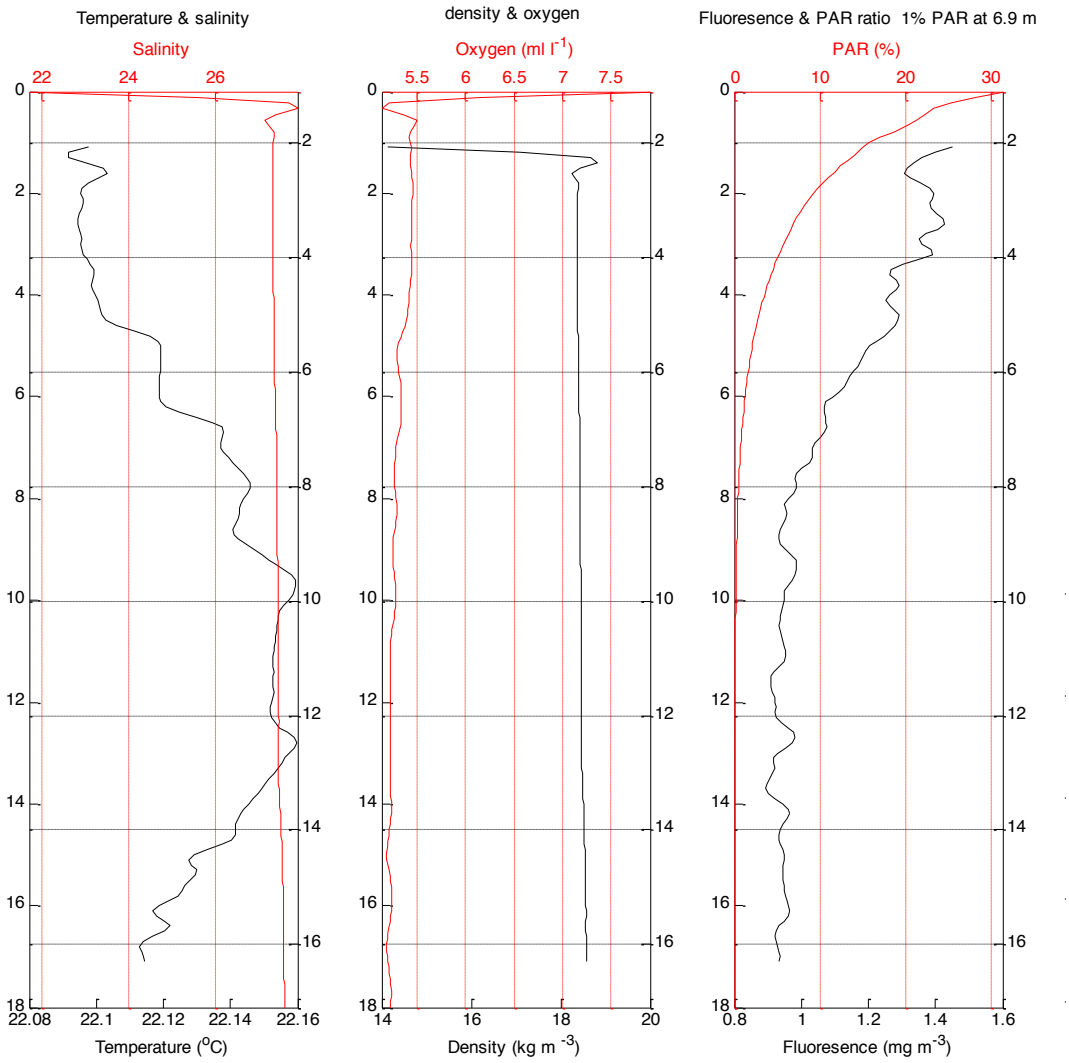


Figure 2i: Water column properties, with depth, measured by the CTD at station A4 on 10 September 2010.

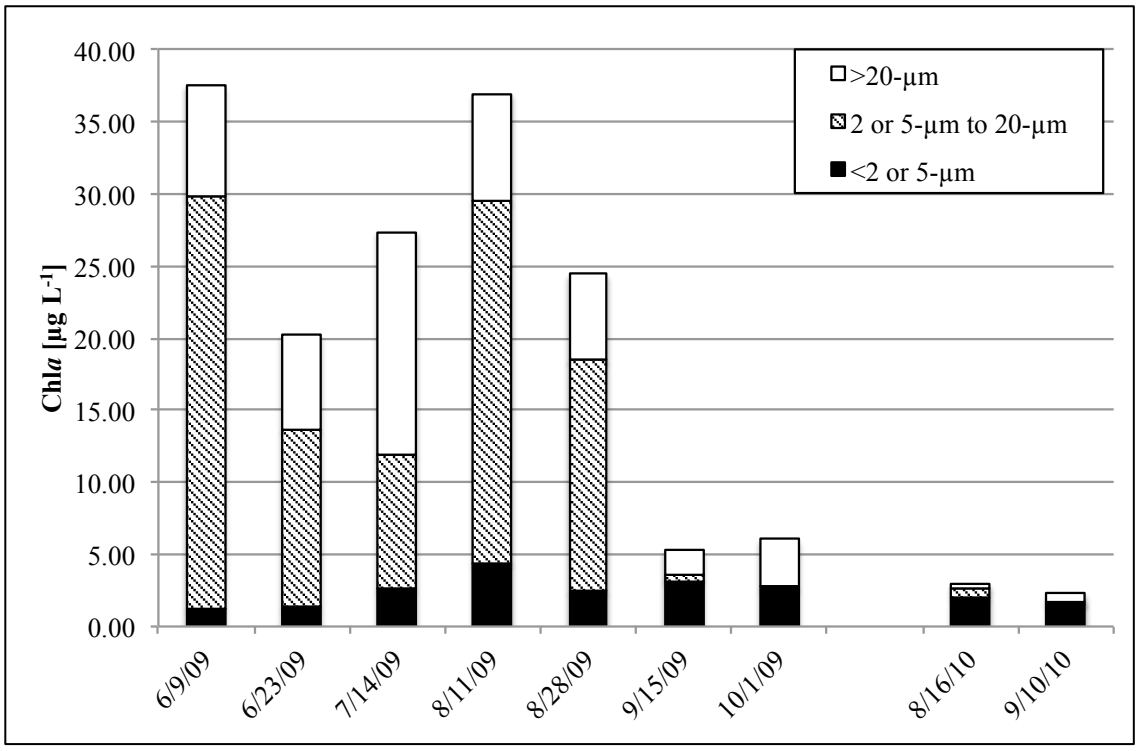


Figure 3: Chl*a* at station A4 in surface waters within each size fraction. During the first 3 cruises, the smallest size fraction was filtered to 2-µm. After 14 July 2009, the smallest size fraction was passed through a to 5-µm filter.

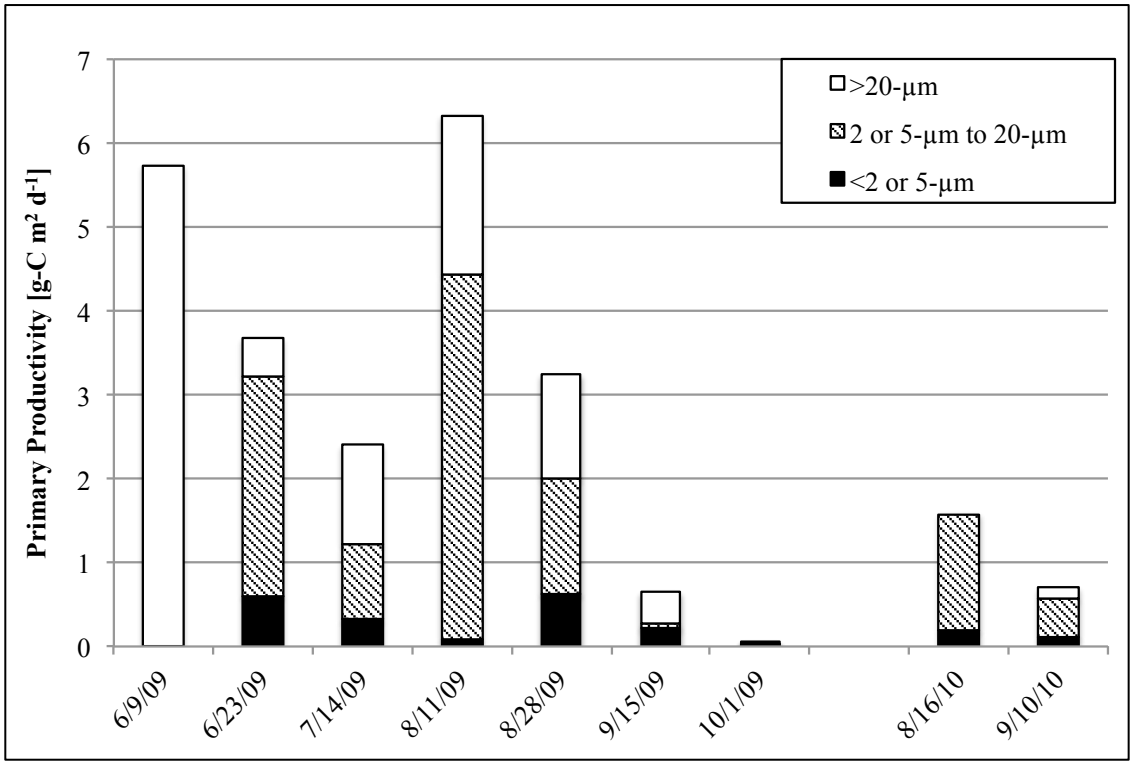


Figure 4: Photic-zone integrated primary productivity at station A4 in surface water from each size fraction. On 6 June, 2009, there was no size-fraction and the bar represents total primary productivity in the photic zone. During the next 2 cruises, the smallest size fraction was filtered to 2-µm. After 14 July, 2009, the smallest size fraction was filtered to 5-µm.

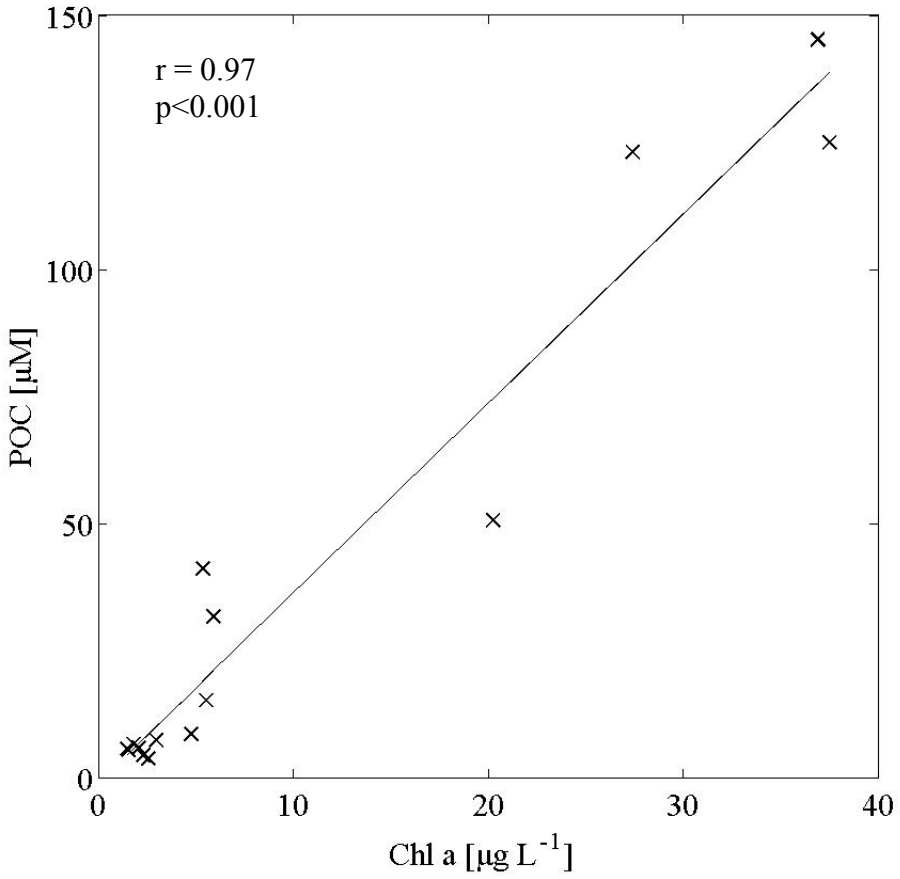


Figure 5: The relationship between Chl*a* and POC measured in surface samples during the summers of 2009 and 2010 at station A4.

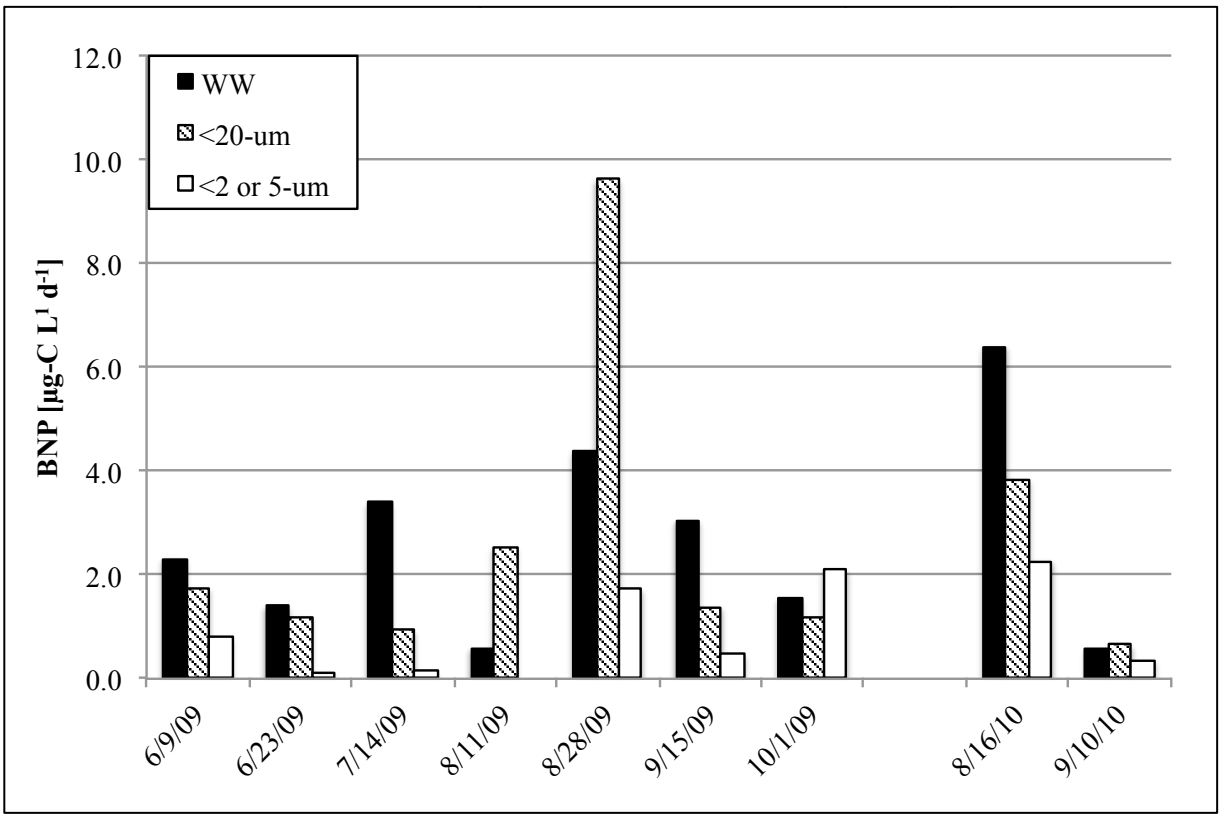


Figure 6a: Bacterial net productivity (BNP) in surface water at station A4 in each size fraction. On 8/11/09, BNP in the <2 or 5-µm fraction was not measured.

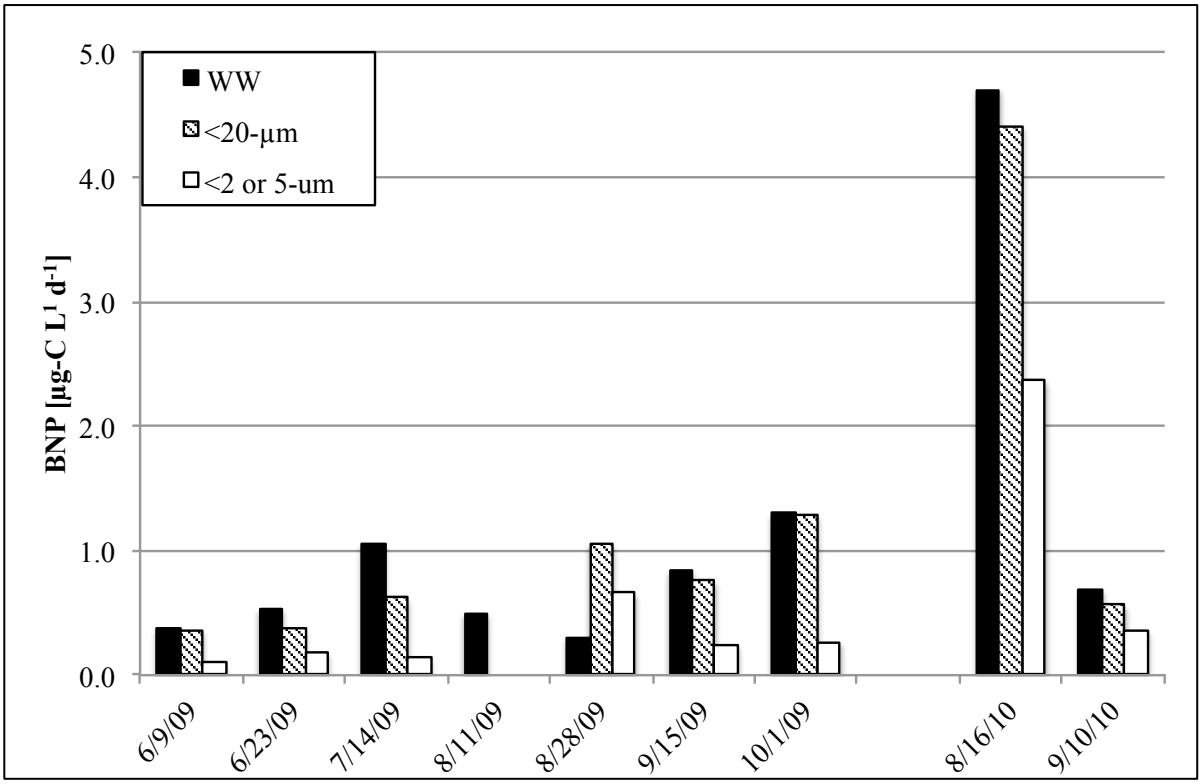


Figure 6b: Bacterial net productivity (BNP) in bottom water at station A4 in each size fraction. On 8/11/09, BNP in the <20-µm and <2 or 5-µm fraction was not measured.

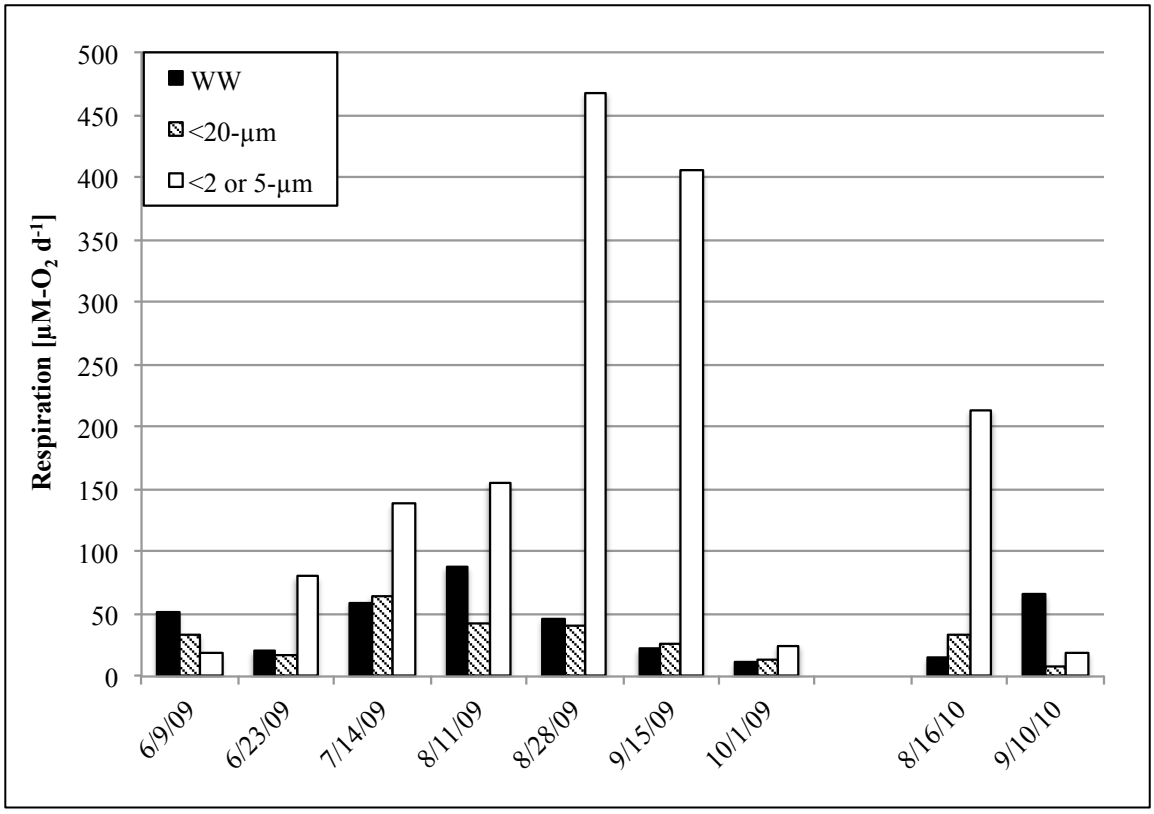


Figure 7a: $O_2$-respiration rates in surface waters at station A4 in each size fraction.

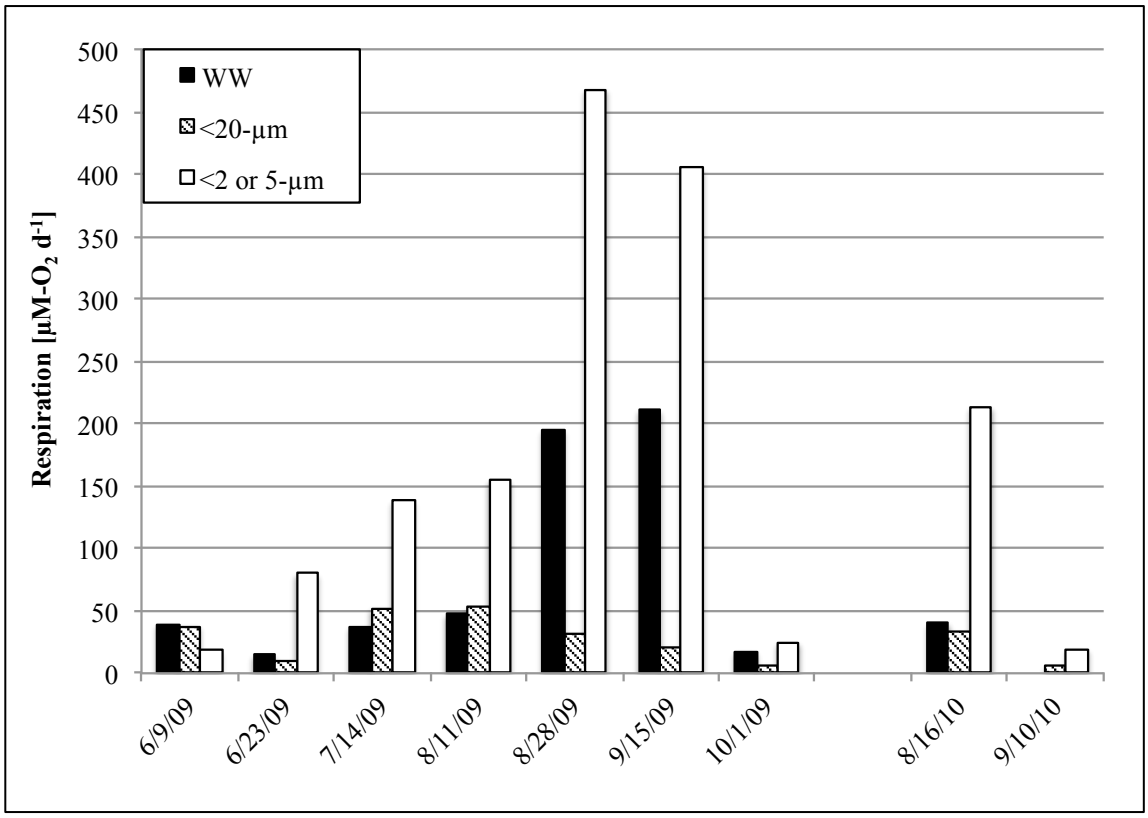


Figure 7b: $O_2$-respiration rates in bottom waters at station A4 in each size fraction. On 10 September, 2010, respiration in the WW fraction was not measured.

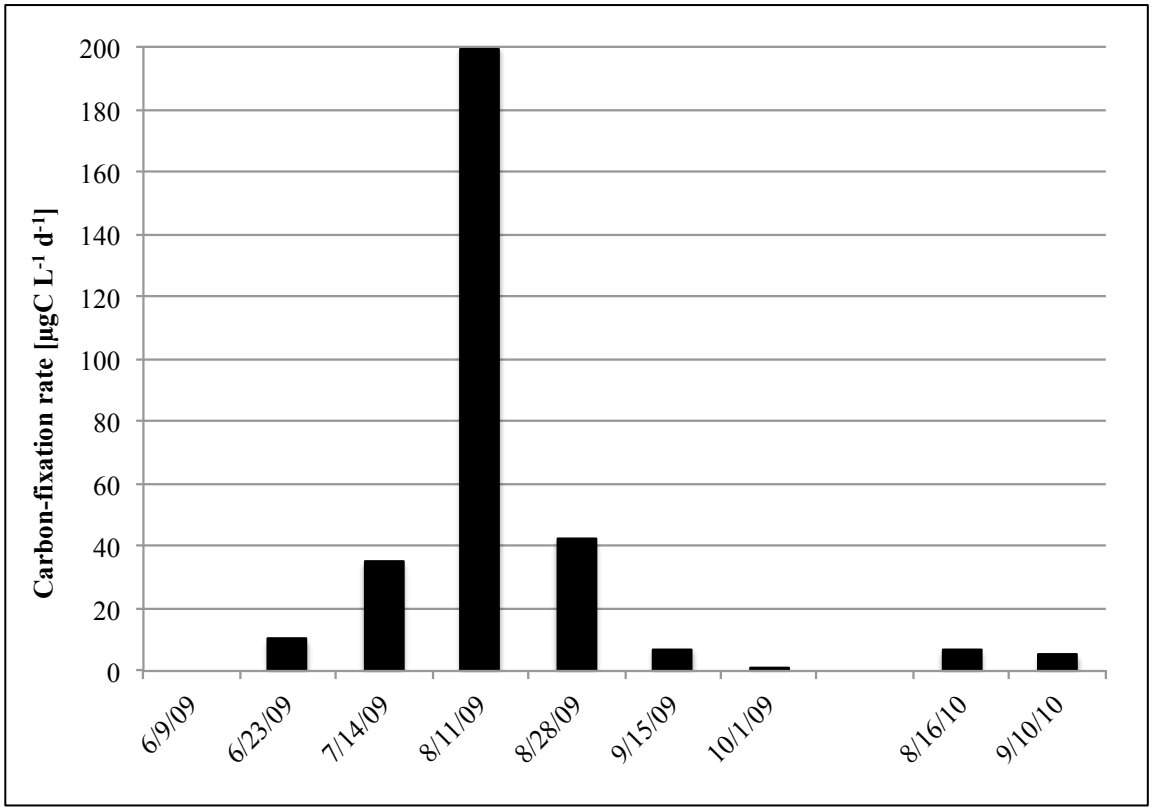


Fig 8a: Rates of dark DIC assimilation (DDA) in surface waters at station A4 during each of the field dates. DDA was below detection on 9 June 2009.

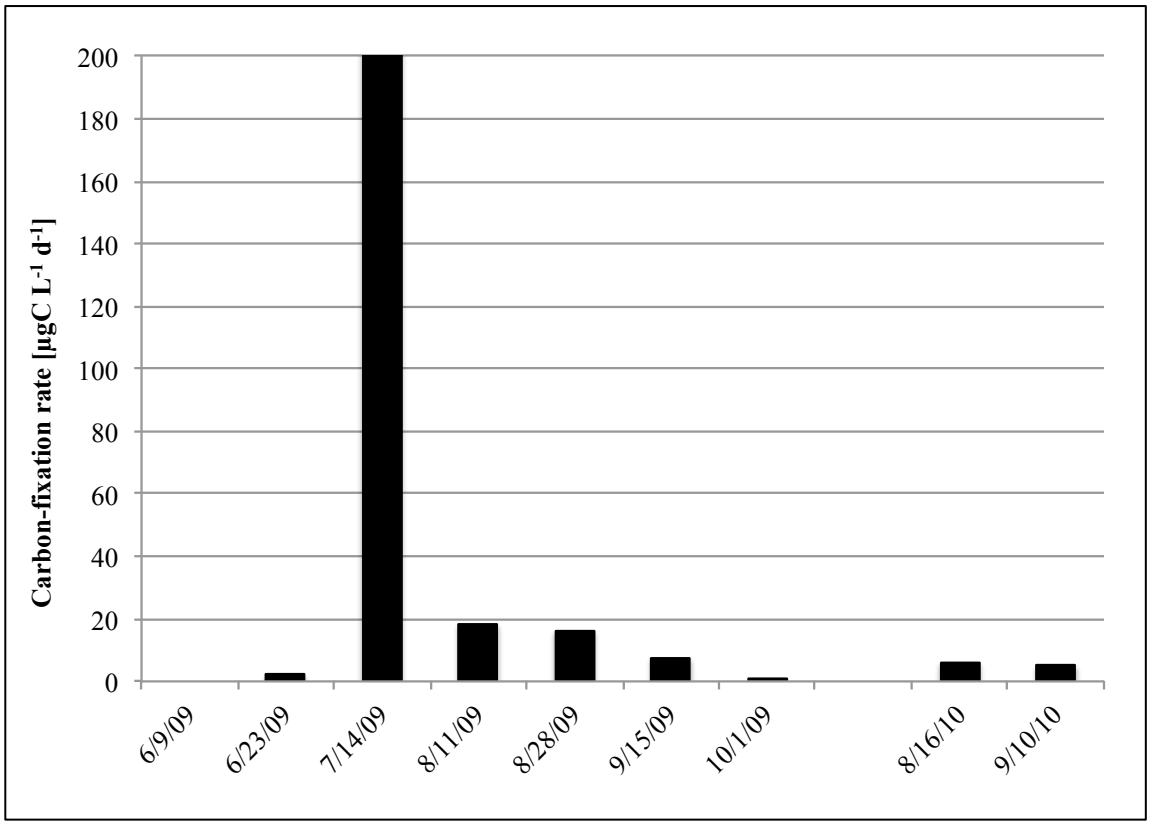


Fig 8b: Rates of dark DIC assimilation (DDA)in bottom waters as station A4 during each of the field dates. DDA was below detection on 9 June 2009.

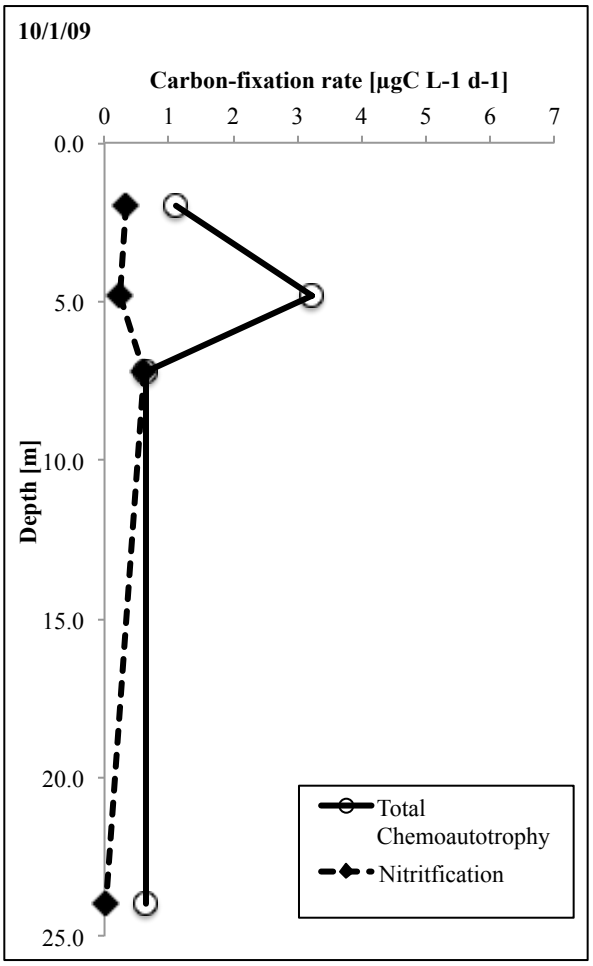


Figure 9a: Depth-profiles of dark DIC assimilation (DDA) rates measured on 1 October 2009 at station A4. Total dark carbon fixation is shown with the circles and solid line. Dark-carbon fixation due to nitrification is shown with the diamonds and dashed line.

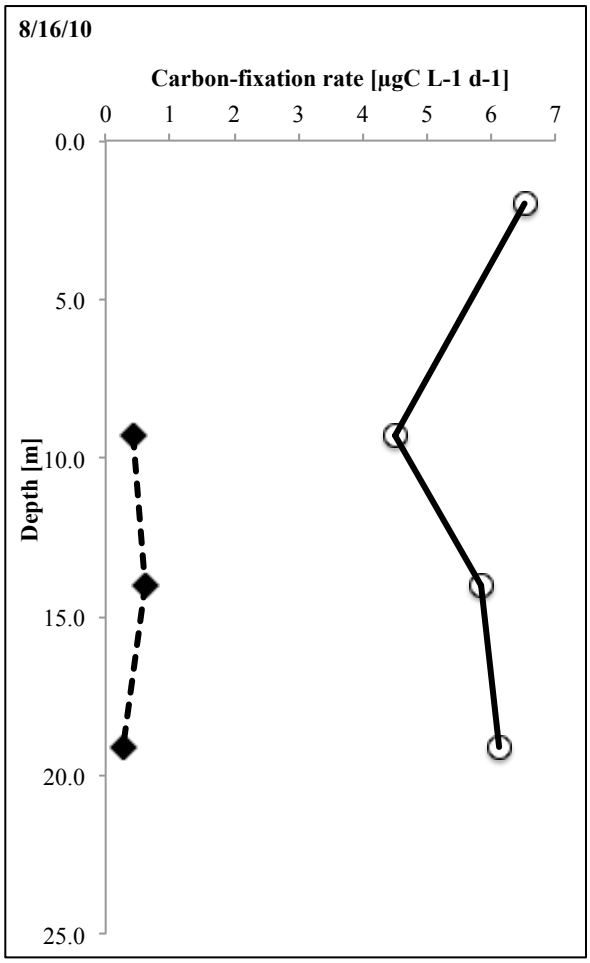


Figure 9b: Depth-profiles of dark DIC assimilation (DDA) rates measured on 16 August 2010 at station A4. Total dark carbon fixation is shown with the circles and solid line. Dark-carbon fixation due to nitrification is shown is the diamonds and dashed line. On this date, the rate of nitrification in the surface sample was greater than the total rate. Therefore it is not presented here.

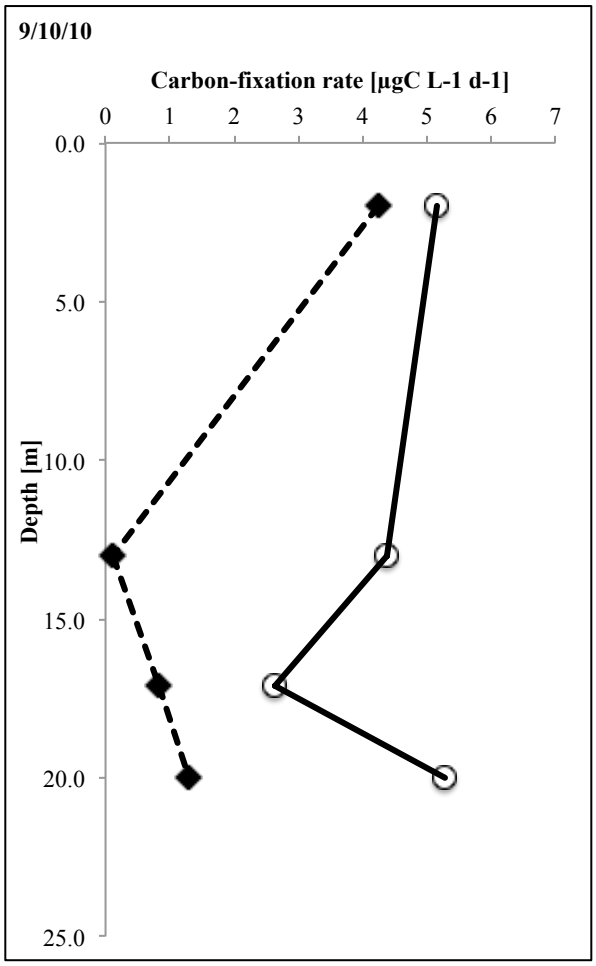


Figure 9c: Depth-profile of the dark DIC assimilation (DDA) rates measured on 10 September 2010 at station A4. Total dark carbon fixation is shown with the circles and solid line. Dark-carbon fixation due to nitrification is shown is the diamonds and dashed line.

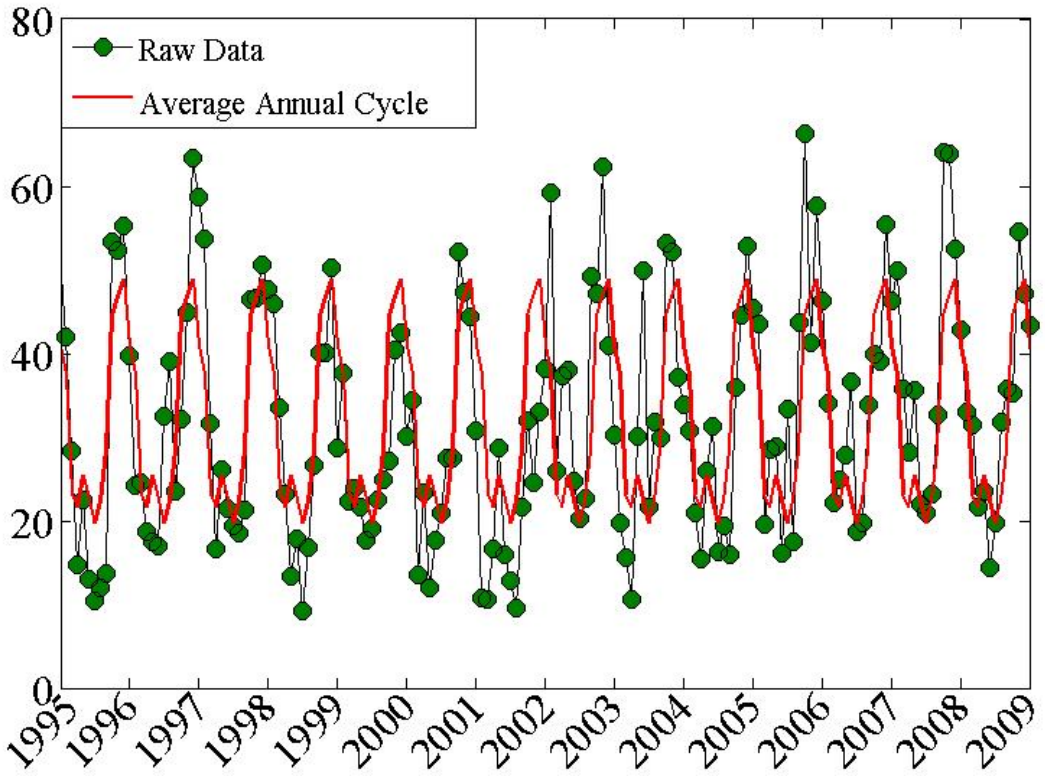


Figure 10a: TDN concentrations (green) and its climatological annual cycle (red) at station A4 in surface water between 1995 and 2009. (Data courtesy of CTDEP)

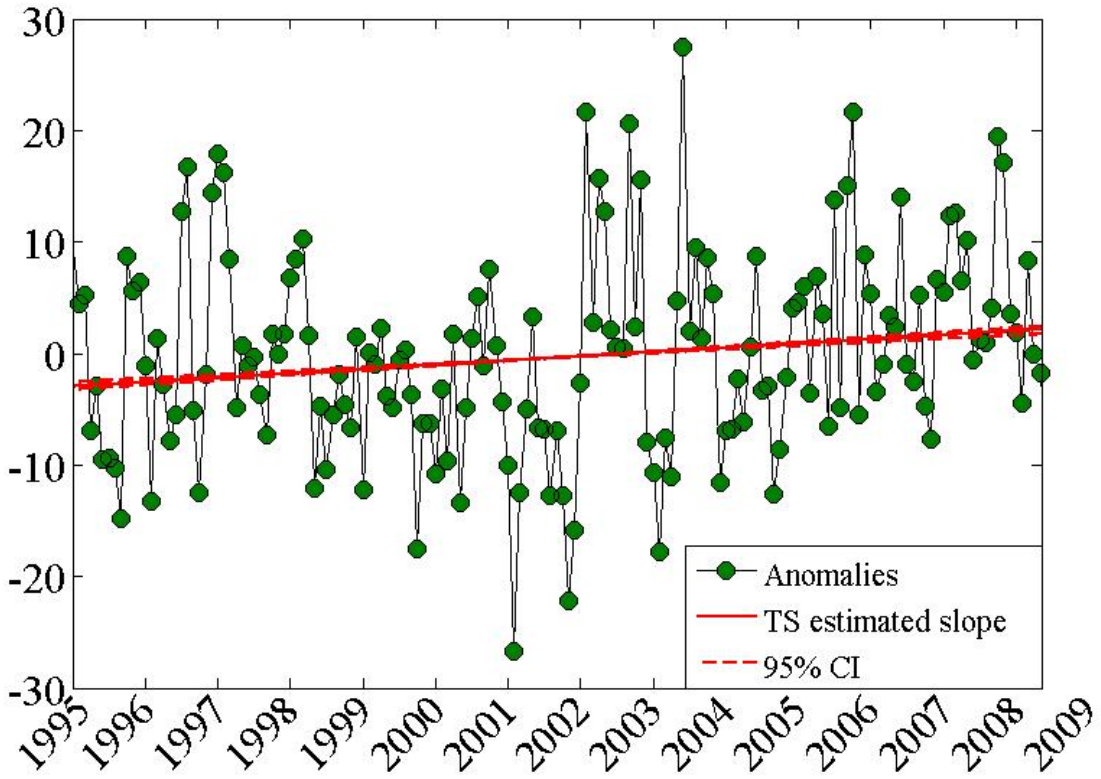


Figure 10b: The anomalies in TDN concentrations (green) were calculated by subtracting the average annual cycle from the raw data in Fig. 10a. The trend was then calculated using the TS estimator (red solid line) as described in the text. The 95% confidence interval of the interannual slope was calculated by bootstrapping (red dashed lines). The trends for each variable at each station in the surface and bottom were calculated in the same fashion. All trends are presented in Tables 5-8.

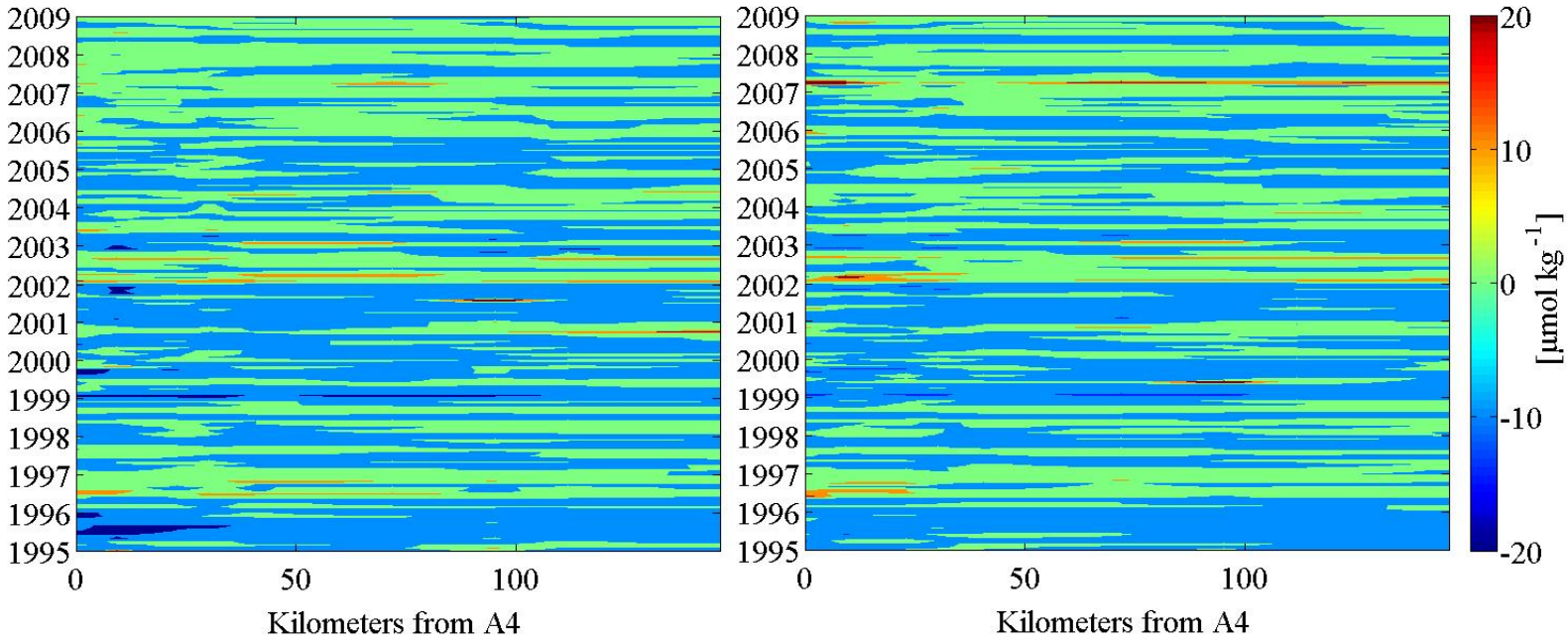


Figure 11: Surface (left) and bottom (right) water DON anomalies from the 9 LIS stations between 1995 and 2009. Estimate of interannual trends and respective confidence intervals are given in Table 7.

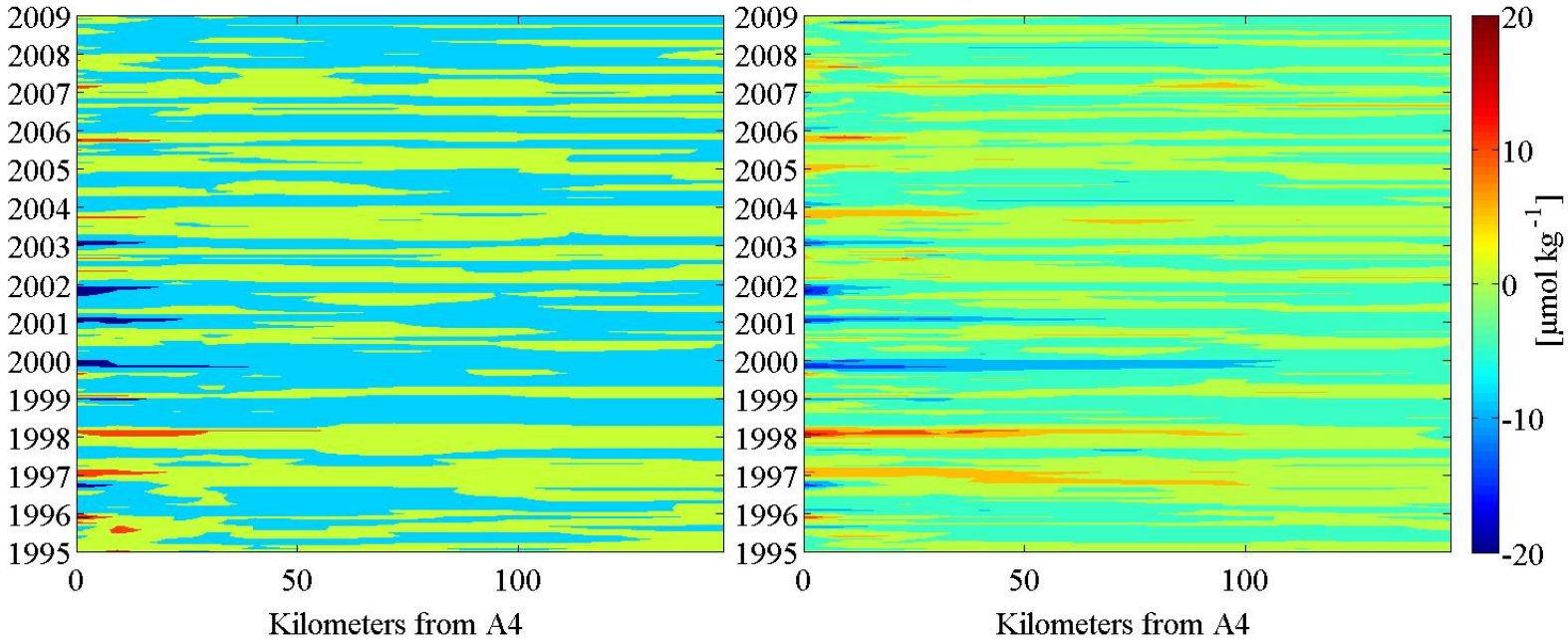


Figure 12: Surface (left) and bottom water (right) DIN anomalies from the 9 LIS stations between 1995 and 2009. Estimate of interannual trends and respective confidence intervals are given in Table 5.

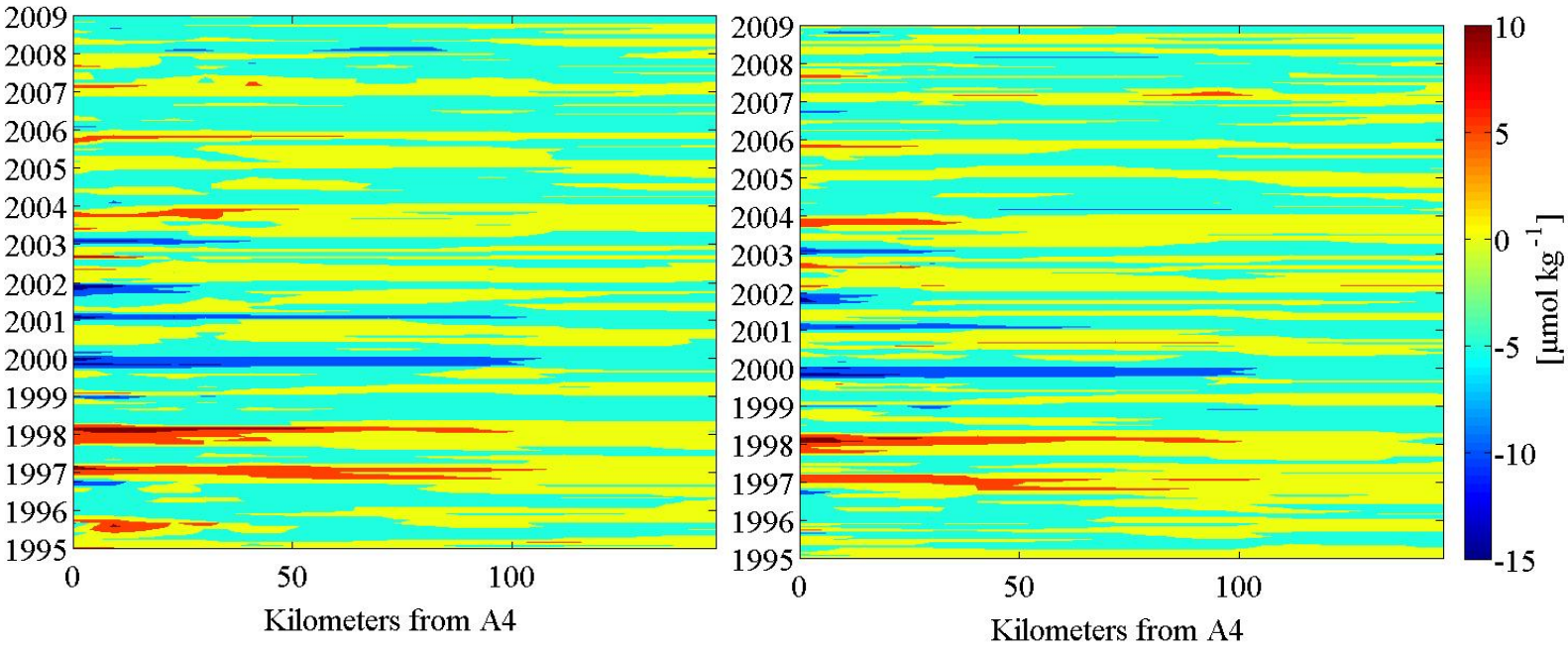


Figure13: Surface (left) and bottom (right) water $NO_x$ anomalies from the 9 LIS stations between 1995 and 2009. Estimate of interannual trends and respective confidence intervals are given in Table 5.

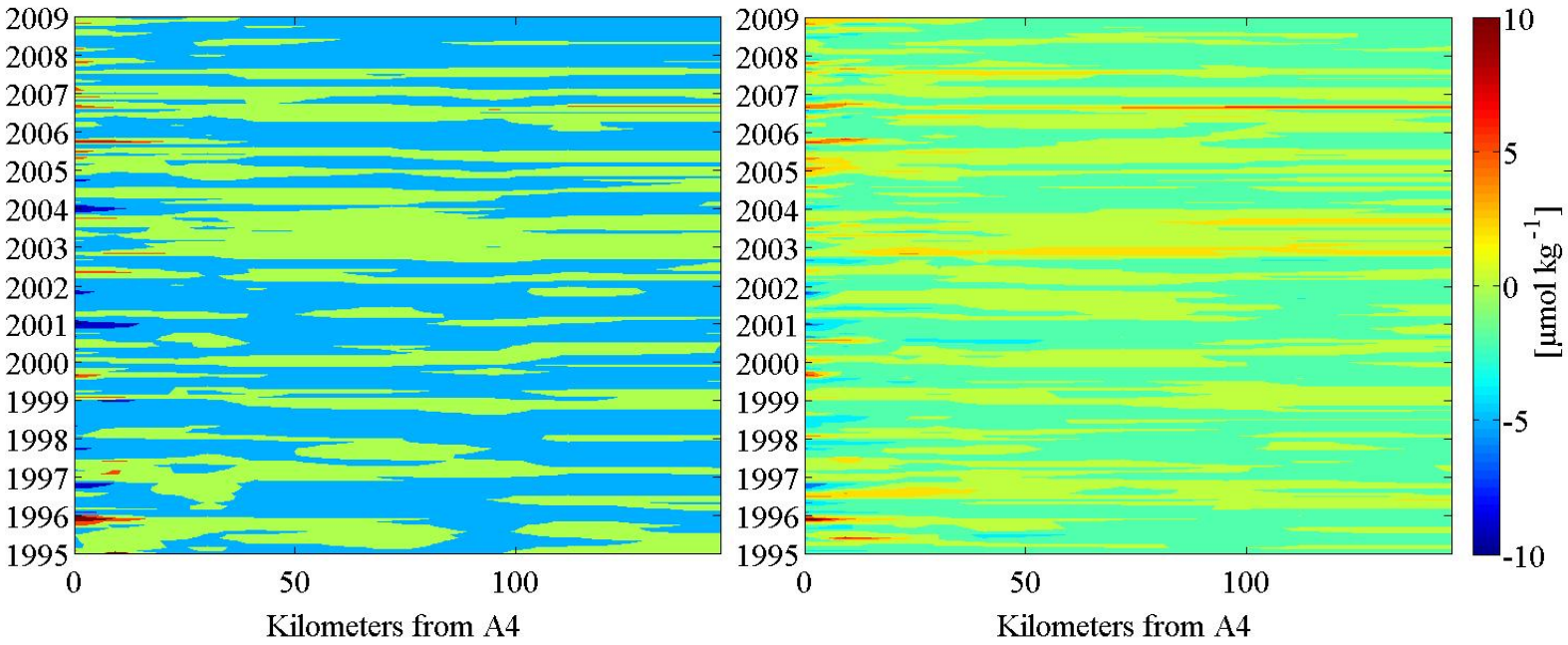


Figure 14: Surface (left) and bottom (right) water $NH_4^+$ anomalies from the 9 LIS stations between 1995 and 2009. Estimate of interannual trends and respective confidence intervals are given in Table 5.

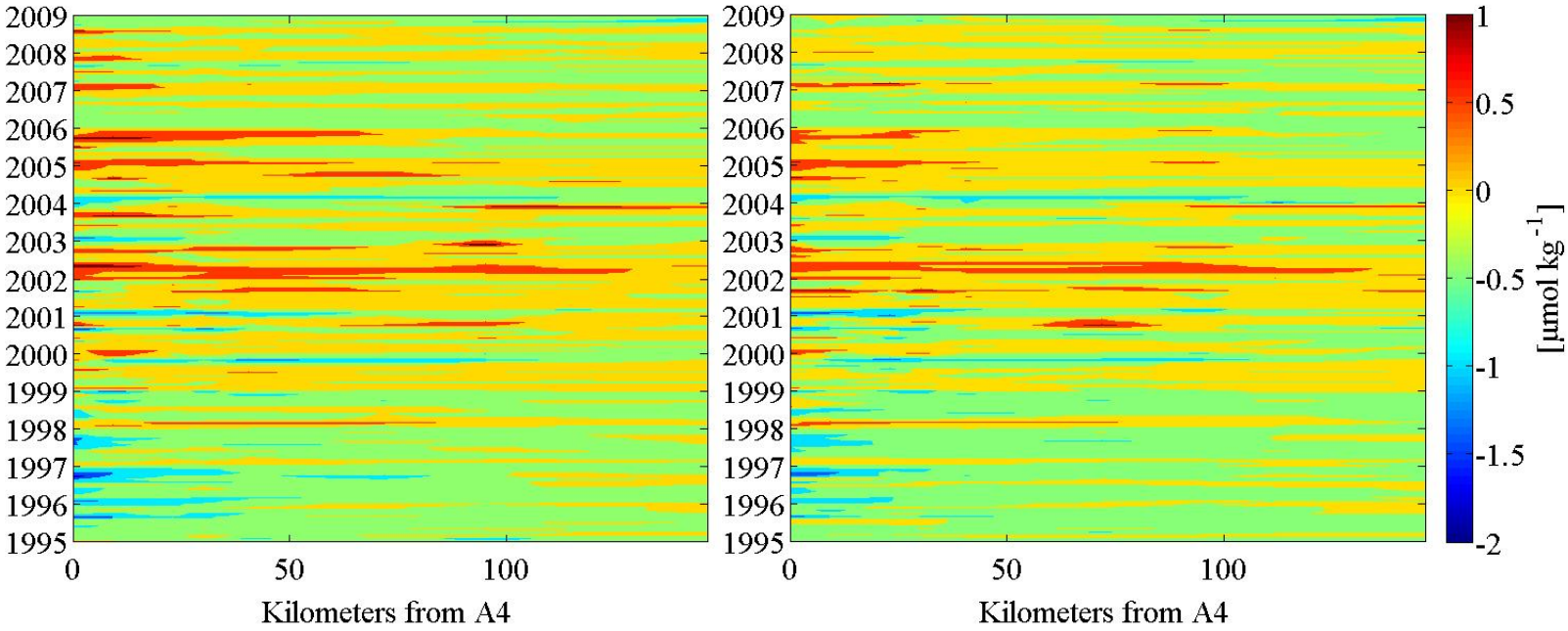


Figure 15: Surface (left) and bottom (right) water DIP anomalies from the 9 LIS stations between 1995 and 2009. Estimate of interannual trends and respective confidence intervals are given in Table 5.

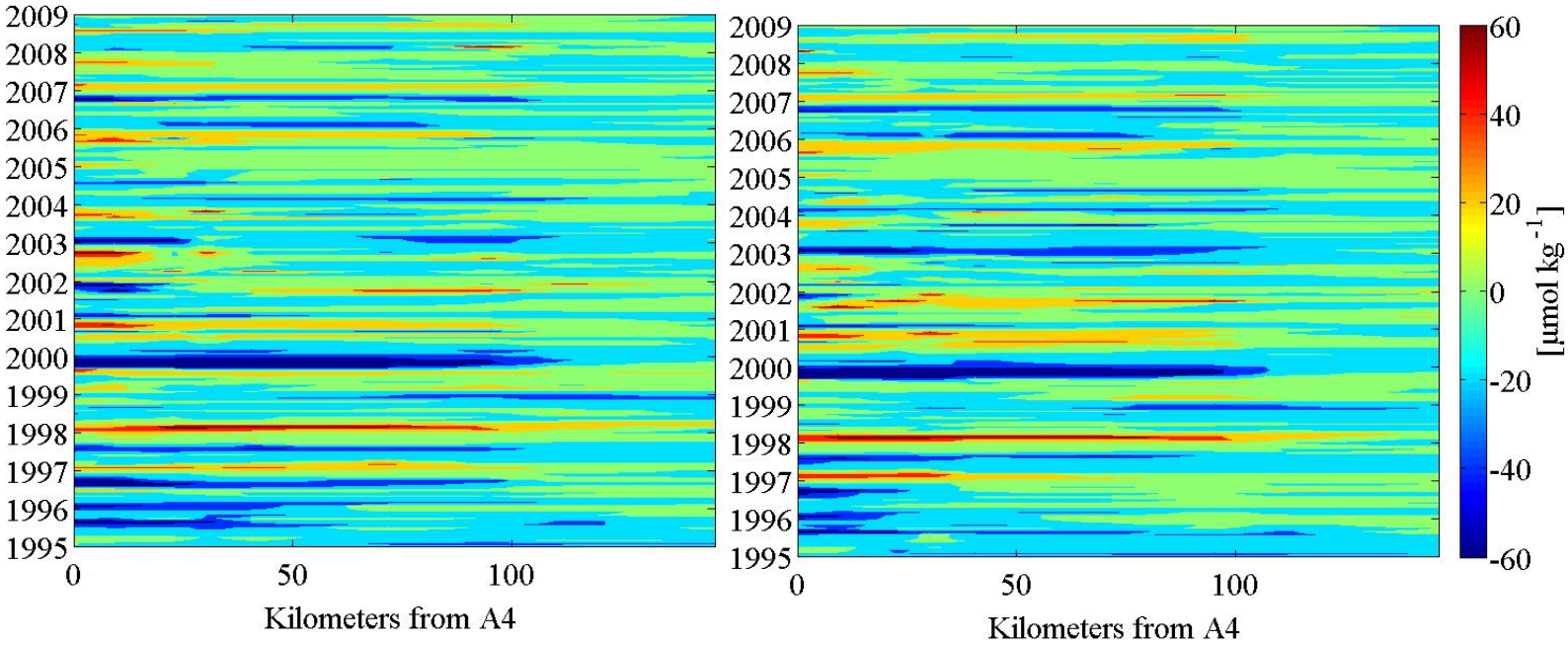


Figure 16: Surface (left) and bottom (right) water DSi anomalies from the 9 LIS stations between 1995 and 2009. Estimate of interannual trends and respective confidence intervals are given in Table 5.

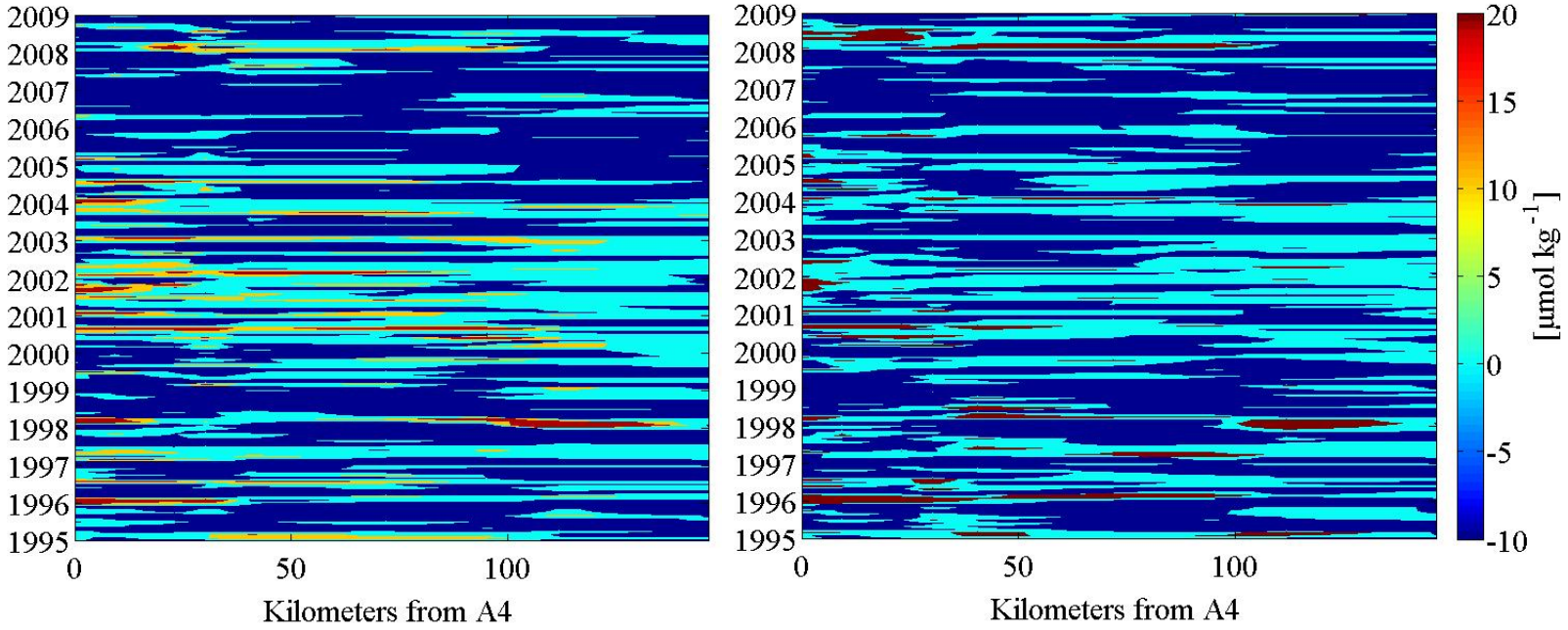


Figure 17: Surface (left) and bottom (right) water BioSi anomalies from the 9 LIS stations between 1995 and 2009. Estimate of interannual trends and respective confidence intervals are given in Table 6.

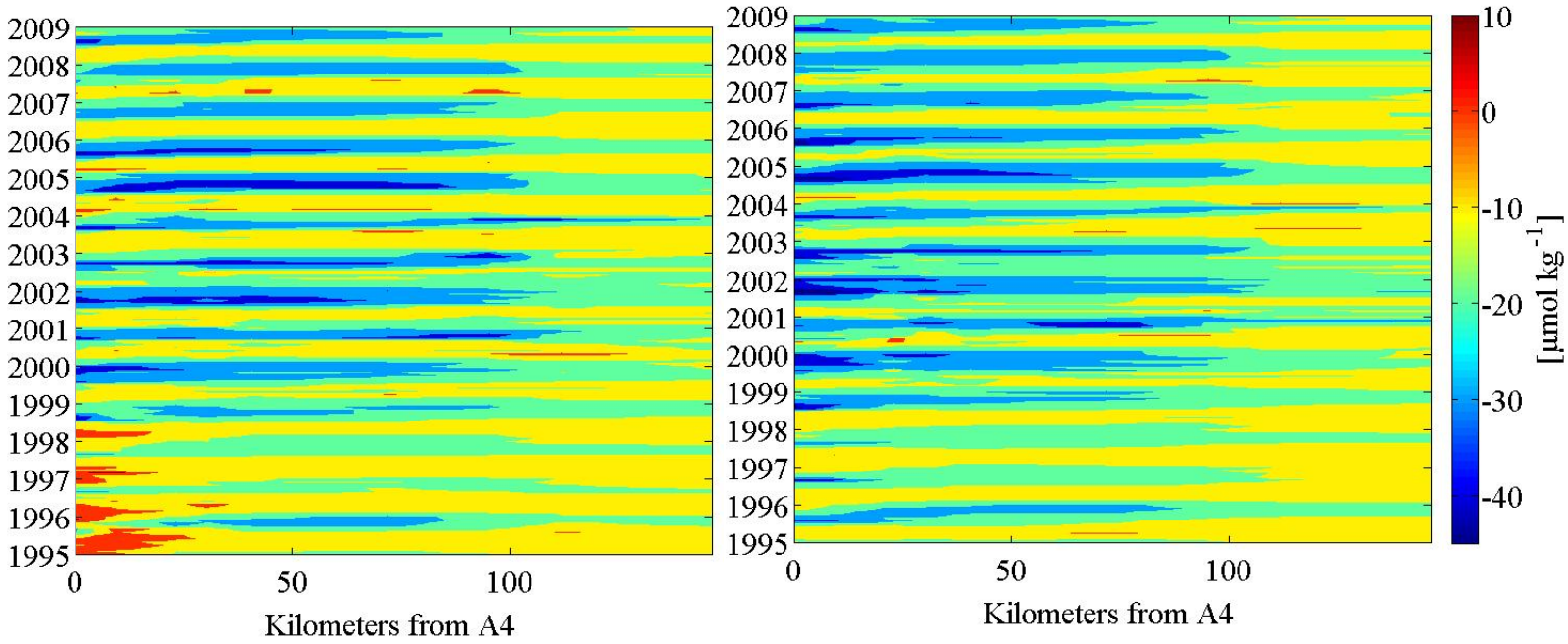


Figure 18: The DINxs parameter from surface (left) and bottom (right) water from the 9 LIS stations between 1995 and 2009. Estimate of interannual trends and respective confidence intervals are given in Table 5.

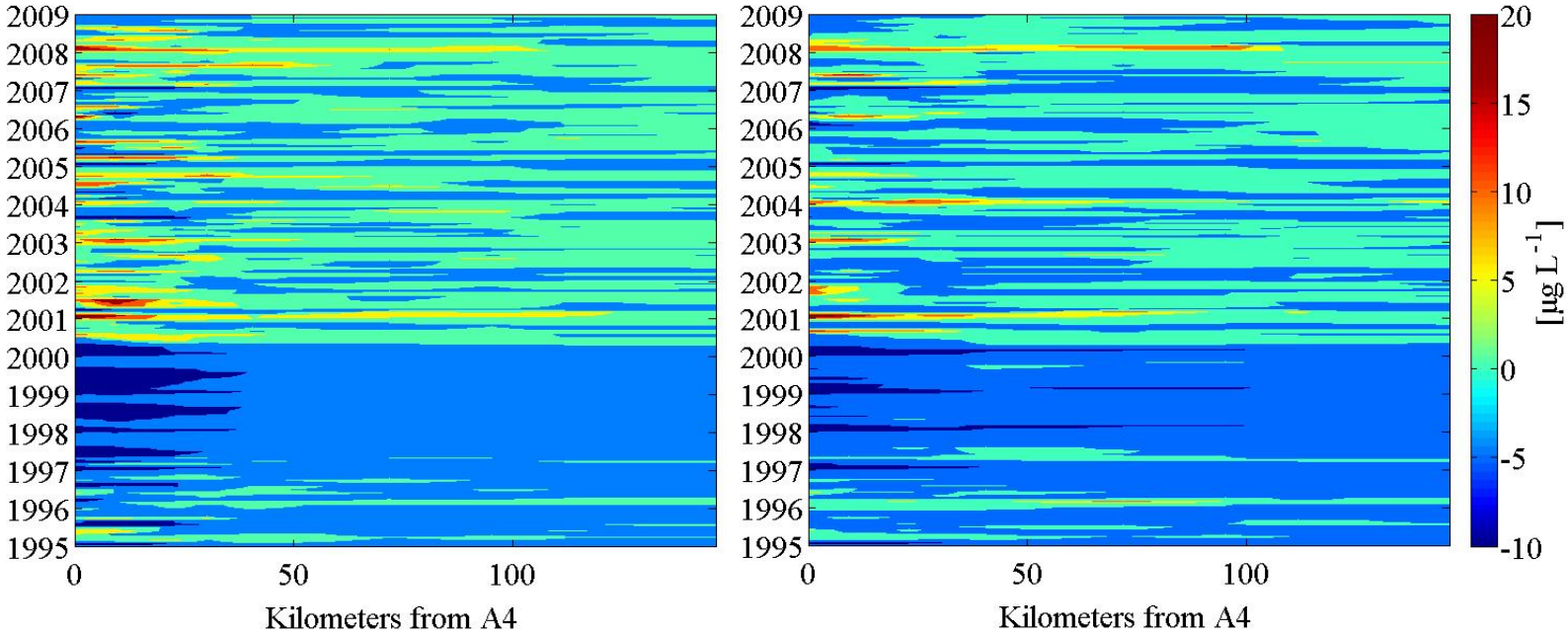


Figure 19: Surface (left) and bottom (right) water Chl*a* anomalies from the 9 LIS stations between 1995 and 2009. Estimate of interannual trends and respective confidence intervals are given in Table 6.

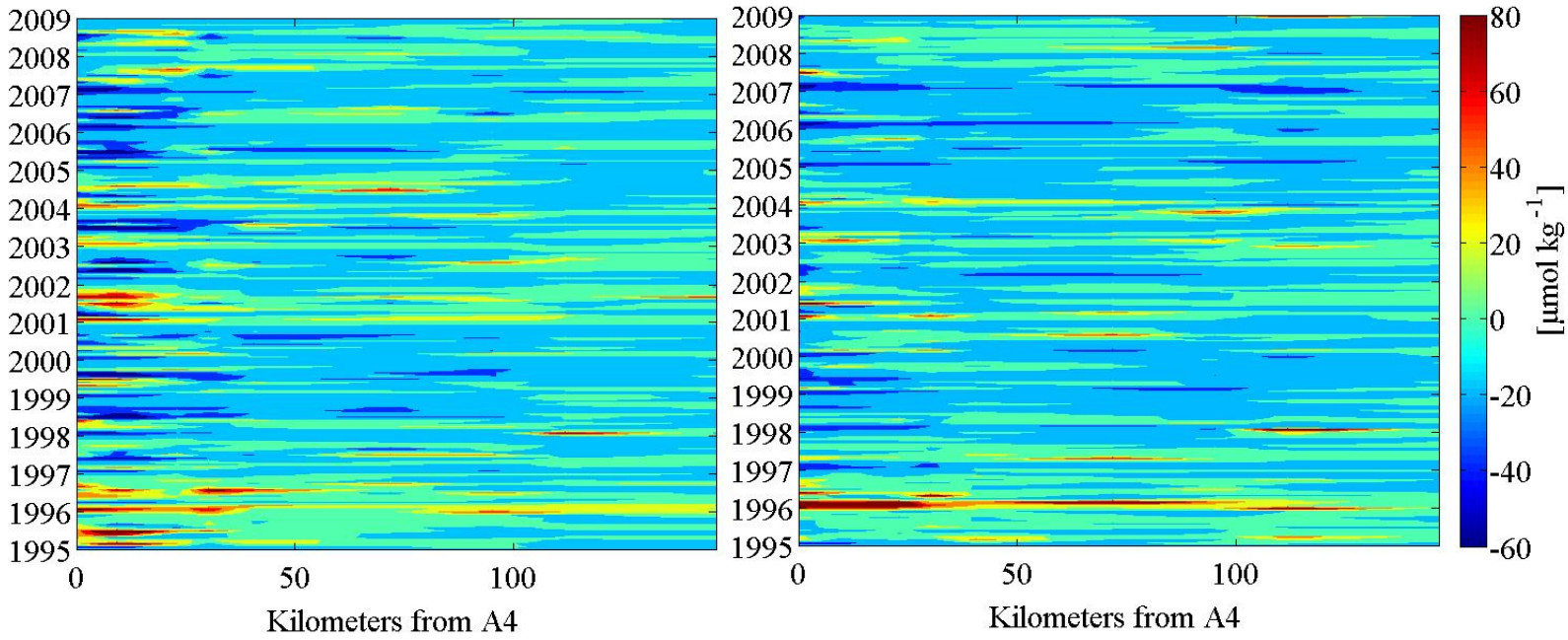


Figure 20: Surface (left) and bottom (right) water PC anomalies from the 9 LIS stations between 1995 and 2009. Estimate of interannual trends and respective confidence intervals are given in Table 6.

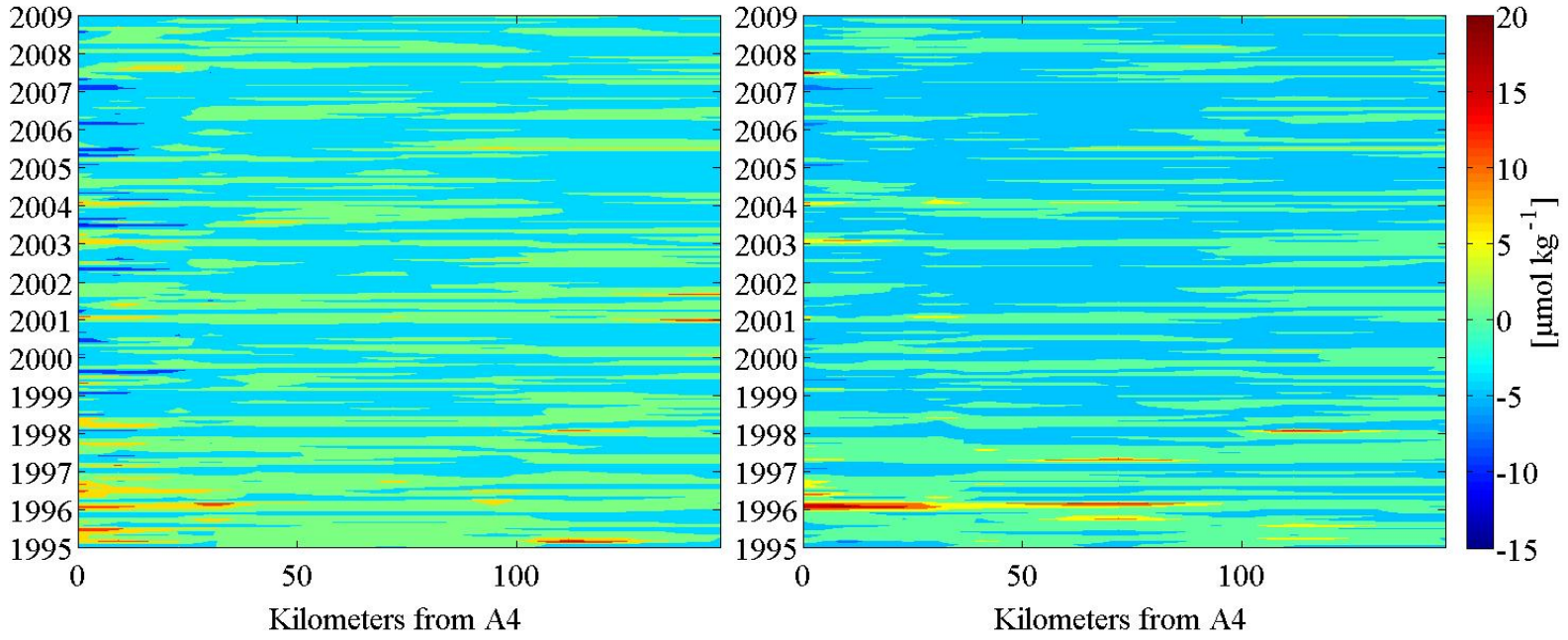


Figure 21: Surface (left) and bottom (right) water PN anomalies from the 9 LIS stations between 1995 and 2009. Estimate of interannual trends and respective confidence intervals are given in Table 6.

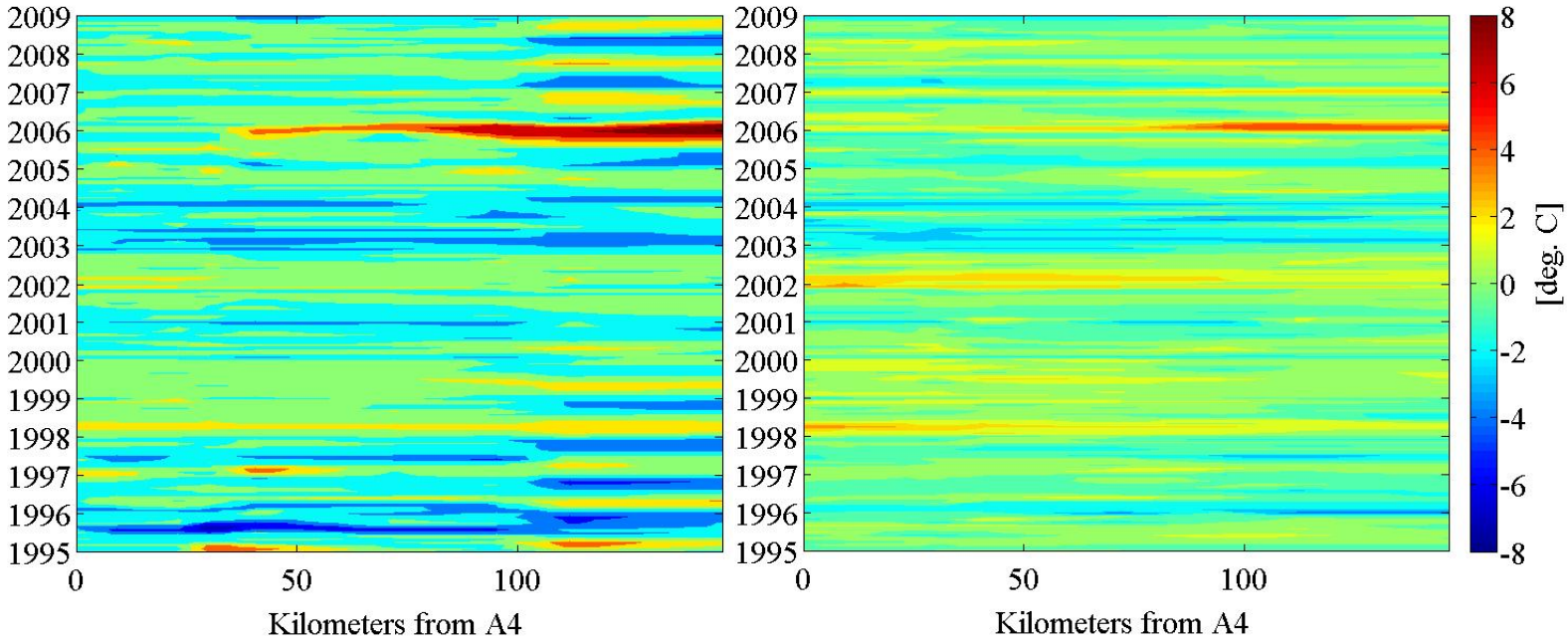


Figure 22: Surface (left) and bottom (right) water temperature anomalies from the 9 LIS stations between 1995 and 2009. Estimate of interannual trends and respective confidence intervals are given in Table 8.

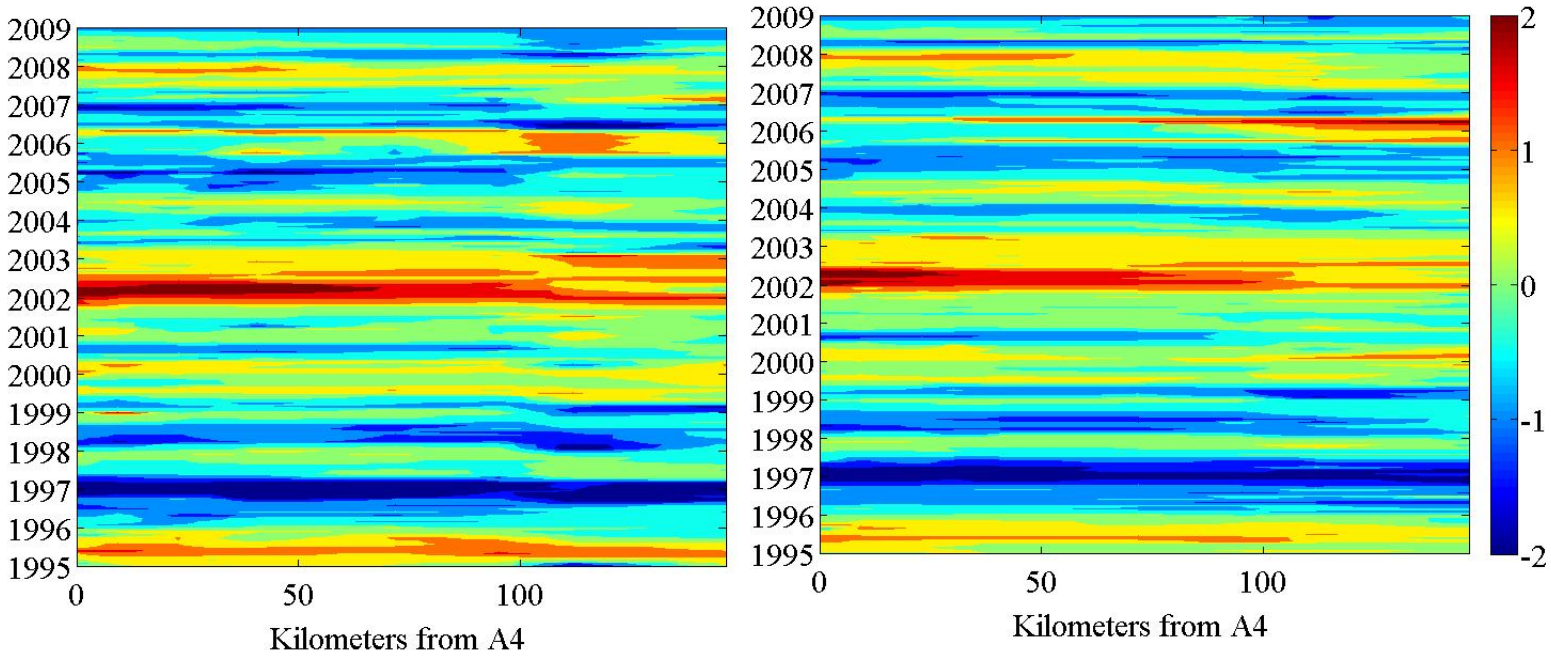


Figure 23: Surface (left) and bottom (right) water salinity anomalies from the 9 LIS stations between 1995 and 2009. Estimate of inerannual trends and respective confidence intervals are given in Table 8.

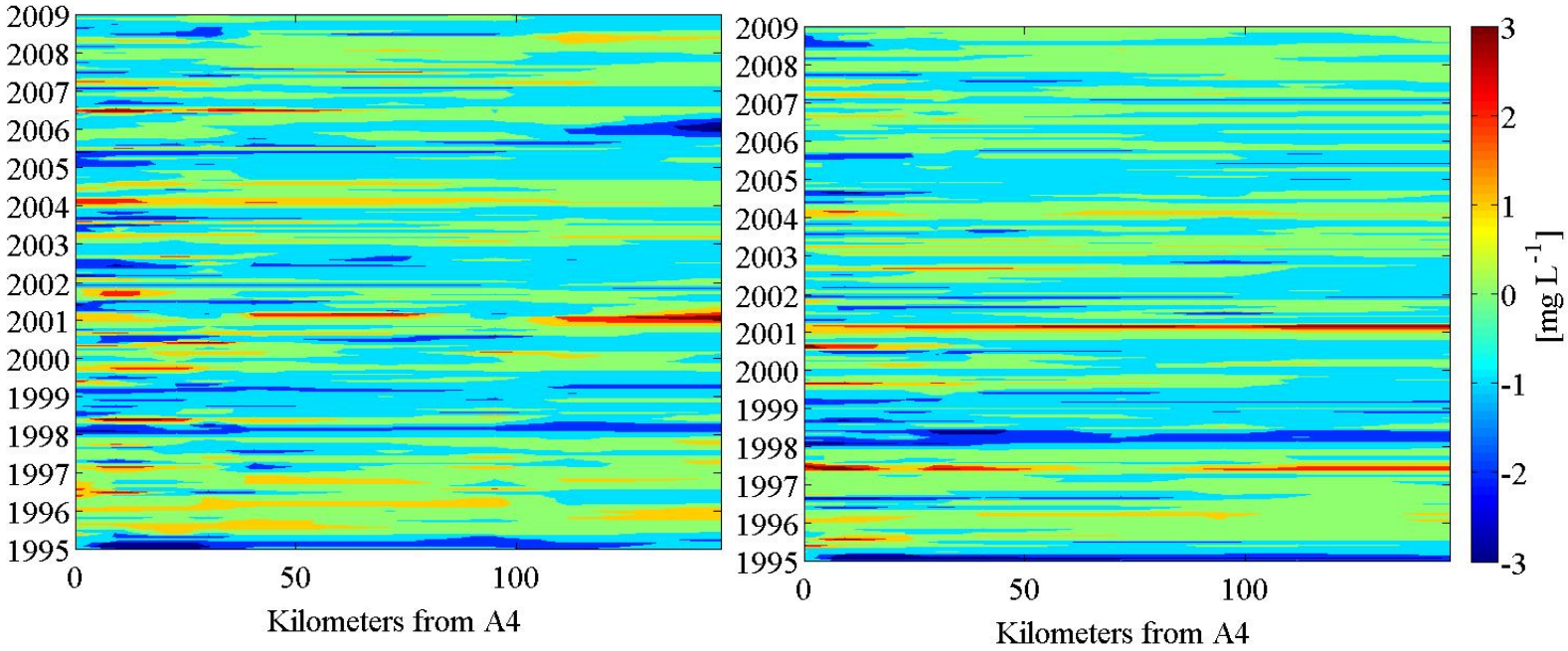


Figure 24: Surface (left) and bottom (right) water DO anomalies from the 9 LIS stations between 1995 and 2009. Estimate of interannual trends and respective confidence intervals are given in Table 8.

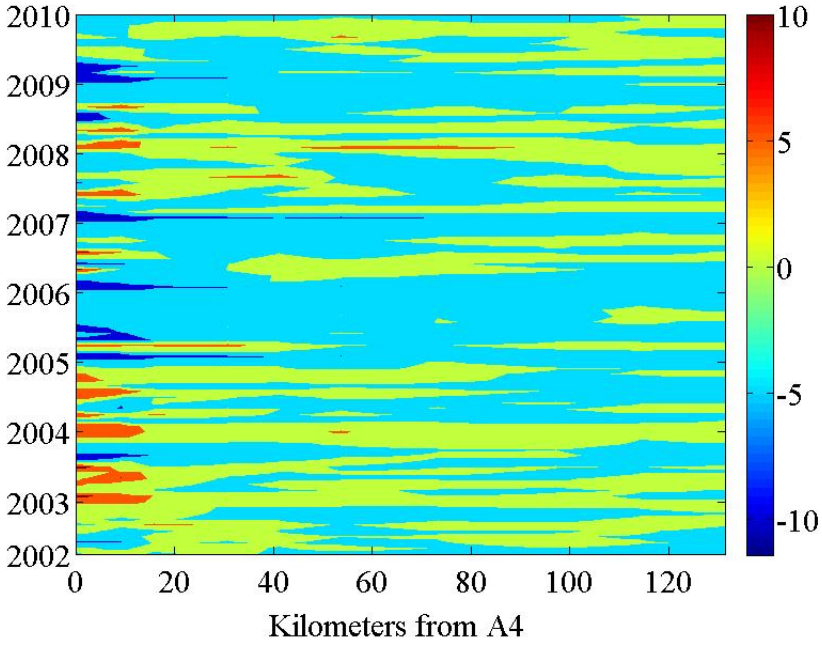


Figure 25: Anomalies of diatom Chl*a* at 10 axial stations in surface water. Trends were calculated using the TS estimator and are given in Table 9.

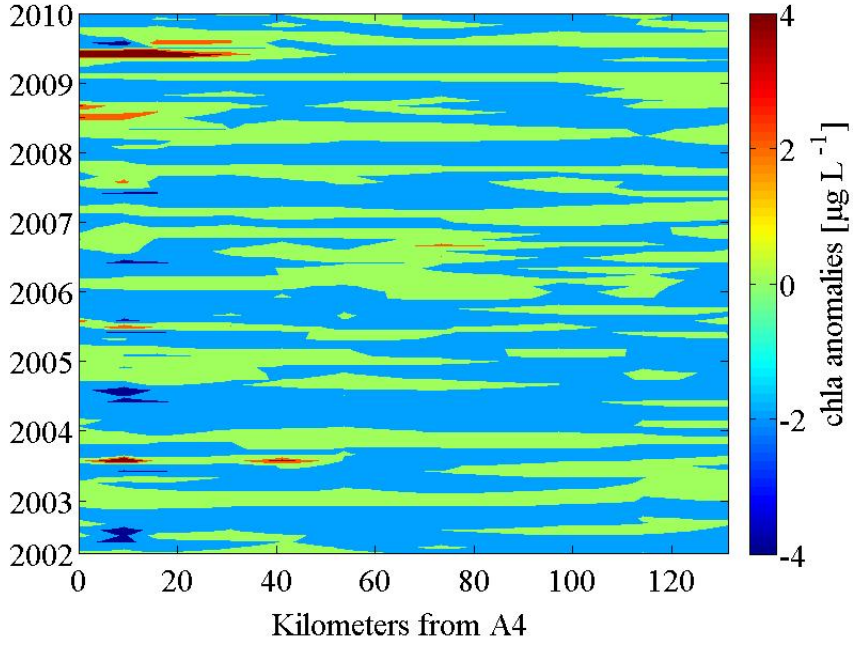


Figure 26: Anomalies of dinoflagellate Chl*a* at 10 axial stations in surface water. Trends were calculated using the TS estimator and are given in Table 9.

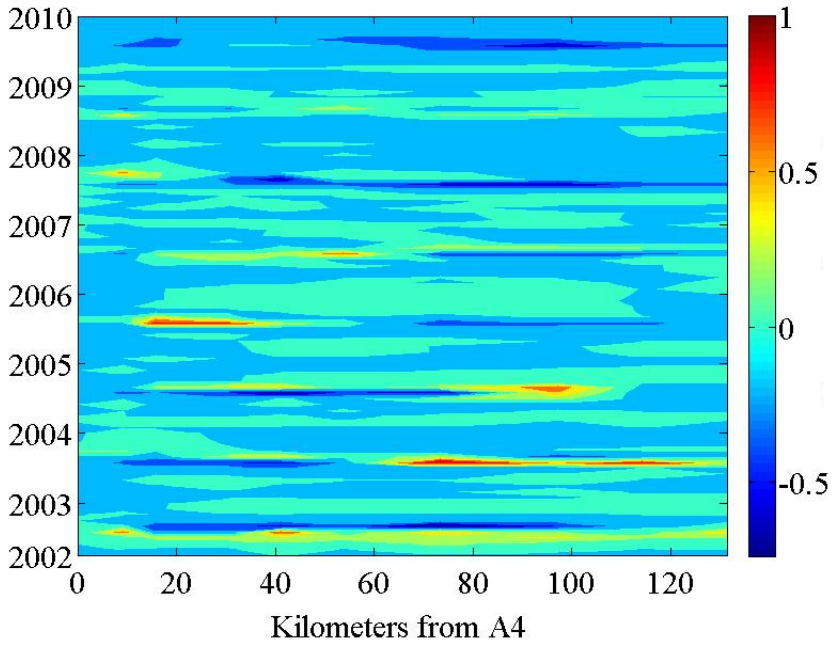


Figure 27: Anomalies of cyanobacteria Chl*a* at 10 axial stations in surface water. Trends were calculated using the TS estimator and are given in Table 9.

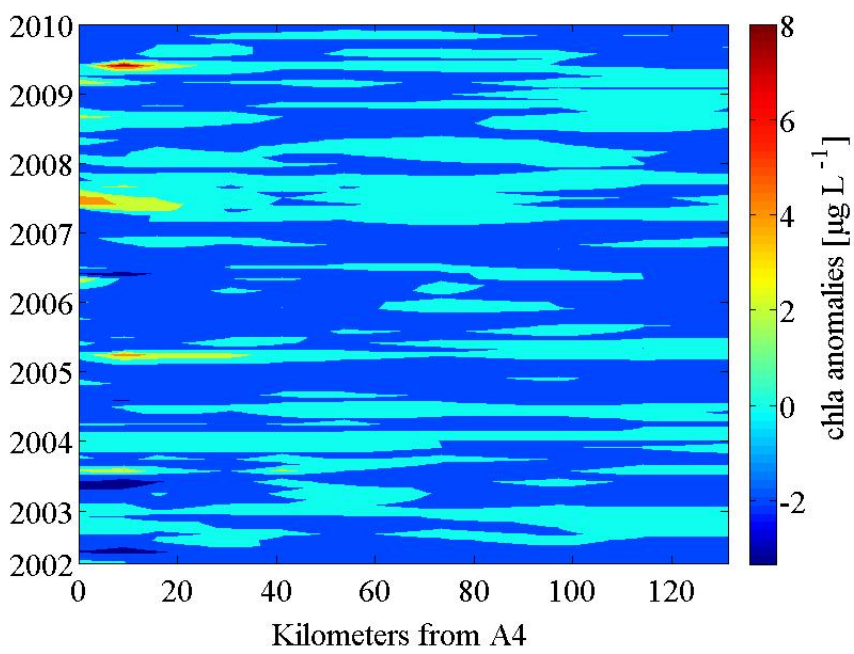


Figure 28: Anomalies of Prynmesiophyseae A Chl*a* at 10 axial stations in surface water. Trends were calculated using the TS estimator and are given in Table 9.

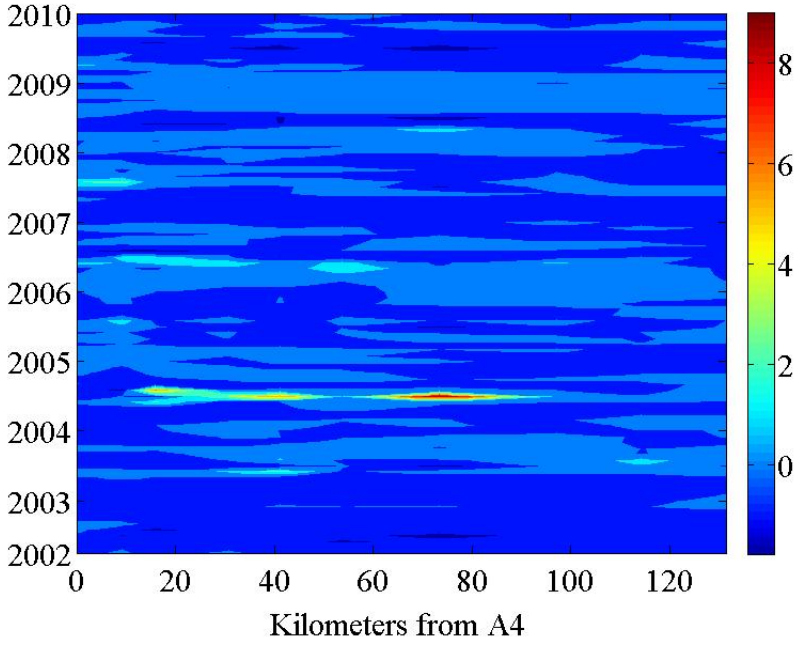


Figure 29: Anomalies of Cryptophyceae Chl*a* at 10 axial stations in surface water. Trends were calculated using the TS estimator and are given in Table 9.

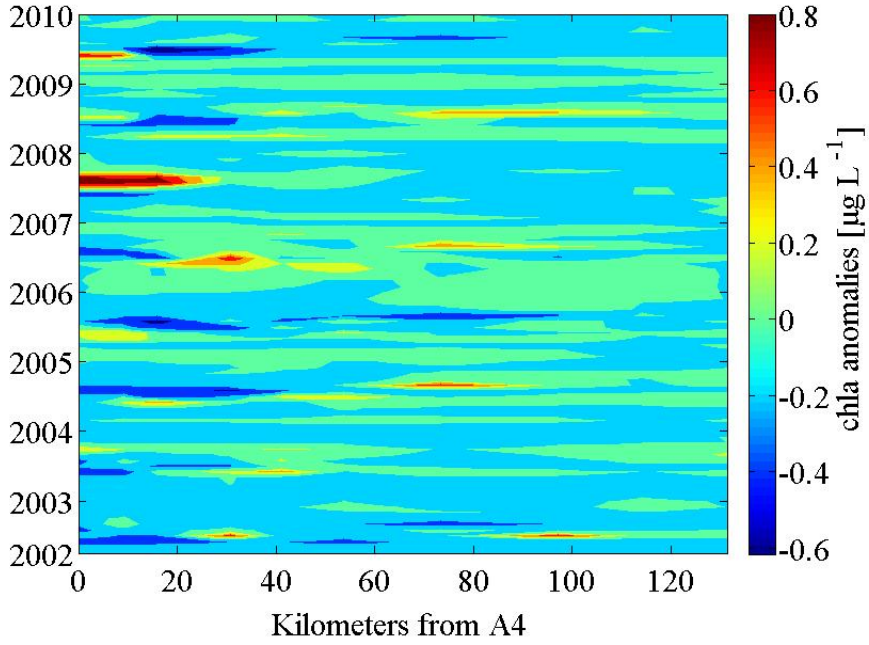


Figure 30: Anomalies of Raphidophyceae Chl*a* at 10 axial stations in surface water. Trends were calculated using the TS estimator and are given in Table 9.

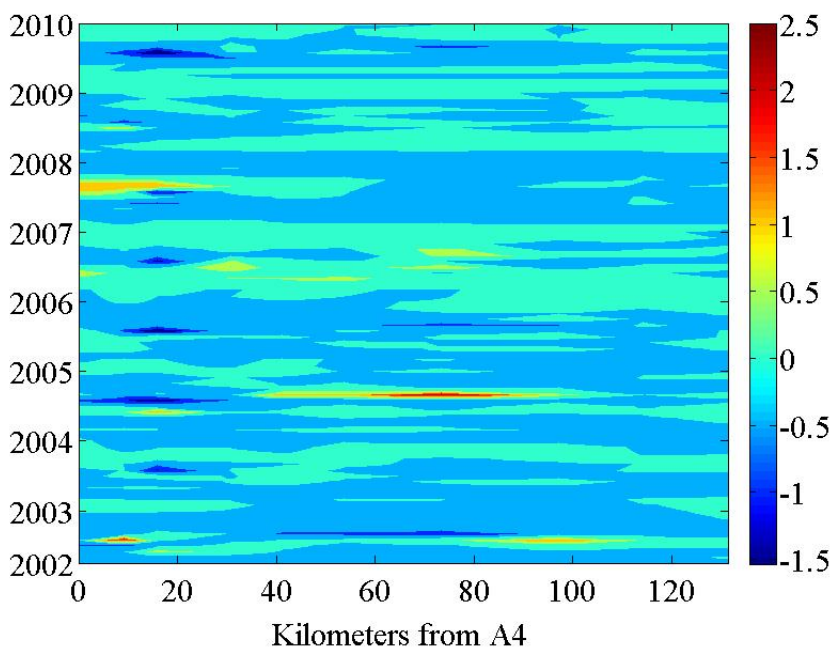


Figure 31: Anomalies of Euglenophyceae Chl*a* at 10 axial stations in surface water. Trends were calculated using the TS estimator and are given in Table 9.

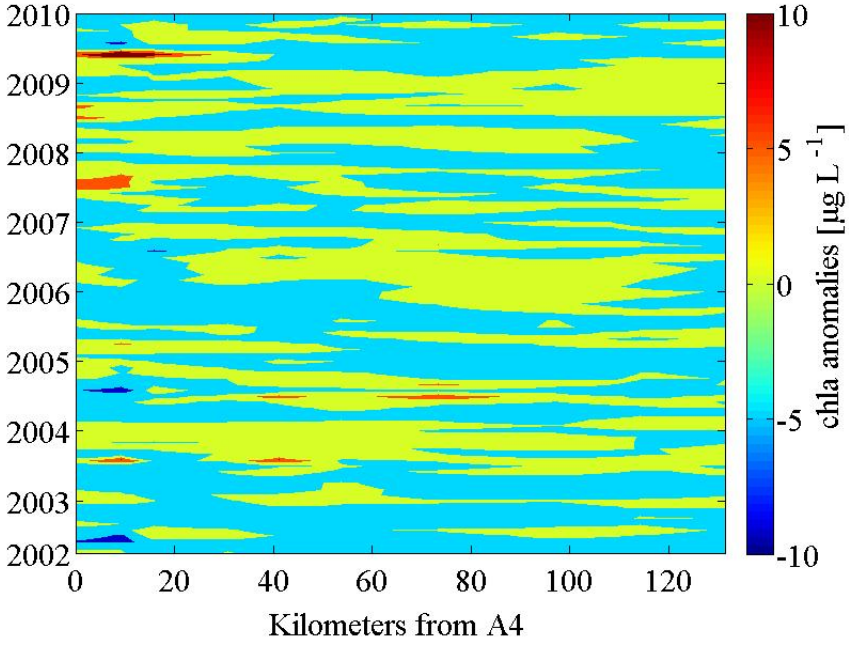


Figure 32: Anomalies of non-diatom Chl*a* at 10 axial stations in surface water. Trends were calculated using the TS estimator and are given in Table 9.

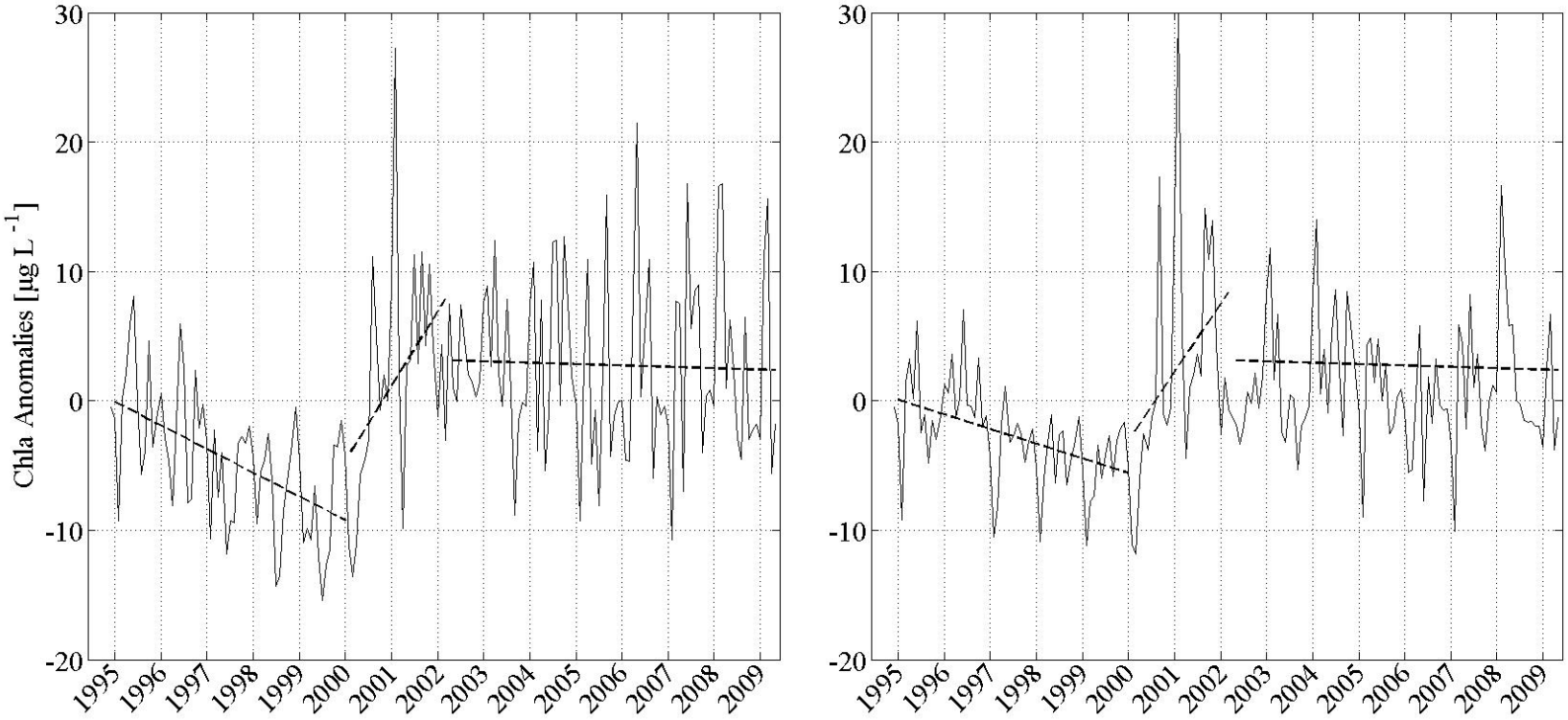


Figure 33: Trends in Chl*a* anomalies in the surface (left) and bottom (right) during the three phases defined in the text. During the first phase, Chl*a* significantly decreased (surface: -1.78 µg $L^{-1}$ $yr^{-1}$, CI = -2.06, -1.54; bottom: -1.11 µg $L^{-1}$ $yr^{-1}$, CI = -1.27, -0.95). During the second phase, Chl*a* significantly increased (surface: 5.81µg $L^{-1}$ $yr^{-1}$, CI = 4.22, 7.56; bottom: 5.23 µg $L^{-1}$ $yr^{-1}$, CI = 3.98, 6.93). During the third phase, Chl*a* significantly decreased (surface: -0.30 µg $L^{-1}$ $yr^{-1}$, CI = -0.43, -0.19; bottom: -0.12 µg $L^{-1}$ $yr^{-1}$, CI = -0.23, -0.03).

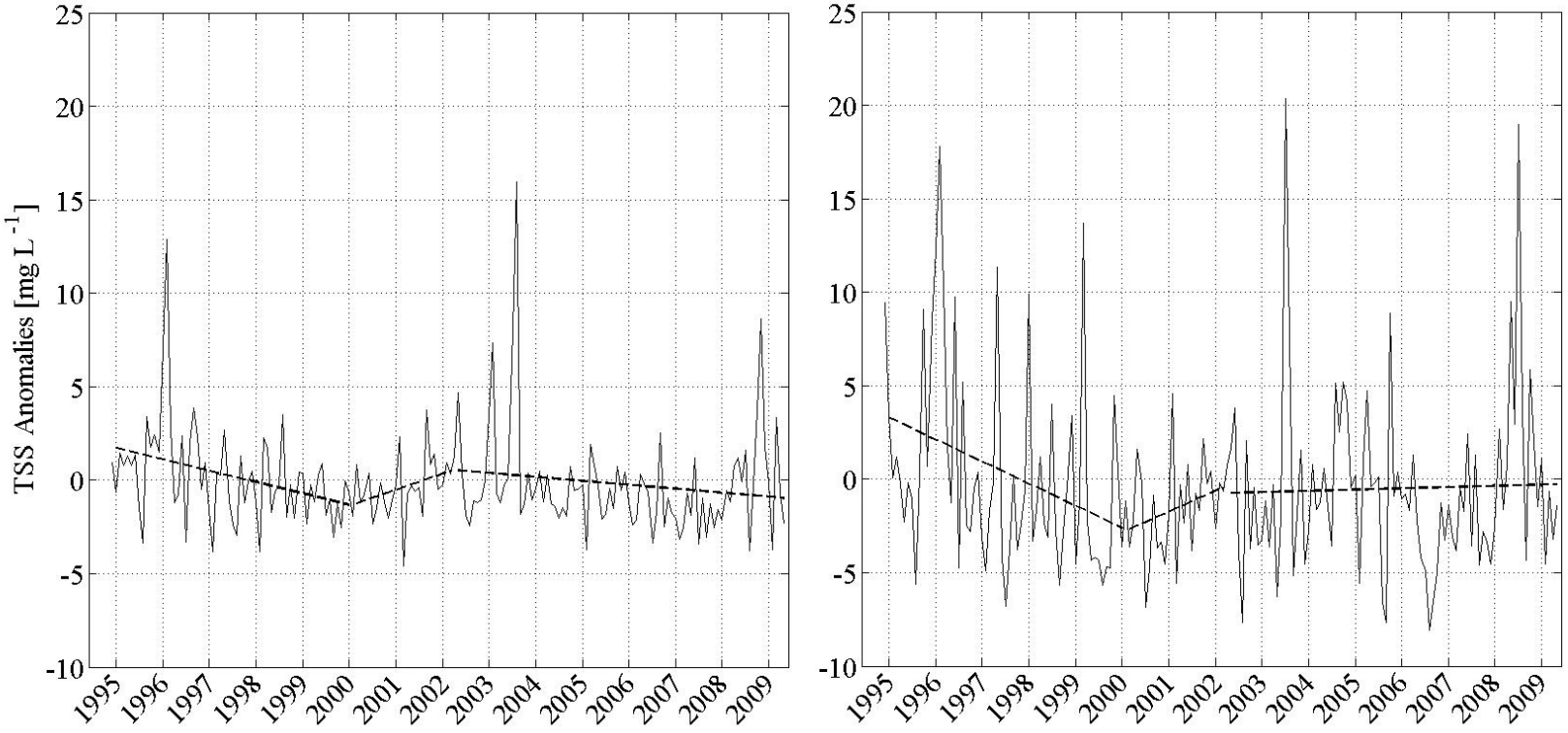


Figure 34: Trends in TSS anomalies in the surface (left) and bottom (right) during the three phases defined in the text. During the first phase, TSS significantly decreased (surface: -0.52 mg $L^{-1}$ $yr^{-1}$, CI = -0.60, -0.41; bottom: -1.02 mg $L^{-1}$ $yr^{-1}$, CI = -1.18, -0.88). During the second phase, TSS significantly increased (surface: 0.88 mg $L^{-1}$ $yr^{-1}$, CI = 0.59, 1.09; bottom: 1.12 mg $L^{-1}$ $yr^{-1}$, CI = 0.49, 1.98). During the third phase, TSS significantly decreased in surface water (-0.14 mg $L^{-1}$ $yr^{-1}$, CI = -0.18, -0.09). However, there was no significant trend in TSS in bottom water during the third phase.

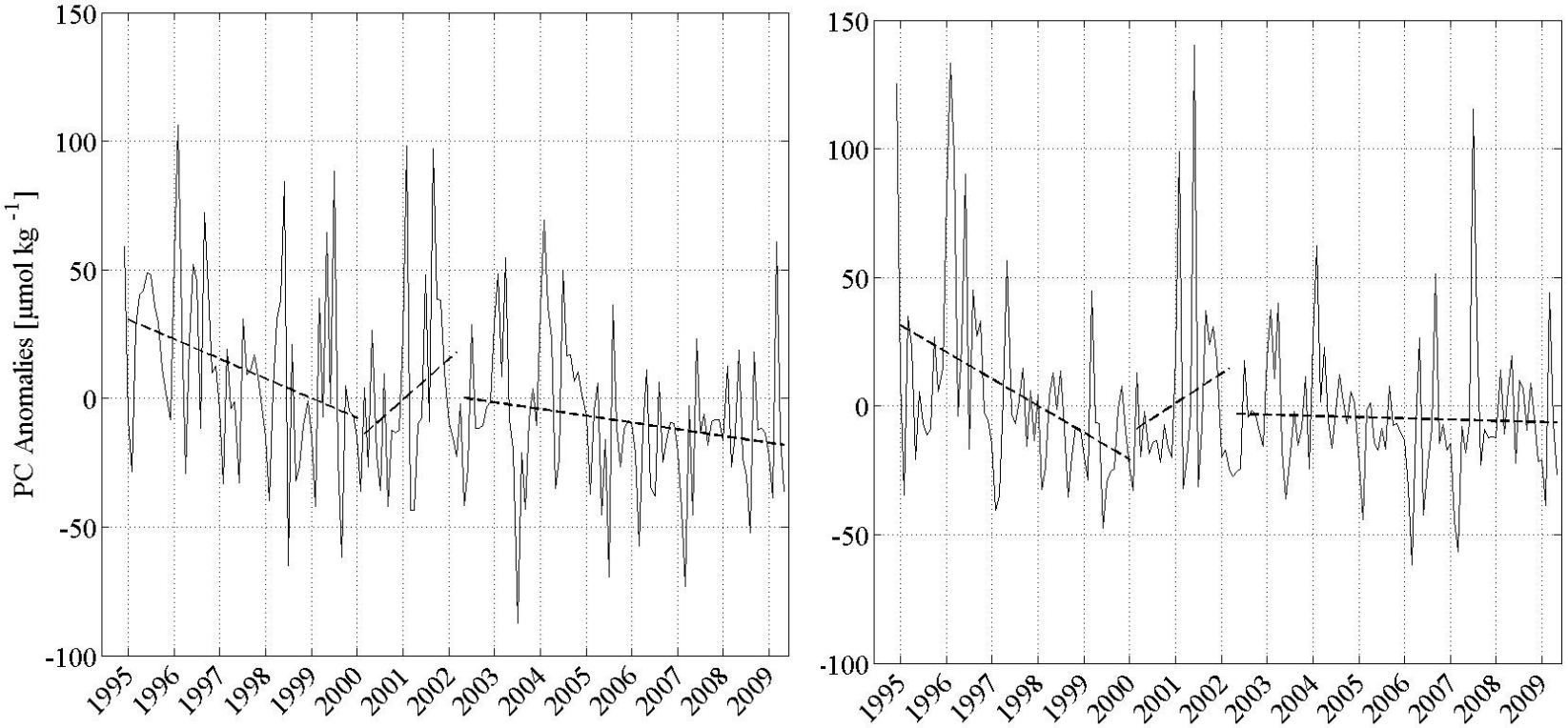


Figure 35: Trends in PC anomalies in the surface (left) and bottom (right) during the three phases defined in the text. During the first phase, PC significantly decreased (surface: -9.17 µmol $kg^{-1}$ $yr^{-1}$, CI = -10.51, -7.49; bottom: -7.48 µmol $kg^{-1}$ $yr^{-1}$, CI = -8.54, -6.08). During the second phase, PC significantly increased (surface: 11.2 µmol $kg^{-1}$ $yr^{-1}$, CI = 3.73, 19.5; bottom: 5.77 µmol $kg^{-1}$ $yr^{-1}$, CI = -0.55, 11.1). During the third phase, PC significantly decreased (surface: -2.64 µmol $kg^{-1}$ $yr^{-1}$, CI = -3.34, -1.95; bottom: -0.87 µmol $kg^{-1}$ $yr^{-1}$, CI = -1.32, -0.33).

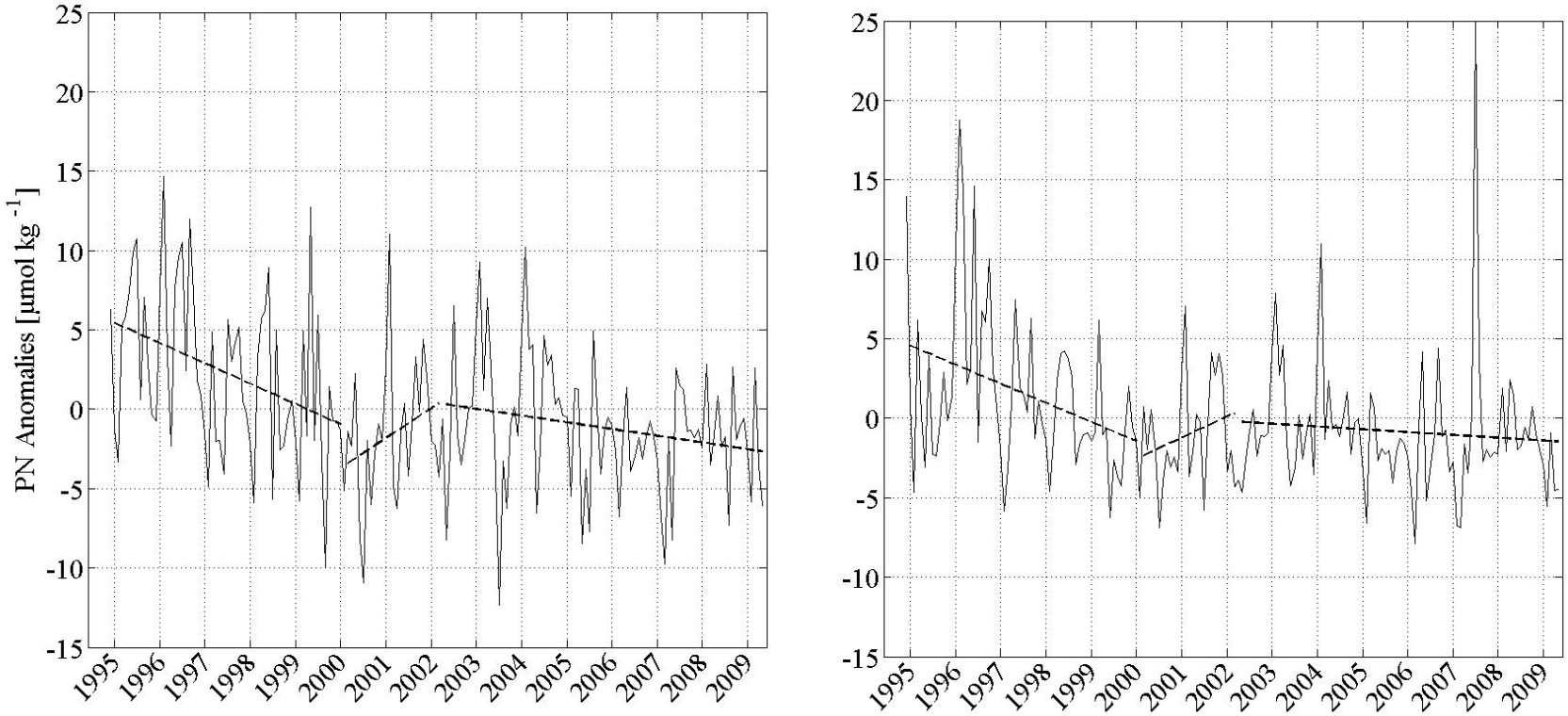


Figure 36: Trends in PN anomalies in the surface (left) and bottom (right) during the three phases defined in the text. During the first phase, PN significantly decreased (surface: -1.31 µmol $kg^{-1}$ $yr^{-1}$, CI = -1.53, -1.00; bottom: -0.89 µmol $kg^{-1}$ $yr^{-1}$, CI = -1.13, -0.71). During the second phase, PN significantly increased (surface: 1.98 µmol $kg^{-1}$ $yr^{-1}$, CI = 0.67, 2.81; bottom: 1.26 µmol $kg^{-1}$ $yr^{-1}$, CI = 0.002, 2.08). During the third phase, PN significantly decreased (surface: -0.39 µmol $kg^{-1}$ $yr^{-1}$, CI = -0.48, -0.30; bottom: -0.18 µmol $kg^{-1}$ $yr^{-1}$, CI = -0.24, -0.13).

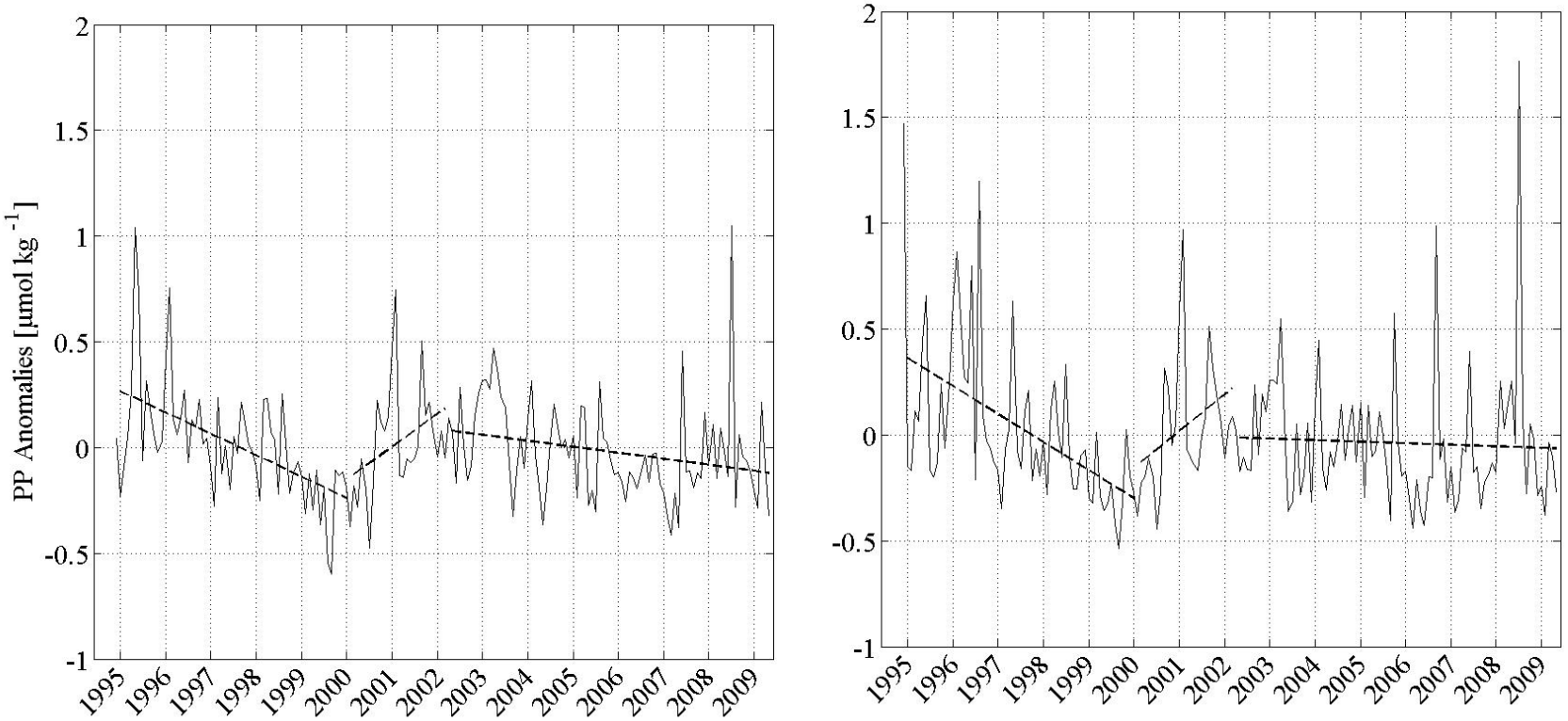


Figure 37: Trends in PP anomalies in the surface (left) and bottom (right) during the three phases defined in the text. During the first phase, PP significantly decreased (surface: -0.08 µmol $kg^{-1}$ $yr^{-1}$, CI = -0.09, -0.07; bottom: -0.10 µmol $kg^{-1}$ $yr^{-1}$, CI = -0.12, -0.09). During the second phase, PP significantly increased (surface: 0.16 µmol $kg^{-1}$ $yr^{-1}$, CI = 0.10, 0.21; bottom: 0.17 µmol $kg^{-1}$ $yr^{-1}$, CI = 0.13, 0.22). During the third phase, PP significantly decreased (surface: -0.04 µmol $kg^{-1}$ $yr^{-1}$, CI = -0.04, -0.03; bottom: -0.02 µmol $kg^{-1}$ $yr^{-1}$, CI = -0.02, -0.01).

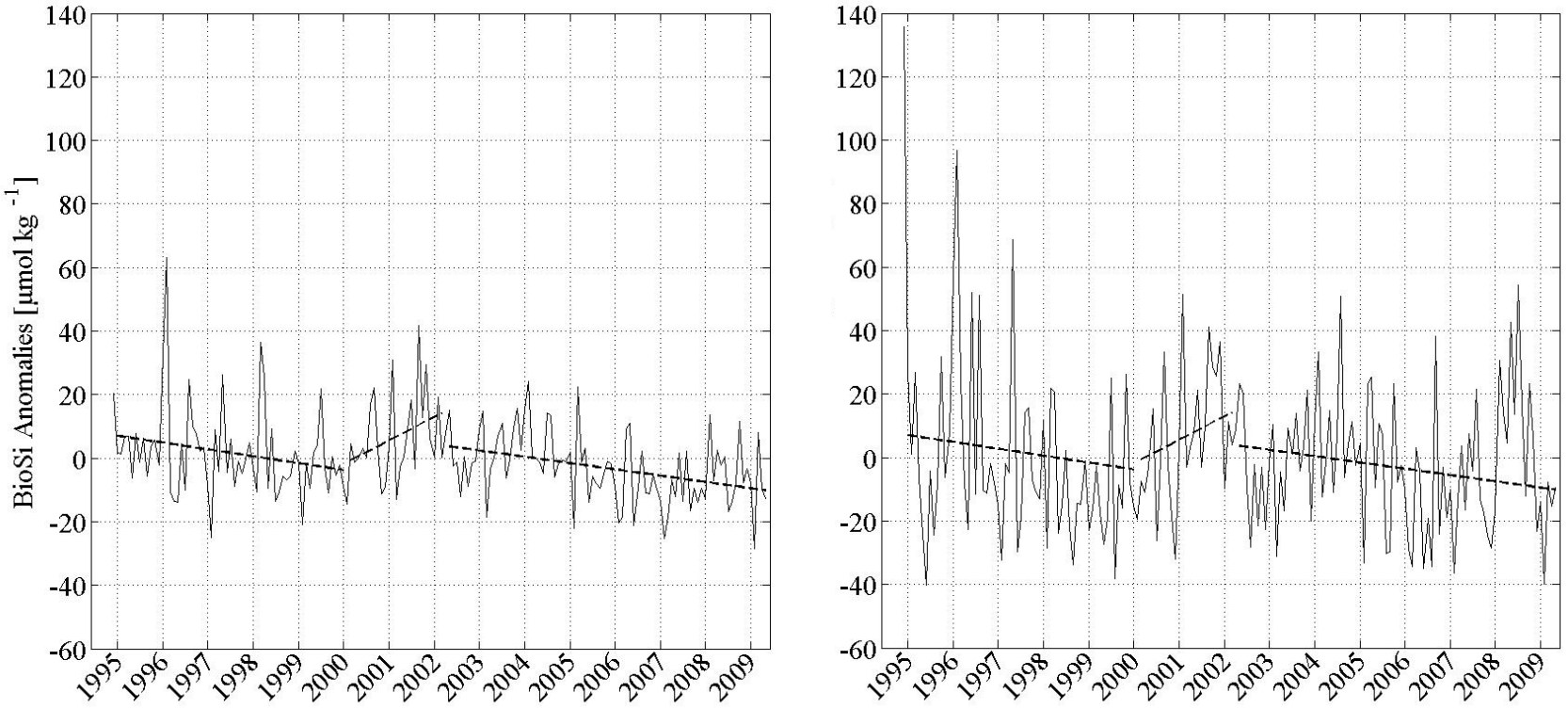


Figure 38: Trends in BioSi anomalies in the surface (left) and bottom (right) during the three phases defined in the text. During the first phase, BioSi significantly decreased (surface: -1.78 µmol $kg^{-1}$ $yr^{-1}$, CI = -2.27, -1.40; bottom: -4.07 µmol $kg^{-1}$ $yr^{-1}$, CI = -5.03, -3.04). During the second phase, BioSi significantly increased (surface: 7.26 µmol $kg^{-1}$ $yr^{-1}$, CI = 3.17, 9.92; bottom: 14.7 µmol $kg^{-1}$ $yr^{-1}$, CI = 10.4, 20.8). During the third phase, BioSi significantly decreased (surface: -1.98 µmol $kg^{-1}$ $yr^{-1}$, CI = -2.19, -1.78; bottom: -1.08 µmol $kg^{-1}$ $yr^{-1}$, CI = -1.55, -0.54).

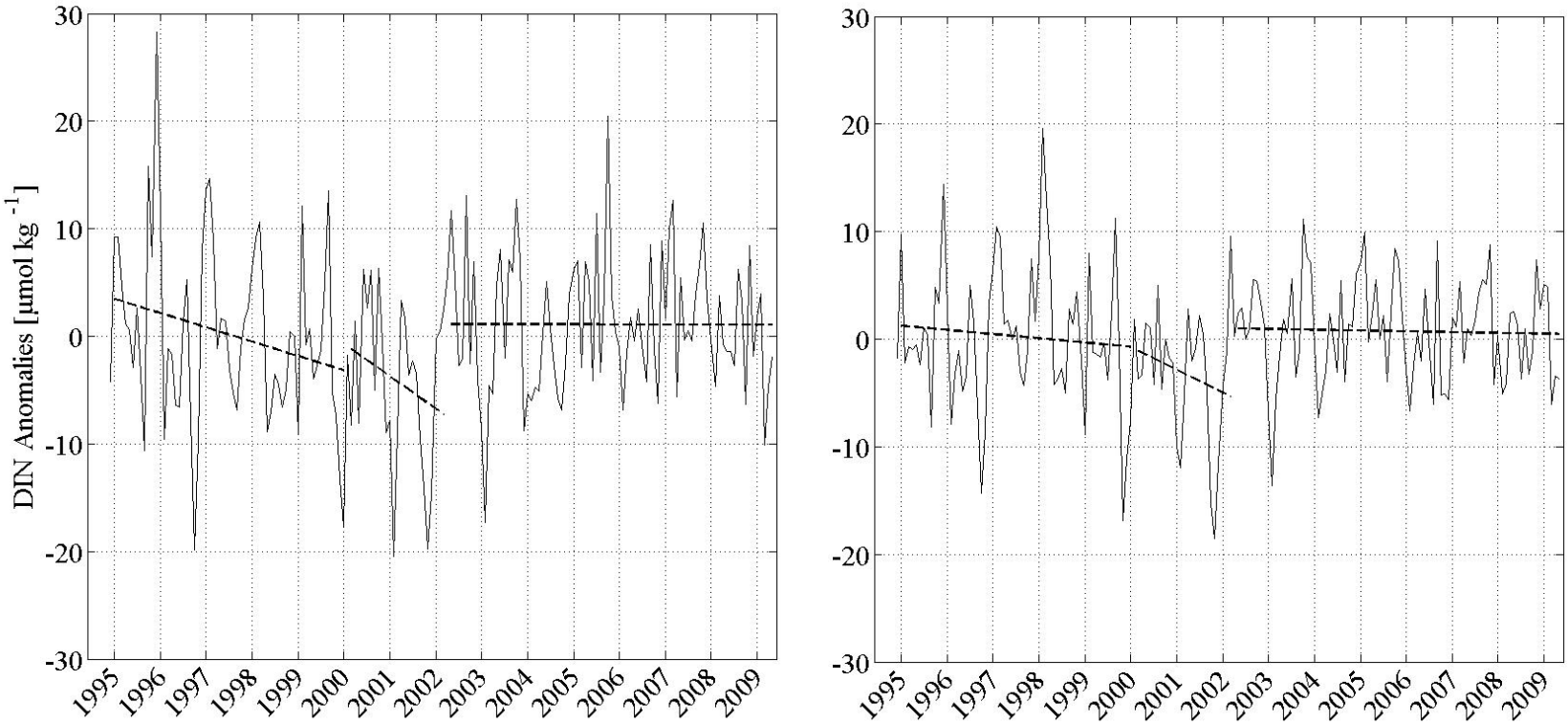


Figure 39: Trends in DIN anomalies in the surface (left) and bottom (right) during the three phases defined in the text. During the first phase, DIN significantly decreased (surface: -1.26 µmol $kg^{-1}$ $yr^{-1}$, CI = -1.70, -0.92; bottom: -0.30 µmol $kg^{-1}$ $yr^{-1}$, CI = -0.67, -0.05). During the second phase, DIN significantly decreased again (surface: -2.81 µmol $kg^{-1}$ $yr^{-1}$, CI = -4.29, -0.81; bottom: -2.02 µmol $kg^{-1}$ $yr^{-1}$, CI = -3.43, -0.80). During the third phase, DIN decreased in surface and bottom waters. However, these changes were not statistically significant.

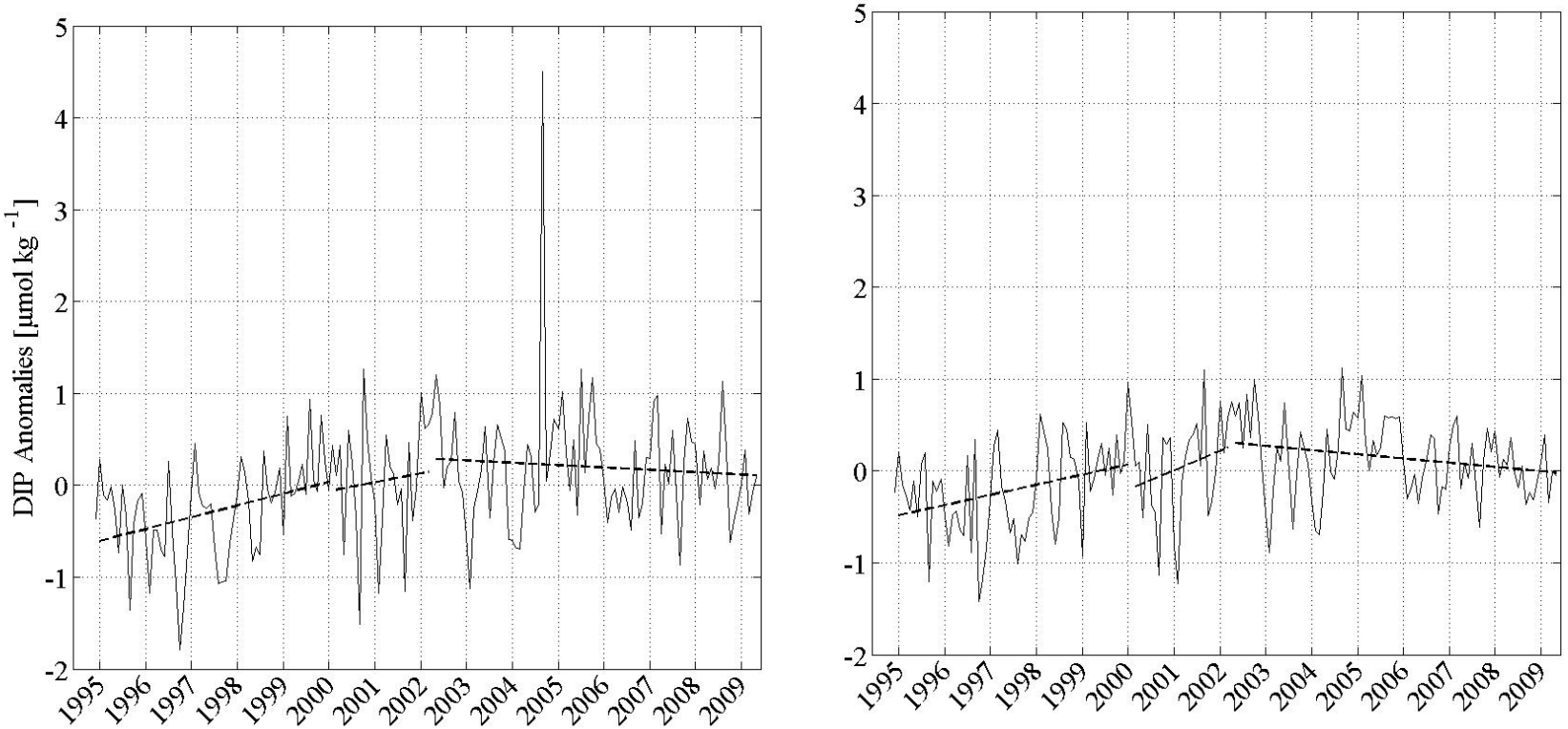


Figure 40: Trends in DIP anomalies in the surface (left) and bottom (right) during the three phases defined in the text. During the first phase, DIP significantly increased (surface: 0.11 µmol $kg^{-1}$ $yr^{-1}$, CI =0.08, 0.13; bottom: 0.11 µmol $kg^{-1}$ $yr^{-1}$, CI =0.08, 0.12). During the second phase, DIP increased in surface water, however this trend was not significant. In bottom water, DIP significantly increased (0.22 µmol $kg^{-1}$ $yr^{-1}$, CI =0.03, 0.34). During the third phase, DIP significantly decreased (surface: -0.02 µmol $kg^{-1}$ $yr^{-1}$, CI = -0.04, -0.006; bottom: -0.06 µmol $kg^{-1}$ $yr^{-1}$, CI = -0.06, -0.05).

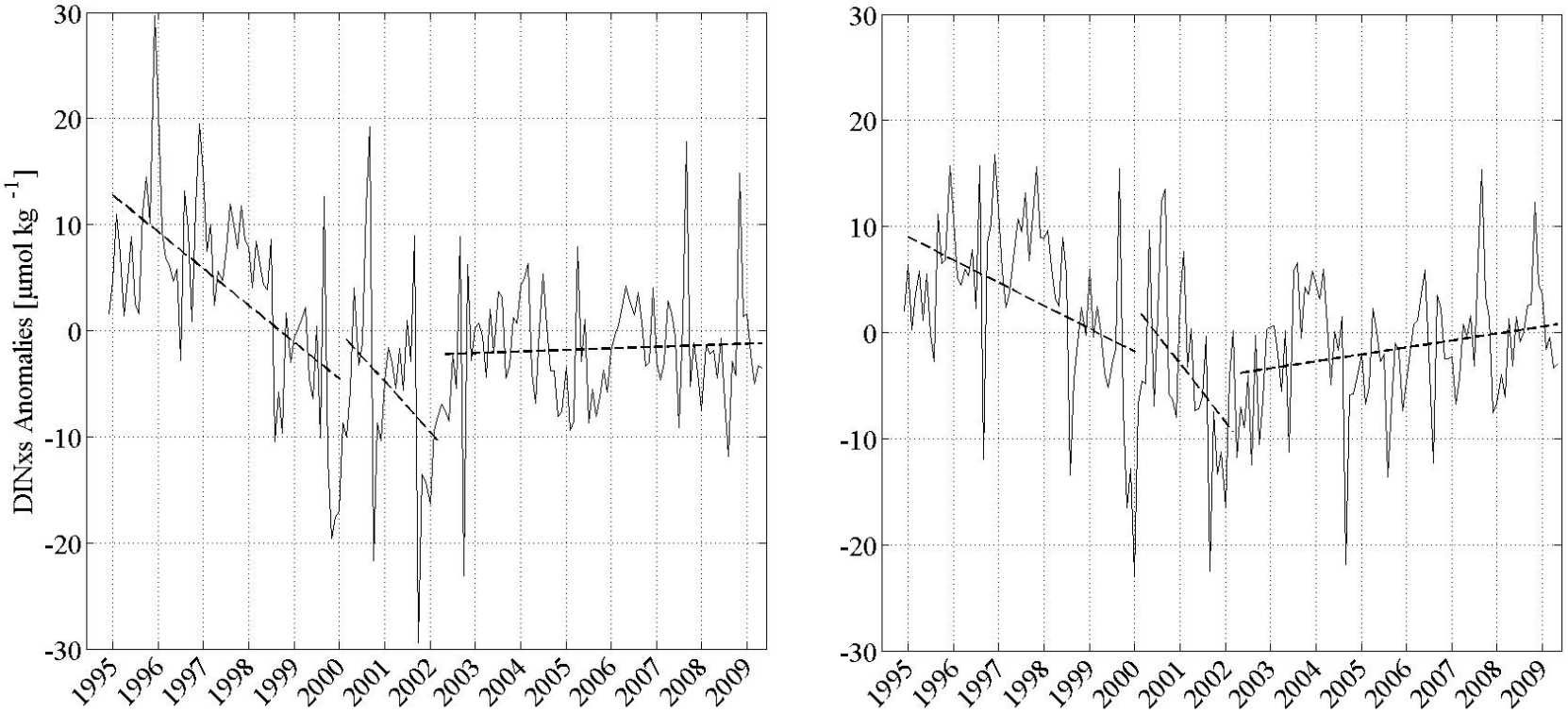


Figure 41: Trends in DINxs anomalies in the surface (left) and bottom (right) during the three phases defined in the text. During the first phase, DINxs significantly decreased (surface: -3.20 µmol $kg^{-1}$ $yr^{-1}$, CI = -3.61, -2.72; bottom: -1.78 µmol $kg^{-1}$ $yr^{-1}$, CI = -2.19, -1.45). During the second phase, DINxs significantly decreased again (surface: -2.87 µmol $kg^{-1}$ $yr^{-1}$, CI = -5.18, -0.65; bottom: -3.84 µmol $kg^{-1}$ $yr^{-1}$, CI = -6.78, -2.01). During the third phase, there were no significant changes in the DINxs parameter in surface water. In bottom water, DINxs significantly increased (0.52 µmol $kg^{-1}$ $yr^{-1}$, CI = 0.39, 0.63).

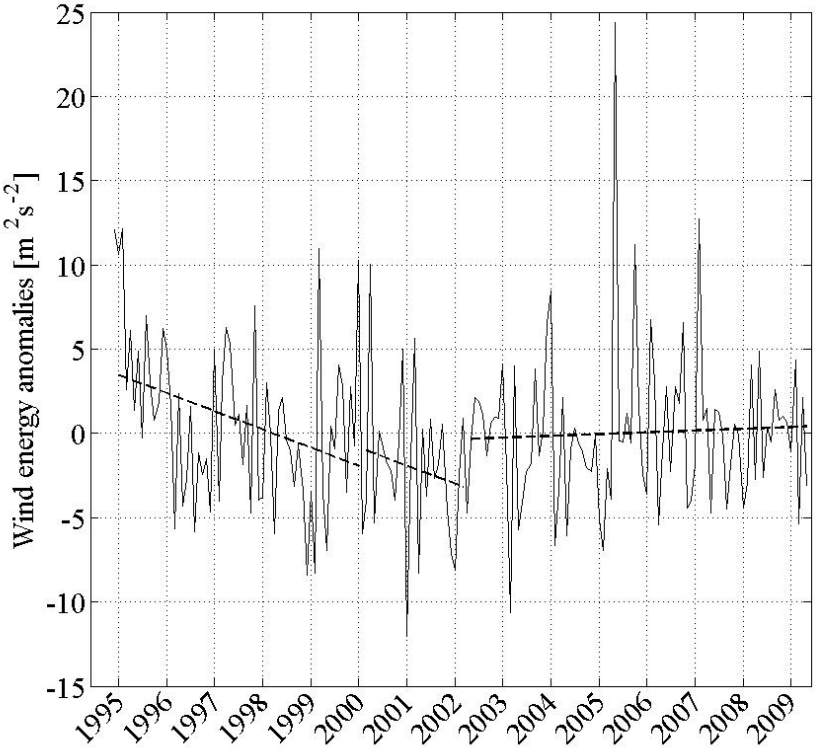


Figure 42: Trends in wind energy anomalies at the Flushing weather station during the three phases defined in the text. During the first phase, wind energy significantly decreased (-1.12 $m^2s^{-2}yr^{-1}$, CI = -1.43, -0.92). During the second and third phases, there were no statistically significant trends in wind energy.

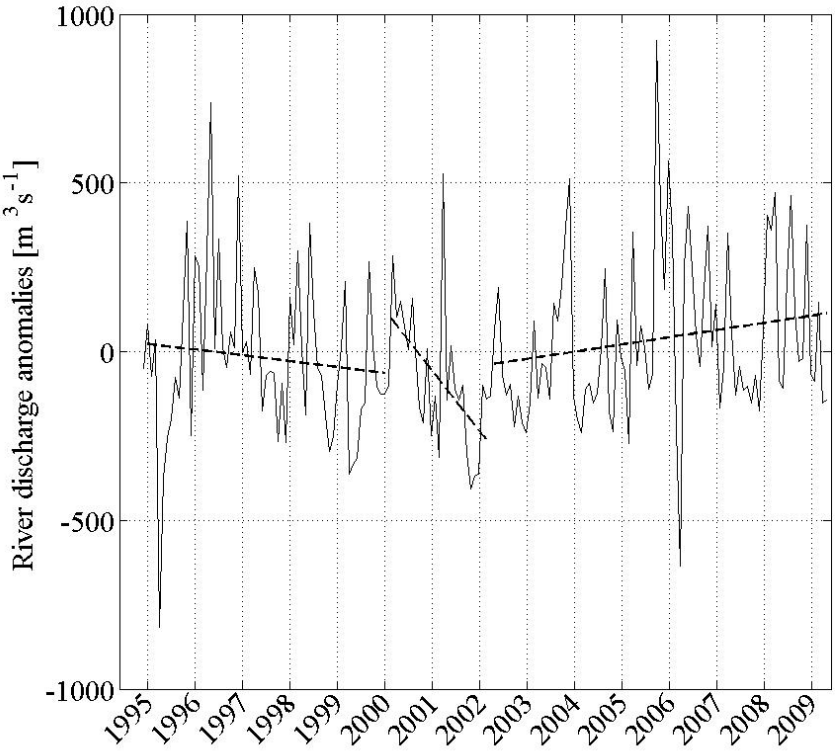


Figure 43: Trends in river discharge anomalies from the Connecticut River during the three phases defined in the text. During the first phase, river discharge significantly decreased (-25.0 $m^3s^{-1}yr^{-1}$, CI = -34.2, -14.8). During the second phase, river discharge continued to significantly decrease (-188.5 $m^3s^{-1}yr^{-1}$, CI = -243.4, -147.8). During the third phase, river discharge increased but this trend was not statistically significant.

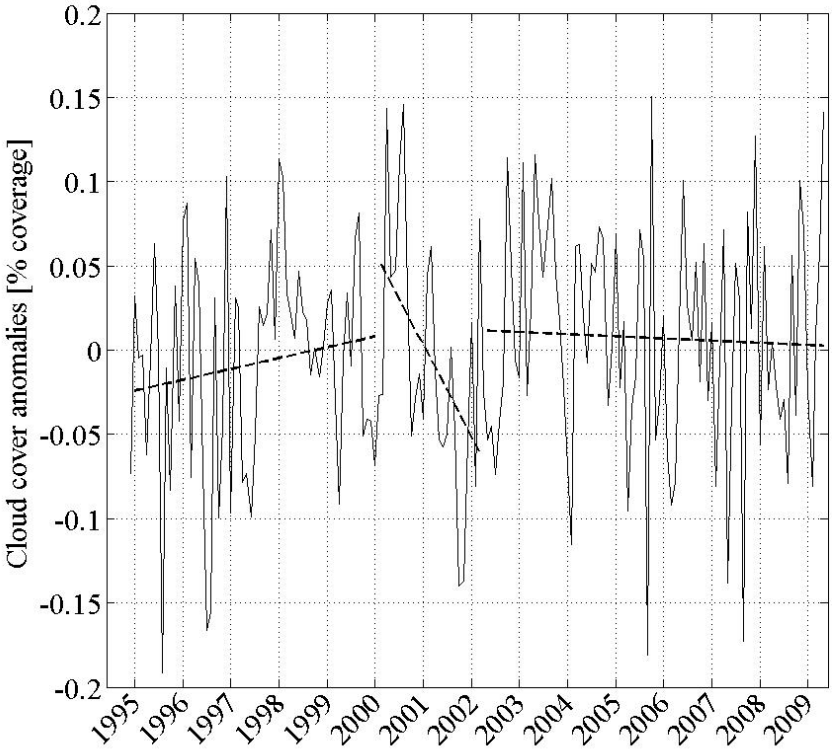


Figure 44: Trends in cloud cover anomalies from the Flushing weather station during the three phases defined in the text. During the first phase, there were no statistically significant trends in cloud cover. During the second phase, cloud cover significantly decreased (-4.96% coverage, CI = -7.17, -3.10). During the third phase, there was no statistically significant trend in cloud cover.

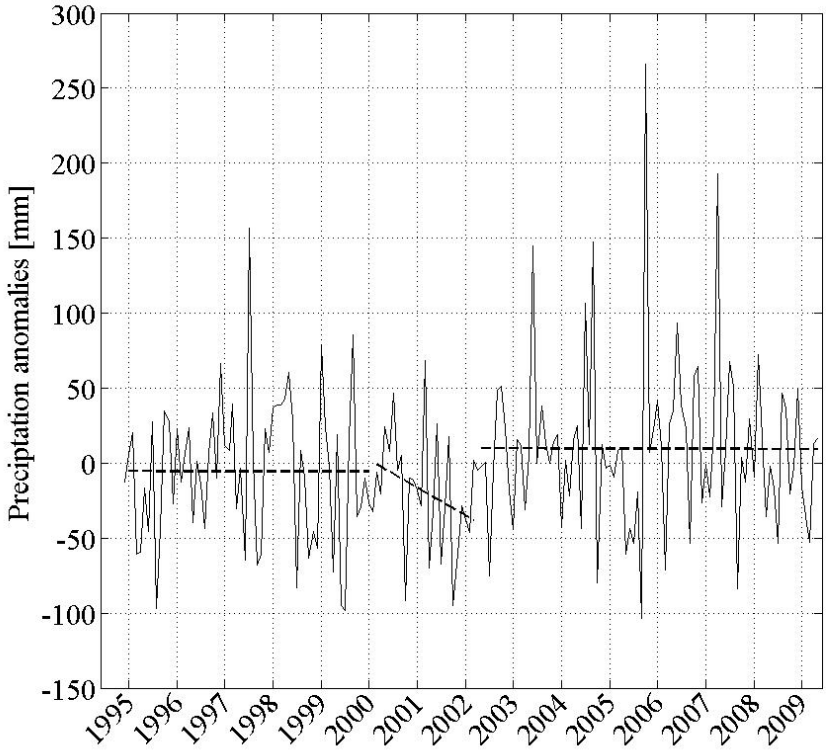


Figure 45: Trends in precipitation anomalies from La Guardia airport during the three phases defined in the text. During the first phase, there were no statistically significant trends in precipitation. During the second phase, precipitation significantly decreased (-21.6 mm $yr^{-1}$, CI = -27.6, -12.2). During the third phase, there was no statistically significant trend in cloud cover.

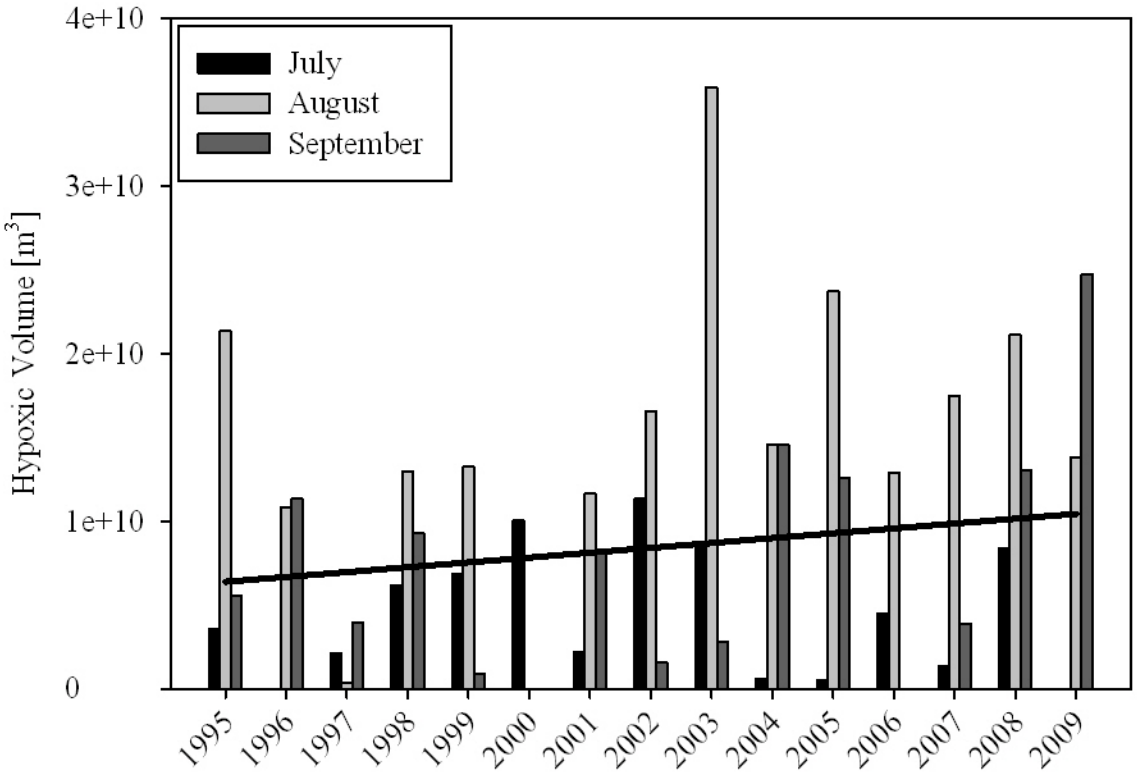


Figure 46: Maximum hypoxic volume ($m^3$) in Long Island Sound during the months of July, August, and September between 1995 and 2009. The black line is the TS-estimated trend of hypoxic volume <3 mg $L^{-1}$ through time. The trend ($2.89x10^8$ $m^3yr^{-1}$) is significant (CI = $1.82x10^8$, $4.77x10^8$).

## Appendix B: Tables

Table 1: Nutrient variables from the 9 field sampling dates during the summers of 2009 and 2010 at station A4. Empty cells indicate no data.

| Date | Depth [m] | $NH_4^+$ [µmol $kg^{-1}$] | $NO_2^- + NO_3^-$ [µmol $kg^{-1}$] | $NO_3^-$ [µmol $kg^{-1}$] | $NO_2^-$ [µmol $kg^{-1}$] | $PO_4^{3-}$ [µmol $kg^{-1}$] | Total DIN [µmol $kg^{-1}$] | DINxs [µmol $kg^{-1}$] | POC [µmol $kg^{-1}$] | PON [µmol $kg^{-1}$] | DOC [µmol $kg^{-1}$] |
|---|---|---|---|---|---|---|---|---|---|---|---|
| 6/9/09 | 2.5 | 0.3 | 3.2 | 2.3 | 0.9 | 0.0 | 3.5 | 3.5 | 124.9 | 50.4 | 139.1 |
| | 8.0 | 5.3 | 1.7 | 0.7 | 1.1 | 0.7 | 7.0 | -4.4 | 63.1 | 1.0 | 163.6 |
| | 11.8 | 5.1 | 0.8 | 0.8 | 0.0 | 09 | 5.9 | -7.9 | 47.2 | 2.5 | 175.9 |
| | 16.5 | 3.6 | 0.6 | 0.6 | 0.0 | 0.7 | 4.2 | -7.3 | 37.3 | 1.0 | 211.9 |
| 6/23/09 | 3.0 | 0.5 | 0.6 | 0.6 | 0.0 | 1.0 | 1.1 | -14.6 | 50.6 | 5.3 | 242.4 |
| | 10.0 | 4.1 | 3.1 | 1.6 | 1.5 | 1.2 | 7.2 | -11.8 | 48.9 | 4.9 | 250.9 |
| | 15.0 | 7.2 | 1.6 | 1.6 | 0.0 | 0.9 | 8.8 | -5.6 | 46.7 | 4.2 | 173.1 |
| | 21.0 | 8.4 | 1.9 | 1.9 | 0.0 | 1.3 | 10.3 | -10.6 | 25.8 | 0.2 | 193.8 |
| 7/14/09 | 1.5 | 0.0 | 0.4 | 0.4 | 0.0 | 1.1 | 0.4 | -16.9 | 123.1 | 13.4 | 191.0 |
| | 9.0 | 1.9 | 0.4 | 0.4 | 0.0 | 1.1 | 2.3 | -16.0 | 28.8 | 0.5 | 235.2 |
| | 19.0 | 1.5 | 0.9 | 0.0 | 0.9 | 0.7 | 2.5 | -8.7 | 29.6 | 0.00 | 205.1 |
| 8/11/09 | 2.1 | 0.0 | 0.8 | 0.8 | 0.0 | 1.3 | 0.8 | -20.1 | 145.2 | 16.1 | |
| | 5.0 | 0.1 | 0.5 | 0.5 | 0.0 | 1.0 | 0.6 | -15.8 | 94.4 | 20.2 | 188.6 |
| | 10.1 | 4.4 | 2.8 | 0.6 | 2.2 | 1.4 | 7.2 | -14.7 | 67.7 | 0.3 | 325.8 |
| | 22.2 | 6.3 | 3.0 | 0.6 | 2.4 | 1.3 | 9.3 | -11.9 | 75.0 | 0.0 | 239.5 |
| 8/28/09 | 2.0 | 0.0 | 2.8 | 2.8 | 0.0 | 0.9 | 2.8 | -11.5 | | | 172.8 |
| | 7.0 | 0.0 | 3.3 | 3.0 | 0.2 | 0.7 | 3.3 | -8.5 | | | |
| | 12.0 | 0.0 | 6.0 | 6.0 | 0.0 | 0.8 | 6.0 | -6.6 | | | |
| | 15.0 | 0.0 | 5.3 | 5.3 | 0.0 | 0.80 | 5.3 | -7.4 | 13.7 | 0.0 | 633.0 |
| 9/15/09 | 1.9 | 8.43 | 3.8 | 2.4 | 1.4 | 1.1 | 12.3 | -5.6 | 41.1 | 0.8 | 201.7 |
| | 4.9 | 9.34 | 4.8 | 3.1 | 1.6 | 1.6 | 14.1 | -10.8 | 22.8 | 1.7 | |
| | 18.4 | 7.67 | 3.0 | 1.7 | 1.2 | 1.3 | 10.6 | -9.9 | 36.1 | 7.1 | 214.2 |
| 10/1/09 | 2.0 | 5.71 | 7.9 | 6.1 | 1.8 | 0.8 | 13.6 | 0.1 | 31.7 | 1.0 | 197.0 |
| | 4.8 | 7.23 | 7.5 | 6.2 | 1.3 | 1.1 | 14.7 | -2.5 | 15.1 | 0.3 | 380.9 |
| | 7.2 | 7.48 | 12.9 | 10.4 | 2.6 | 2.1 | 20.4 | -12.7 | 28.6 | 0.4 | 224.6 |
| | 24.0 | 7.45 | 12.6 | 9.9 | 2.7 | 1.9 | 20.0 | -10.7 | 43.9 | 0.5 | 633.0 |
| 8/16/10 | 2.0 | 2.23 | 11.0 | | | 0.0 | 13.2 | 13.2 | 83.6 | 7.3 | |
| | 9.3 | 0.70 | 5.4 | | | 1.7 | 6.1 | -20.6 | 34.1 | 6.5 | |
| | 14.0 | 0.00 | 4.4 | | | 1.8 | 4.4 | -23.6 | 58.0 | 5.4 | |
| | 19.1 | 1.53 | 6.2 | | | 2.5 | 7.7 | -31.7 | 33.1 | 5.8 | |
| 9/10/10 | 2.0 | 0.20 | 19.1 | | | 2.5 | 19.3 | -21.1 | 48.3 | 4.3 | |
| | 13.0 | 0.00 | 20.7 | | | 2.7 | 20.7 | -22.8 | 85.1 | 8.5 | |
| | 17.8 | 0.00 | 19.5 | | | 2.4 | 19.5 | -18.4 | 62.5 | 3.7 | |
| | 17.1 | 0.07 | 21.0 | | | 2.5 | 21.1 | -18.9 | 40.9 | 5.6 | |

Table 2: Chl*a*, phaeopigments, and primary productivity rates in the photic zone from the 9 field sampling dates during the summers of 2009 and 2010 at station A4. Empty cells indicate no data. Between 9 June, 2009 and 15 September, 2009, Chl*a* was only measured in surface water samples.

| Date | Depth [m] | Chl*a* WW [µg $L^{-1}$] | Chl*a* <20-µm fraction [µg $L^{-1}$] | Chl*a* <2/5-µm fraction [µg $L^{-1}$] | Phaeo-pigments WW [µg $L^{-1}$] | Phaeo-pigments <20-µm fraction [µg $L^{-1}$] | Phaeo-pigments <2/5-µm fraction [µg $L^{-1}$] | Photic Zone Integrated PP WW [gC $m^{-2}$ $d^{-1}$] | Photic Zone Integrated PP <20-µm fraction [gC $m^{-2}$ $d^{-1}$] | Photic Zone Integrated PP <2/5-µm fraction [gC $m^{-2}$ $d^{-1}$] |
|---|---|---|---|---|---|---|---|---|---|---|
| 6/9/09 | 2.5 | 37.5 | 29.8 | 1.3 | 5.8 | 7.4 | 0.4 | 5.7 | | |
| 6/23/09 | 3.0 | 20.3 | 13.7 | 1.4 | 3.0 | 6.1 | 0.9 | 3.7 | 3.2 | 0.6 |
| 7/14/09 | 1.5 | 27.4 | 11.9 | 2.6 | 1.3 | 2.1 | 0.9 | 2.4 | 1.2 | 0.3 |
| 8/11/09 | 2.1 | 36.9 | 29.5 | 4.4 | 4.1 | 4.2 | 2.6 | 1.9 | 4.4 | 0.1 |
| 8/28/09 | 2.0 | 24.4 | 18.5 | 2.4 | 5.8 | 4.8 | 1.8 | 3.2 | 2.0 | 0.6 |
| 9/15/09 | 1.9 | 5.4 | 3.5 | 3.2 | 1.6 | 0.9 | 0.6 | 0.7 | 0.3 | 0.2 |
| 10/1/09 | 2.0 | 5.9 | 2.6 | 2.7 | 2.2 | 1.4 | 1.1 | 0.1 | <0.1 | <0.1 |
| | 4.8 | 5.5 | 2.6 | | 1.8 | 1.0 | | | | |
| 8/16/10 | 2.0 | 3.0 | 2.6 | 2.0 | 2.1 | 1.8 | 1.5 | 0.9 | 1.6 | 0.2 |
| | 9.3 | 1.8 | 1.6 | 1.4 | 2.4 | 2.0 | 0.4 | | | |
| | 14.0 | 1.6 | 1.3 | 1.2 | 1.9 | 2.6 | 1.1 | | | |
| | 19.1 | 2.1 | 1.7 | 1.4 | 1.1 | 2.5 | 1.1 | | | |
| 9/10/10 | 2.0 | 2.3 | 1.7 | 1.6 | 1.2 | 0.9 | 0.3 | 0.7 | 0.6 | 0.1 |
| | 13.0 | 4.8 | 3.5 | 2.0 | 1.5 | 1.0 | 1.1 | | | |
| | 17.8 | 2.6 | 1.9 | 0.7 | 0.6 | 0.6 | 0.4 | | | |
| | 17.1 | 1.5 | 0.9 | 0.8 | 0.4 | 1.0 | 0.7 | | | |

Table 3: Bacterial abundances, biomass, and net productivity from the 9 field sampling dates during the summers of 2009 and 2010 at station A4. Empty cells indicate no data.

| Date | Depth [m] | Bacterial Abundance [x$10^8$ cells $L^{-1}$] | Bacterial Biomass [µgC $L^{-1}$] | BNP, WW [µgC $L^{-1}$ $d^{-1}$] | BNP, <20-µm fraction [µgC $L^{-1}$ $d^{-1}$] | BNP, <2/5-µm fraction [µgC $L^{-1}$ $d^{-1}$] |
|---|---|---|---|---|---|---|
| 6/9/09 | 2.5 | 20.1 | 74.4 | 2.3 | 1.8 | 0.8 |
| | 8.0 | 16.4 | 60.7 | 0.4 | 0.5 | 0.4 |
| | 11.8 | 17.2 | 63.6 | 0.6 | 0.4 | 0.1 |
| | 16.5 | 10.1 | 37.3 | 0.4 | 0.4 | 0.1 |
| 6/23/09 | 3.0 | 3.6 | 13.4 | 1.4 | 1.2 | 0.1 |
| | 10.0 | 4.6 | 17.0 | 0.8 | 0.5 | 0.3 |
| | 15.0 | 8.4 | 30.9 | 0.7 | 0.6 | 0.2 |
| | 21.0 | 9.6 | 35.5 | 0.5 | 0.4 | 0.2 |
| 7/14/09 | 1.5 | 13.1 | 48.5 | 3.4 | 0.9 | 0.2 |
| | 9.0 | 11.7 | 43.3 | 1.1 | 0.2 | 0.2 |
| | 19.0 | 6.2 | 22.8 | 1.1 | 0.6 | 0.1 |
| 8/11/09 | 2.1 | 10.8 | 40.0 | 0.6 | 2.5 | |
| | 5.0 | 9.9 | 36.6 | 0.6 | 1.2 | 0.2 |
| | 10.1 | 7.9 | 29.0 | 0.3 | 0.4 | 0.2 |
| | 22.2 | 8.0 | 29.7 | 0.5 | | |
| 8/28/09 | 2.0 | 5.4 | 19.8 | 4.4 | 9.6 | 1.7 |
| | 7.0 | 4.6 | 17.0 | 2.6 | 3.3 | 1.6 |
| | 12.0 | | | 0.7 | | 0.8 |
| | 15.0 | 5.7 | 21.1 | 0.3 | 1.1 | 0.7 |
| 9/15/09 | 1.9 | 4.5 | 16.7 | 3.1 | 1.4 | 0.5 |
| | 4.9 | 3.0 | 11.1 | 1.3 | 1.9 | 0.2 |
| | 18.4 | 3.7 | 13.8 | 0.8 | 0.8 | 0.2 |
| 10/1/09 | 2.0 | 7.6 | 28.0 | 1.6 | 1.2 | 2.1 |
| | 4.8 | 2.6 | 9.6 | 1.0 | 0.4 | |
| | 7.2 | 3.2 | 11.8 | 1.2 | 1.3 | 0.2 |
| | 24.0 | 4.5 | 16.8 | 1.3 | 1.3 | 0.3 |
| 8/16/10 | 2.0 | 1.9 | 7.0 | 6.4 | 3.8 | 2.3 |
| | 9.3 | | | 8.8 | 8.0 | 4.1 |
| | 14.0 | | | 8.0 | 2.7 | 0.6 |
| | 19.1 | | | 4.7 | 4.4 | 2.4 |
| 9/10/10 | 2.0 | 0.9 | 3.4 | 0.6 | 0.7 | 0.4 |
| | 13.0 | 14.5 | 53.6 | 0.6 | 0.5 | 0.4 |
| | 17.8 | 4.8 | 17.9 | 0.5 | 0.4 | 0.2 |
| | 17.1 | 11.4 | 42.0 | 0.7 | 0.6 | 0.4 |

Table 4: Respiration, total DDA, and nitrification rates from the 9 field sampling dates during the summers of 2009 and 2010 at station A4. Empty cells indicate no data. These nitrification rates were measured with ATU-inhibition only.

| Date | Depth [m] | $O_2$-Respiration, WW [µM $d^{-1}$] | $O_2$-Respiration, <20-µm fraction [µM $d^{-1}$] | $O_2$-Respiration, <2/5-µm fraction [µM $d^{-1}$] | DDA [µgC $L^{-1}$ $d^{-1}$] | Nitrification [µgC $L^{-1}$ $d^{-1}$] |
|---|---|---|---|---|---|---|
| 6/9/09 | 2.5 | 51.9 | 32.7 | 18.7 | 0.0 | |
| | 8.0 | 40.2 | 50.4 | 40.0 | 0.0 | |
| | 11.8 | 25.7 | 38.9 | 31.7 | 0.0 | |
| | 16.5 | 39.5 | 37.9 | 32.3 | 0.0 | |
| 6/23/09 | 3.0 | 20.2 | 17.3 | 80.1 | 10.2 | |
| | 10.0 | 22.6 | 16.6 | 17.0 | 21.9 | |
| | 15.0 | 7.5 | 5.7 | 9.9 | 1.7 | |
| | 21.0 | 15.0 | 9.6 | 5.6 | 2.2 | |
| 7/14/09 | 1.5 | 59.1 | 63.9 | 138.7 | 35.1 | |
| | 9.0 | 40.3 | 49.5 | 94.7 | 8.2 | |
| | 19.0 | 37.6 | 51.6 | 175.8 | 229.1 | |
| 8/11/09 | 2.1 | 87.2 | 43.1 | 155.1 | 199.7 | |
| | 5.0 | | 18.5 | | 0.0 | |
| | 10.1 | 6.3 | 2.9 | 97.8 | 0.0 | |
| | 22.2 | 47.5 | 52.8 | 317.9 | 18.5 | |
| 8/28/09 | 2.0 | 46.3 | 39.9 | 468.2 | 42.2 | |
| | 7.0 | 41.3 | 23.4 | 50.2 | 69.9 | |
| | 12.0 | 33.0 | 30.2 | 40.7 | 20.1 | |
| | 15.0 | 194.8 | 32.2 | 114.1 | 16.4 | |
| 9/15/09 | 1.9 | 21.7 | 25.6 | 405.1 | 7.1 | |
| | 4.9 | 17.0 | 21.0 | 199.9 | 4.5 | |
| | 18.4 | 210.6 | 21.1 | 378.0 | 7.5 | |
| 10/1/09 | 2.0 | 12.5 | 12.9 | 25.0 | 1.1 | 0.8 |
| | 4.8 | 6.0 | 3.9 | 23.1 | 3.2 | 3.0 |
| | 7.2 | 3.4 | 4.2 | 23.1 | 0.7 | 0.0 |
| | 24.0 | 17.5 | 6.5 | 23.3 | 0.6 | 0.6 |
| 8/16/10 | 2.0 | 146 | 33.8 | 213.6 | 6.3 | 9.6 |
| | 9.3 | 6.8 | 6.5 | 60.0 | 4.5 | 4.1 |
| | 14.0 | 8.5 | 8.1 | | 5.8 | 5.2 |
| | 19.1 | 40.2 | 33.0 | 58.9 | 6.1 | 5.9 |
| 9/10/10 | 2.0 | 65.4 | 8.4 | 19.6 | 5.2 | 0.9 |
| | 13.0 | 8.7 | 7.8 | 16.3 | 4.4 | 4.3 |
| | 17.8 | 6.5 | 6.3 | 42.0 | 2.6 | 1.8 |
| | 17.1 | 14.6 | 6.0 | 31.2 | 5.3 | 4.0 |

Table 5a: Trends in inorganic nutrients in surface water from 1994 to 2009. Slopes were estimated with the TS-estimator and the 95% confidence intervals (shown in parentheses) were estimated by bootstrapping. A slope is considered significantly different than zero if its confidence intervals do not cross zero. Significant trends are shown in bold.

| | TDN [µmol kg$^{-1}$ yr$^{-1}$] | DIN [µmol kg$^{-1}$ yr$^{-1}$] | $NH_4^+$ [µmol kg$^{-1}$ yr$^{-1}$] | $NO_x$ [µmol kg$^{-1}$ yr$^{-1}$] | TDP [µmol kg$^{-1}$ yr$^{-1}$] | DIP [µmol kg$^{-1}$ yr$^{-1}$] | DSi [µmol kg$^{-1}$ yr$^{-1}$] | DINxs [µmol kg$^{-1}$ yr$^{-1}$] |
|---|---|---|---|---|---|---|---|---|
| **A4** | **0.38** (0.33, 0.42) | **0.10** (0.05, 0.15) | **0.14** (0.11, 0.16) | -0.01 (-0.04, 0.01) | **0.05** (0.05, 0.05) | **0.04** (0.04, 0.05) | **1.03** (0.88, 1.16) | **-0.69** (-0.72, -0.64) |
| **B3** | **0.17** (0.13, 0.21) | -0.15 (-0.18,0.12) | **-0.04** (-0.06, -0.03) | **-0.10** (-0.12, -0.08) | **0.03** (0.03, 0.04) | **0.03** (0.03, 0.03) | **1.09** (0.94, 1.26) | **-0.76** (-0.80, -0.72) |
| **C2** | **0.18** (0.15, 0.21) | **-0.11** (-0.13, -0.09) | **-0.01** (-0.02, -0.01) | **-0.09** (-0.10, -0.08) | **0.03** (0.02, 0.03) | **0.03** (0.02, 0.03) | **0.91** (0.82, 1.04) | **-0.52** (-0.55, -0.49) |
| **D3** | **0.10** (0.07, 0.13) | **-0.04** (-0.06, -0.02) | -0.01 (-0.01, 0.00) | -0.01 (-0.02, 0.00) | **0.03** (0.03, 0.03) | **0.03** (0.02, 0.03) | **1.28** (1.17, 1.40) | **-0.48** (-0.51, -0.46) |
| **E1** | **0.14** (0.10, 0.17) | -0.01 (-0.02, 0.01) | **0.02** (0.01, 0.02) | **-0.02** (-0.04, -0.01) | **0.02** (0.02, 0.02) | **0.02** (0.02, 0.02) | **0.84** (0.75, 0.95) | **-0.35** (-0.38, -0.32) |
| **H4** | **0.05** (0.02, 0.08) | **-0.08** (-0.10, -0.07) | 0.00 (-0.01, 0.00) | **-0.07** (-0.08, -0.06) | **0.01** (0.01, 0.01) | **0.01** (0.01, 0.01) | **0.14** (0.04, 0.23) | **-0.29** (-0.31, -0.26) |
| **I2** | 0.00 (-0.03,0.02) | **-0.06** (-0.08, -0.05) | **0.00** (0.00, 0.00) | **-0.07** (-0.08, -0.06) | **0.01** (0.01, 0.02) | **0.01** (0.01, 0.01) | **0.49** (0.40, 0.57) | **-0.25** (-0.27, -0.23) |
| **J2** | **0.11** (0.09, 0.14) | **-0.10** (-0.11, -0.09) | **-0.01** (-0.02, -0.01) | **-0.08** (-0.09, -0.08) | **0.00** (0.00, 0.00) | **0.00** (0.00, 0.00) | **0.12** (0.05, 0.20) | **-0.12** (-0.14, -0.11) |
| **M3** | **0.14** (0.12, 0.16) | **-0.04** (-0.05, -0.03) | **0.00** (0.00, 0.00) | **-0.04** (-0.05, -0.04) | **0.00** (0.00, 0.00) | **0.00** (0.00, 0.01) | **0.24** (0.20, 0.29) | **-0.10** (-0.12, -0.08) |

Table 5b: Trends in inorganic nutrients in bottom water from 1994 to 2009. Slopes were estimated with the TS-estimator and the 95% confidence intervals (shown in parentheses) were estimated by bootstrapping. A slope is considered significantly different than zero if its confidence intervals do not cross zero. Significant trends are shown in bold.

| | TDN [µmol kg$^{-1}$ yr$^{-1}$] | DIN [µmol kg$^{-1}$ yr$^{-1}$] | $NH_4^+$ [µmol kg$^{-1}$ yr$^{-1}$] | $NO_x$ [µmol kg$^{-1}$ yr$^{-1}$] | TDP [µmol kg$^{-1}$ yr$^{-1}$] | DIP [µmol kg$^{-1}$ yr$^{-1}$] | DSi [µmol kg$^{-1}$ yr$^{-1}$] | DINxs [µmol kg$^{-1}$ yr$^{-1}$] |
|---|---|---|---|---|---|---|---|---|
| **A4** | **0.21** (0.16, 0.25) | **0.06** (0.03, 0.10) | **0.10** (0.08, 0.11) | -0.01 (-0.03, 0.00) | **0.03** (0.03, 0.04) | **0.03** (0.03, 0.03) | **0.87** (0.73, 1.02) | **-0.52** (-0.56, -0.47) |
| **B3** | **0.12** (0.07, 0.16) | **-0.05** (-0.07, -0.03) | **0.03** (0.02, 0.04) | **-0.04** (-0.06, -0.02) | **0.03** (0.03, 0.03) | **0.03** (0.03, 0.03) | **0.78** (0.63, 0.89) | **-0.45** (-0.48, -0.41) |
| **C2** | **0.05** (0.02, 0.09) | **-0.06** (-0.13, -0.09) | 0.00 (-0.01, 0.01) | **-0.04** (-0.05, -0.02) | **0.02** (0.02, 0.03) | **0.02** (0.02, 0.03) | **0.78** (0.68, 0.89) | **-0.47** (-0.49, -0.41) |
| **D3** | **0.14** (0.11, 0.17) | -0.01 (-0.03, 0.00) | **0.02** (0.01, 0.03) | **-0.03** (-0.05, -0.02) | **0.02** (0.02, 0.03) | **0.02** (0.02, 0.02) | **0.39** (0.31, 0.49) | **-0.36** (-0.39, -0.34) |
| **E1** | **0.10** (0.07, 0.12) | **-0.03** (-0.05, -0.02) | 0.00 (-0.01, 0.00) | **-0.04** (-0.05, -0.02) | **0.02** (0.01, 0.02) | **0.02** (0.02, 0.02) | **0.43** (0.34, 0.52) | **-0.38** (-0.41, -0.35) |
| **H4** | **0.03** (0.00, 0.06) | **-0.06** (-0.08, -0.05) | **0.02** (0.02, 0.03) | **-0.09** (-0.10, -0.08) | **0.00** (0.00, 0.01) | **0.01** (0.01, 0.01) | **0.19** (0.08, 0.28) | **-0.26** (-0.28, -0.24) |
| **I2** | **0.03** (0.00,0.06) | **-0.09** (-0.08, -0.05) | **0.02** (0.02, 0.03) | **-0.12** (-0.13, -0.11) | **0.00** (0.00, 0.01) | **0.01** (0.01, 0.01) | **0.12** (0.04, 0.23) | **-0.22** (-0.25, -0.20) |
| **J2** | **0.03** (0.01, 0.05) | **-0.09** (-0.10, -0.08) | **0.00** (0.00, 0.01) | **-0.09** (-0.10, -0.08) | **0.00** (0.00, 0.00) | **0.00** (0.00, 0.00) | **0.18** (0.13, 0.24) | **-0.09** (-0.11, -0.07) |
| **M3** | **0.12** (0.10, 0.14) | **-0.04** (-0.04, -0.03) | 0.00 (-0.01, 0.00) | **-0.02** (-0.03, -0.02) | **0.00** (0.00, 0.00) | **0.00** (0.00, 0.00) | **0.09** (0.05, 0.12) | **-0.04** (-0.05, -0.02) |

Table 6a: Trends in biomass indices and particulate nutrient ratios in surface water from 1994 to 2009. Slopes were estimated with the TS-estimator and the 95% confidence intervals (shown in parentheses) were estimated by bootstrapping. A slope is considered significantly different than zero if its confidence intervals do not cross zero. Significant trends are shown in bold.

| | Chl *a* [µg $L^{-1}$ $yr^{-1}$] | TSS [mg $L^{-1}$ $yr^{-1}$] | BioSi [µmol $kg^{-1}$ $yr^{-1}$] | PC [µmol $kg^{-1}$ $yr^{-1}$] | PN [µmol $kg^{-1}$ $yr^{-1}$] | PC:PN [$yr^{-1}$] | PN:PP [$yr^{-1}$] | PN:BioSi [$yr^{-1}$] |
|---|---|---|---|---|---|---|---|---|
| **A4** | **0.55** (0.51, 0.58) | **-0.10** (-0.11, -0.09) | **-0.74** (-0.79, -0.67) | **-2.47** (-2.63, -2.28) | **-0.37** (-0.40, -0.34) | **0.03** (0.03, 0.04) | **-0.22** (-0.26, -0.19) | 0.00 (0.00, 0.00) |
| **B3** | 0.48 (0.44, 0.51) | **-0.04** (-0.05, -0.03) | **-0.36** (-0.42, -0.30) | **-1.32** (-1.53, -1.12) | **-0.21** (-0.23, -0.18) | **0.05** (0.04, 0.06) | **-0.30** (-0.34, -0.26) | 0.00 (-0.01, 0.00) |
| **C2** | **0.32** (0.30, 0.35) | **-0.04** (-0.05, -0.04) | **-0.17** (-0.22, -0.13) | **-0.65** (-0.78, -0.54) | **-0.15** (-0.16, -0.13) | **0.07** (0.06, 0.08) | **-0.24** (-0.28, -0.19) | 0.00 (-0.01, 0.00) |
| **D3** | **0.31** (0.29, 0.33) | **-0.09** (-0.10, -0.07) | **-0.27** (-0.32, -0.22) | **-0.64** (-0.75, -0.54) | **-0.12** (-0.13, -0.10) | **0.06** (0.05, 0.07) | **-0.22** (-0.27, -0.17) | 0.00 (0.00, 0.00) |
| **E1** | **0.20** (0.19, 0.22) | **0.01** (0.00, 0.02) | **-0.19** (-0.23, -0.14) | **-0.55** (-0.62, -0.47) | **-0.14** (-0.15, -0.13) | **0.08** (0.08, 0.09) | **-0.46** (-0.52, -0.40) | -0.01 (-0.01, 0.00) |
| **H4** | **0.18** (0.17, 0.16) | **-0.06** (-0.07, -0.05) | **-0.21** (-0.25, -0.17) | **-0.22** (-0.30, -0.14) | **-0.07** (-0.07, -0.06) | **0.08** (0.07, 0.09) | **-0.19** (-0.24, -0.14) | 0.00 (0.00, 0.00) |
| **I2** | **0.17** (0.16, 0.18) | **0.01** (0.01, 0.03) | -0.01 (-0.04, 0.02) | **-0.10** (-0.15, -0.04) | **-0.08** (-0.09, -0.07) | **0.12** (0.11, 0.13) | **-0.45** (-0.51, -0.41) | **-0.01** (-0.01, -0.01) |
| **J2** | **0.17** (0.16, 0.18) | **-0.11** (-0.13, -0.10) | **-0.26** (-0.30, -0.23) | **-0.18** (-0.25, -0.11) | **-0.11** (-0.12, -0.10) | **0.15** (0.14, 0.16) | **-0.28** (-0.34. -0.24) | 0.00 (0.00, 0.00) |
| **M3** | **0.14** (0.14, 0.15) | -0.01 (-0.02, 0.00) | **-0.08** (-0.10, -0.07) | **-0.17** (-0.22, -0.12) | **-0.03** (-0.03, -0.02) | **0.01** (0.00, 0.03) | **-0.19** (-0.27, -0.14) | 0.00 (0.00, 0.00) |

Table 6b: Trends in biomass indices and particulate nutrient ratios in bottom water from 1994 to 2009. Slopes were estimated with the TS-estimator and the 95% confidence intervals (shown in parentheses) were estimated by bootstrapping. A slope is considered significantly different than zero if its confidence intervals do not cross zero. Significant trends are shown in bold.

| | Chl *a* [µg $L^{-1}$ $yr^{-1}$] | TSS [mg $L^{-1}$ $yr^{-1}$] | BioSi [µmol $kg^{-1}$ $yr^{-1}$] | PC [µmol $kg^{-1}$ $yr^{-1}$] | PN [µmol $kg^{-1}$ $yr^{-1}$] | PC:PN [$yr^{-1}$] | PN:PP [$yr^{-1}$] | PN:BioSi [$yr^{-1}$] |
|---|---|---|---|---|---|---|---|---|
| **A4** | **0.24** (0.22, 0.27) | **-0.03** (-0.06, -0.01) | **-0.23** (-0.36, -0.11) | **-0.87** (-1.02, -0.74) | **-0.23** (-0.25, -0.21) | **0.10** (0.09, 0.11) | **-0.19** (-0.21, -0.15) | 0.00 (-0.01, 0.00) |
| **B3** | **0.26** (0.24, 0.28) | **-0.07** (-0.09, -0.05) | **-0.41** (-0.50, -0.31) | **-0.58** (-0.68, -0.49) | **-0.15** (-0.16, -0.13) | **0.09** (0.08, 0.10) | **-0.27** (-0.31, -0.25) | 0.00 (0.00, 0.00) |
| **C2** | **0.19** (0.18, 0.21) | **-0.06** (-0.08, -0.05) | **-0.29** (-0.37, -0.21) | **-0.54** (-0.62, -0.49) | **-0.10** (-0.12, -0.09) | **0.07** (0.06, 0.08) | **-0.23** (-0.26, -0.19) | 0.00 (0.00, 0.00) |
| **D3** | **0.17** (0.16, 0.18) | **-0.14** (-0.16, -0.12) | **-0.59** (-0.66, -0.53) | **-0.68** (-0.76, -0.61) | **-0.16** (-0.17, -0.15) | **0.10** (0.09, 0.11) | **-0.27** (-0.31, -0.24) | 0.00 (0.00, 0.00) |
| **E1** | **0.10** (0.09, 0.11) | **-0.16** (-0.18, -0.14) | **-0.71** (-0.79, -0.65) | **-0.69** (-0.76, -0.62) | **-0.13** (-0.14, -0.12) | **0.08** (0.07, 0.09) | **-0.46** (-0.50, -0.41) | 0.00 (0.00, 0.00) |
| **H4** | **0.09** (0.08, 0.10) | **-0.05** (-0.07, -0.04) | **-0.05** (-0.11, 0.02) | **-0.25** (-0.32, -0.19) | **-0.09** (-0.10, -0.08) | **0.13** (0.12, 0.14) | **-0.50** (-0.54, -0.46) | 0.00 (0.00, 0.00) |
| **I2** | **0.15** (0.14, 0.15) | **0.02** (0.00, 0.03) | 0.03 (-0.04, 0.09) | 0.00 (-0.06, 0.07) | **-0.07** (-0.08, -0.06) | **0.11** (0.09, 0.12) | **-0.31** (-0.35, -0.28) | 0.00 (0.00, 0.00) |
| **J2** | **0.21** (0.20, 0.22) | **-0.23** (-0.26, -0.20) | **-0.43** (-0.50, -0.37) | **-0.54** (-0.62, -0.48) | **-0.09** (-0.10, -0.08) | **0.09** (0.08, 0.11) | **-0.17** (-0.22. -0.13) | 0.00 (0.00, 0.00) |
| **M3** | **0.15** (0.14, 0.16) | **-0.06** (-0.07, -0.05) | **-0.10** (-0.12, -0.08) | **-0.18** (-0.22, -0.15) | **-0.04** (-0.05, -0.04) | **0.06** (0.04, 0.07) | **-0.26** (-0.32, -0.21) | 0.00 (0.00, 0.00) |

Table 7a: Trends in dissolved organic nutrients and total nutrients (organic + inorganic) in surface water from 1994 to 2009. Slopes were estimated with the TS-estimator and the 95% confidence intervals (shown in parentheses) were estimated by bootstrapping. A slope is considered significantly different than zero if its confidence intervals do not cross zero. Significant trends are shown in bold.

| | DOC [µg $L^{-1}$ $yr^{-1}$] | DON [µg $L^{-1}$ $yr^{-1}$] | TOC [µmol $kg^{-1}$ $yr^{-1}$] | Total N [µmol$kg^{-1}$ $yr^{-1}$] | Total P [µmol $kg^{-1}$ $yr^{-1}$] | Total Si [µmol $kg^{-1}$ $yr^{-1}$] |
|---|---|---|---|---|---|---|
| **A4** | **2.38** (1.97, 2.79) | **0.24** (0.21, 0.26) | **0.89** (0.37, 1.34) | **-0.09** (-0.13, -0.04) | **0.04** (0.04, 0.04) | **0.13** (0.02, 0.25) |
| **B3** | **2.29** (1.96, 2.77) | **0.33** (0.30, 0.37) | **1.51** (0.93, 2.03) | **-0.07** (-0.12, -0.01) | **0.03** (0.02, 0.03) | **0.70** (0.57, 0.87) |
| **C2** | **2.34** (1.98, 2.74) | **0.28** (0.25, 0.30) | **2.38** (1.99, 2.88) | **0.06** (0.03, 0.09) | **0.02** (0.02, 0.02) | **0.76** (0.64, 0.86) |
| **D3** | **3.33** (2.90, 3.84) | **0.14** (0.12, 0.16) | **2.96** (2.52, 3.51) | **-0.08** (-0.12, -0.05) | **0.03** (0.02, 0.03) | **0.87** (0.76, 0.98) |
| **E1** | **2.92** (2,54, 3.31) | **0.15** (0.13, 0.18) | **2.37** (1.94, 2.78) | -0.03 (-0.06, 0.01) | **0.02** (0.02, 0.02) | **0.51** (0.39, 0.61) |
| **H4** | **2.12** (1.70, 2.52) | **0.15** (0.13, 0.18) | **2.26** (1.86, 2.69) | -0.02 (-0.05, 0.01) | **0.01** (0.01, 0.01) | **-0.13** (-0.21, -0.04) |
| **I2** | **2.53** (2.06, 3.02) | **0.08** (0.06, 0.10) | **2.02** (1.55, 2.53) | **-0.12** (-0.15, -0.09) | **0.01** (0.01, 0.02) | **0.38** (0.30, 0.48) |
| **J2** | **3.35** (2.88, 3.87) | **0.22** (0.20, 0.24) | **3.34** (2.80, 3.91) | -0.01 (-0.04, 0.02) | 0.00 (0.00, 0.00) | **-0.17** (-0.25, -0.10) |
| **M3** | **2.14** (1.79, 2.55) | **0.19** (0.17, 0.21) | **2.05** (1.67, 2.53) | **0.10** (0.07, 0.12) | 0.00 (0.00, 0.00) | **0.14** (0.10, 0.18) |

Table 7b: Trends in dissolved organic nutrients and total nutrients (organic + inorganic) in bottom water from 1994 to 2009. Slopes were estimated with the TS-estimator and the 95% confidence intervals (shown in parentheses) were estimated by bootstrapping. A slope is considered significantly different than zero if its confidence intervals do not cross zero. Significant trends are shown in bold.

| | DOC [µg $L^{-1}$ $yr^{-1}$] | DON [µg $L^{-1}$ $yr^{-1}$] | TOC [µmol $kg^{-1}$ $yr^{-1}$] | Total N [µmol$kg^{-1}$ $yr^{-1}$] | Total P [µmol $kg^{-1}$ $yr^{-1}$] | Total Si [µmol $kg^{-1}$ $yr^{-1}$] |
|---|---|---|---|---|---|---|
| **A4** | **2.78** (2.34, 3.17) | **0.14** (0.11, 0.17) | **2.07** (1.63, 2.61) | **-0.09** (-0.13, -0.04) | **0.02** (0.01, 0.02) | **0.37** (0.19, 0.50) |
| **B3** | **3.19** (2.79, 3.62) | **0.15** (0.12, 0.18) | **3.00** (2.47, 3.52) | -0.02 (-0.07, 0.02) | **0.02** (0.02, 0.03) | **0.24** (0.06, 0.39) |
| **C2** | **0.88** (0.53, 1.31) | **0.13** (0.11, 0.14) | **0.56** (0.20, 0.95) | **-0.10** (-0.14, -0.07) | **0.02** (0.02, 0.02) | **0.39** (0.23, 0.53) |
| **D3** | **2.63** (2.16, 3.00) | **0.15** (0.13, 0.17) | **1.56** (1.15, 2.06) | **-0.08** (-0.12, -0.05) | **0.02** (0.01, 0.02) | **-0.47** (-0.60, -0.36) |
| **E1** | **3.60** (3.04, 4.13) | **0.14** (0.12, 0.16) | **2.46** (2.07, 3.01) | **-0.10** (-0.13, -0.07) | **0.01** (0.01, 0.02) | **-0.35** (-0.46, -0.23) |
| **H4** | **1.27** (0.93, 1.65) | **0.09** (0.07, 0.12) | **1.17** (0.76, 1.52) | **-0.13** (-0.17, -0.10) | 0.00 (0.00, 0.01) | 0.07 (-0.04, 0.20) |
| **I2** | **2.40** (1.93, 2.79) | **0.13** (0.11, 0.15) | **2.80** (2.37, 3.29) | **-0.04** (-0.07, -0.01) | **0.01** (0.00, 0.01) | **0.19** (0.08, 0.29) |
| **J2** | **3.26** (2.78, 3.91) | **0.12** (0.10, 0.15) | **2.94** (2.46, 3.39) | **-0.06** (-0.09, -0.04) | -0.01 (-0.01, 0.00) | **-0.34** (-0.42, -0.27) |
| **M3** | **2.69** (2.27, 3.10) | 0.15 (0.13, 0.17) | **2.60** (2.18, 3.06) | **0.07** (0.05, 0.09) | 0.00 (0.00, 0.00) | -0.01 (-0.04, 0.03) |

Table 8a: Trends in physical variables in surface water from 1994 to 2009. Slopes were estimated with the TS-estimator and the 95% confidence intervals (shown in parentheses) were estimated by bootstrapping. A slope is considered significantly different than zero if its confidence intervals do not cross zero. Significant trends are shown in bold.

| | **Temperature [°C $yr^{-1}$]** | **Salinity [$yr^{-1}$]** | **Density [kg $m^{-3}$ $yr^{-1}$]** | **DO [mg $L^{-1}$ $yr^{-1}$]** |
|---|---|---|---|---|
| **A4** | **-0.03** (-0.04, -0.02) | 0.00 (0.00, 0.01) | 0.00 (0.00, 0.01) | **-0.04** (-0.05, -0.04) |
| **B3** | -0.01 (-0.02, 0.00) | 0.00 (0.00, 0.01) | 0.00 (-0.01, 0.00) | -0.01 (-0.02, 0.00) |
| **C2** | -0.01 (-0.02, 0.00) | 0.00 (0.00, 0.01) | 0.00 (0.00, 0.01) | -0.01 (-0.02, 0.00) |
| **D3** | -0.01 (-0.02, 0.00) | 0.00 (-0.00, 0.01) | 0.00 (0.00, 0.00) | 0.00 (-0.01, 0.00) |
| **E1** | **-0.02** (-0.03, -0.01) | 0.00 (-0.00, 0.01) | 0.00 (-0.01, 0.00) | 0.00 (0.00, 0.01) |
| **H4** | **0.03** (0.02, 0.04) | **-0.02** (-0.03, -0.02) | **-0.02** (-0.03, -0.02) | 0.00 (-0.01, 0.00) |
| **I2** | **0.04** (0.03, 0.05) | -0.01 (-0.01, 0.00) | **-0.02** (-0.02, -0.02) | 0.00 (-0.01, 0.00) |
| **J2** | 0.01 (-0.01, 0.03) | **0.02** (0.01, 0.02) | **0.01** (0.00, 0.01) | 0.00 (0.00, 0.01) |
| **M3** | **0.01** (0.00, 0.02) | 0.00 (0.00, 0.00) | -0.01 (-0.01, 0.00) | -0.01 (-0.02, 0.01) |

Table 8b: Trends in physical variables in bottom water from 1994 to 2009. Slopes were estimated with the TS-estimator and the 95% confidence intervals (shown in parentheses) were estimated by bootstrapping. A slope is considered significantly different than zero if its confidence intervals do not cross zero. Significant trends are shown in bold.

| | **Temperature [°C yr$^{-1}$]** | **Salinity [yr$^{-1}$]** | **Density [kg m$^{-3}$ yr$^{-1}$]** | **DO [mg L$^{-1}$ yr$^{-1}$]** |
|---|---|---|---|---|
| **A4** | **-0.04** (-0.04, -0.03) | 0.00 (0.00, 0.00) | 0.00 (0.00, 0.01) | **-0.02** (-0.02, -0.01) |
| **B3** | **-0.04** (-0.05, -0.03) | -0.01 (-0.01, 0.00) | 0.00 (0.00, 0.01) | 0.00 (-0.01, 0.00) |
| **C2** | **-0.02** (-0.03, -0.02) | 0.00 (-0.01, 0.00) | 0.00 (0.00, 0.01) | **0.01** (0.00, 0.01) |
| **D3** | **-0.03** (-0.03, -0.02) | 0.00 (0.00, 0.01) | **0.01** (0.00, 0.01) | **0.01** (0.00, 0.01) |
| **E1** | **-0.05** (-0.06, -0.04) | **0.01** (0.00, 0.01) | **0.02** (0.01, 0.02) | 0.01 (0.00, 0.01) |
| **H4** | **-0.03** (-0.04, -0.02) | **0.01** (0.01, 0.02) | **0.01** (0.01, 0.02) | 0.01 (0.01, 0.02) |
| **I2** | 0.00 (-0.01, 0.00) | **0.02** (0.01, 0.02) | **0.01** (0.01, 0.01) | 0.01 (0.00, 0.01) |
| **J2** | 0.00 (0.00, 0.01) | **0.01** (0.01, 0.02) | **0.01** (0.00, 0.01) | 0.00 (0.00, 0.01) |
| **M3** | **0.03** (0.02, 0.03) | **0.01** (0.01, 0.02) | 0.00 (0.00, 0.01) | 0.00 (0.00, 0.01) |

Table 9: Trends in phytoplankton functional groups from 2002 to 2010. Trends are in units of Chl *a* per year. Slopes were estimated with the TS-estimator and the 95% confidence intervals (shown in parentheses) were estimated by bootstrapping. A slope is considered significantly different than zero if its confidence intervals do not cross zero. Significant trends are shown in bold.

| | Diatom (Chl *a*) [µg $L^{-1}$ $yr^{-1}$] | Dinoflagellate (Chl *a*) [µg $L^{-1}$ $yr^{-1}$] | Cyano-bacteria (Chl *a*) [µg $L^{-1}$ $yr^{-1}$] | Prymnesio-phyceae-A (Chl *a*) [µg $L^{-1}$ $yr^{-1}$] | Crypto-phyceae (Chl *a*) [µg $L^{-1}$ $yr^{-1}$] | Raphido-phyceae (Chl *a*) [µg $L^{-1}$ $yr^{-1}$] | Eugleno-phyceae (Chl *a*) [µg $L^{-1}$ $yr^{-1}$] | Non-diatom Chl *a* [µg $L^{-1}$ $yr^{-1}$] |
|---|---|---|---|---|---|---|---|---|
| **A4** | **-0.62** (-0.72, -0.53) | **6.85 x $10^{-3}$** (4.90 x $10^{-5}$, 1.33 x $10^{-3}$ ) | 0.00 (0.00, 0.00) | **0.06** (0.04, 0.08) | **0.02** (0.02, 0.03) | **7.12 x $10^{-3}$** (5.39 x $10^{-3}$, 9.19 x $10^{-3}$) | **6.97 x $10^{-3}$** (3.37 x $10^{-3}$, 1.17 x $10^{-2}$) | **0.14** (0.11, 0.18) |
| **B3** | **-0.18** (-0.25, -0.12) | **4.56 x $10^{-2}$** (3.46 x $10^{-2}$, 5.54 x $10^{-2}$) | **-6.23 x $10^{-4}$** (-9.62 x $10^{-4}$, -3.64 x $10^{-4}$) | **0.05** (0.02, 0.07) | **0.04** (0.03, 0.04) | **7.64 x $10^{-3}$** (5.16 x $10^{-3}$, 1.00 x $10^{-2}$) | **1.19 x $10^{-2}$** (8.09 x $10^{-3}$, 1.54 x $10^{-2}$) | **0.18** (0.15, 0.22) |
| **C1** | **-0.17** (-0.22, -0.13) | **3.61 x $10^{-2}$** (2.68 x $10^{-2}$, 4.72 x $10^{-2}$) | 0.0 (-5.20 x $10^{-4}$, 3.43 x $10^{-4}$) | **0.07** (0.06, 0.09) | **0.03** (0.03, 0.04) | **6.15E x $10^{-3}$** (4.14 x $10^{-3}$, 8.00 x $10^{-3}$) | **4.77 x $10^{-3}$** (6.32 x $10^{-4}$, 8.19 x $10^{-3}$) | **0.16** (0.13, 0.19) |
| **D3** | **-0.07** (-0.12, -0.03) | **1.72 x $10^{-2}$** (9.71 x $10^{-3}$, 2.46 x $10^{-2}$) | **-1.34 x $10^{-3}$** (-1.93 x $10^{-3}$, -8.27 x $10^{-4}$) | **0.02** (0.01, 0.03) | **0.01** (0.01, 0.02) | **2.87 x $10^{-3}$** (1.31 x $10^{-3}$, 4.44 x $10^{-3}$) | **7.11 x $10^{-3}$** (4.58 x $10^{-3}$, 9.27 x $10^{-3}$) | **0.07** (0.05, 0.10) |
| **E1** | -0.01 (-0.04, 0.02) | -2.03 x $10^{-2}$ (-4.51 x $10^{-3}$, 3.98 x $10^{-3}$) | **-4.93 x $10^{-3}$** (-5.92 x $10^{-3}$, -4.10 x $10^{-3}$) | 0.00 (-0.01, 0.01) | **0.02** (0.01, 0.02) | **5.11 x $10^{-3}$** (3.56 x $10^{-3}$, 6.50 x $10^{-3}$) | **4.59 x $10^{-3}$** (2.25 x $10^{-3}$, 7.35 x $10^{-3}$) | **0.03** (0.02, 0.05) |
| **F2** | 0.00 (-0.03, 0.02) | 1.98 x $10^{-3}$ (-1.46 x $10^{-3}$, 5.22 x $10^{-3}$) | **-1.66 x $10^{-3}$** (-2.55 x $10^{-3}$, -9.12 x $10^{-4}$) | **0.00** (0.00, 0.01) | **0.02** (0.01, 0.02) | **1.40 x $10^{-3}$** (6.73 x $10^{-4}$, 2.58 x $10^{-3}$) | **4.77 x $10^{-3}$** (1.95 x $10^{-3}$, 6.72 x $10^{-3}$) | **0.02** (0.00, 0.04) |
| **H4** | **-0.04** (-0.06, -0.03) | **4.03 x $10^{-3}$** (8.00 x $10^{-4}$, 6.92 x $10^{-3}$) | **-5.70 x $10^{-3}$** (-6.98 x $10^{-3}$, -4.60 x $10^{-3}$) | **0.01** (0.01, 0.02) | **0.02** (0.01, 0.02) | **1.52 x $10^{-3}$** (5.24 x $10^{-4}$, 2.72 x $10^{-3}$) | **8.84 x $10^{-3}$** (6.22 x $10^{-3}$, 1.10 x $10^{-2}$) | **0.03** (0.01, 0.05) |
| **I2** | 0.01 (-0.01, 0.02) | 2.04 x $10^{-3}$ (-9.91 x $10^{-4}$, 5.21 x $10^{-3}$) | **-5.14 x $10^{-3}$** (-6.12 x $10^{-3}$, -4.26 x $10^{-3}$) | **0.01** (0.01, 0.01) | **0.02** (0.01, 0.02) | -7.31 x $10^{-5}$ (-8.75 x $10^{-4}$, 4.70 x $10^{-4}$) | 2.67 x $10^{-3}$ (-2.77 x $10^{-4}$, 4.79 x $10^{-3}$) | **0.03** (0.01, 0.04) |
| **J2** | **0.05** (0.03, 0.07) | **4.04 x $10^{-3}$** (2.31 x $10^{-3}$, 5.60 x $10^{-3}$) | **-1.09 x $10^{-3}$** (-1.46 x $10^{-3}$, -7.66 x $10^{-4}$) | **0.01** (0.01, 0.01) | **0.01** (0.01, 0.01) | **6.73 x $10^{-4}$** (1.59 x $10^{-4}$, 1.43 x $10^{-3}$) | **1.06 x $10^{-2}$** (8.93 x $10^{-3}$, 1.18 x $10^{-2}$) | **0.03** (0.03, 0.04) |
| **K2** | **0.07** (0.05, 0.09) | **4.65 x $10^{-3}$** (3.41 x $10^{-3}$, 5.90 x $10^{-3}$) | **-1.48 x $10^{-3}$** (-1.92 x $10^{-3}$, -1.14 x $10^{-3}$) | **0.01** (0.01, 0.01) | **0.01** (0.00, 0.01) | 0.00 (-4.25 x $10^{-4}$, 1.85 x $10^{-4}$) | 1.27 x $10^{-3}$ (-6.72 x $10^{-6}$, 2.26 x $10^{-3}$) | **0.03** (0.02, 0.04) |

Table 10: Correlation coefficients and p-values between TSS and other variables at all stations in western and central LIS in surface and bottom waters. Only significant relationships are listed.

| Station | Depth | Correlation coefficient and significance (p-value) between TSS and listed variable |
|---|---|---|
| A4 | Surface | DIP (r = -0.24, p <0.001), DSi (r = -0.28, p <0.001), PC (r = 0.19, p = 0.01), PN (r = 0.18, p = 0;02), PP (r = 0.39, p <0.001), BioSi (r = 0.47, p <0.001), DINxs (r = 0.16, p = 0.04) |
| | Bottom | Chl a (r = 0.15, p = 0.05), TDP (r = -0.20, p < 0.001), NH4 (r = 0.15, p = 0.04), DIP (r = -0.15, p = 0.05), PC (r = 0.44, p < 0.001), PN (r = 0.37, p <0.001), PP (r = 0.58, p <0.001), BioSi (r = 0.63, p< 0.001), total N (r = 0.21, p <0.001), total Si (r = 0.41, p < 0.001), DINxs (r = 0.20, p < 0.001), |
| B3 | Surface | Chl a (r = 0.16, p = 0.03), DSi (p = 0.05, r = -0.14), PC (r =0.20, p < 0.001), PN(r =0.23, p < 0.001), PP(r =0.32, p < 0.001), BioSi (r =0.28, p < 0.001), DINxs (r = 0.18, p = 0.01) |
| | Bottom | PC (r =0.36, p<0.001), PN (r = 0.29, p<0.001), PP (r = 0.43, p<0.001), BioSi (r = 0.57, p<0.001), total N (r = 0.16, p = 0.03), total Si (r = 0.29, p <0.001), water density (r = 0.16, p = 0.03) |
| C2 | Surface | PP (r = 0.20, p<0.001), BioSi (r = 0.20, p <0.001) |
| | Bottom | Chl a (r = , p<0.001), PC (r = 0.57, p <0.001), PN (r = 0.49, p <0.001), PP (r = 0.49, p <0.001), BioSi (r = 0.67, p <0.001), total C (r = 0.18, p = 0.02), total N (r = 0.20, p <0.001), total Si (r = 0.49, p <0.001), total precipitation (r = 0.18, p = 0.02) |
| D3 | Surface | PC (r = 0.15, p = 0.05), PN (r = 0.19, p = 0.01), PP (r = 0.21, p < 0.001), BioSi (r = 0.18, p = 0.02) |
| | Bottom | PC (r = 0.15, p < 0.001), PN (r = 0.19, p < 0.001), PP (r = 0.21, p < 0.001), BioSi (r = 0.18, p < 0.001), total N (r = 0.15, p = 0.05), total Si (r = 0.24, p < 0.001) |
| E1 | Surface | Chl a (r = 0.23, p <0.001), PC (r = 0.24, p <0.001), PN (r = 0.27, p <0.001), PP (r = 0.23, p <0.001), BioSi (r = 18, p = 0.02), total N (r = 0.18, p = 0.02) |
| | Bottom | PC (r = 0.36, p < 0.001), PN (r = 0.26, p < 0.001), PP (r = 0.40, p < 0.001), BioSi (r = 0.42, p < 0.001), total N (r = 0.22, p < 0.001), total Si (r = 0.22, p < 0.001) |

## Appendix C

Table A1: ATP concentrations from the 9 field sampling dates during the summers of 2009 and 2010 at station A4. Empty cells indicate samples in which the measured ATP concentrations were less than the analytical blanks, and therefore no ATP could be measured.

| Date | Depth [m] | ATP, WW [ng $L^{-1}$] | ATP, <20-µm [ng $L^{-1}$] | ATP, <2/5-µm [ng $L^{-1}$] |
|---|---|---|---|---|
| 6/9/09 | 2.5 | 3633.3 | 2793.7 | 395.4 |
| | 8.0 | 958.9 | 687.3 | 396.7 |
| | 11.8 | 904.6 | 490.4 | 297.9 |
| | 16.5 | 674.5 | 386.0 | 259.3 |
| 6/23/09 | 3.0 | 3111.4 | 2168.3 | 569.5 |
| | 10.0 | 2671.6 | 2705.2 | 609.5 |
| | 15.0 | 1360.8 | 1081.9 | 685.3 |
| | 21.0 | | | |
| 7/14/09 | 1.5 | 3574.5 | 4020.3 | 605.6 |
| | 9.0 | 1375.9 | 840.2 | 575.9 |
| | 19.0 | 692.9 | 816.4 | 511.8 |
| 8/11/09 | 2.1 | 2759.3 | 640.7 | 343.8 |
| | 5.0 | 1038.3 | 855.2 | |
| | 10.1 | 223.2 | 135.2 | |
| | 22.2 | 105.4 | | |
| 8/28/09 | 2.0 | 317.1 | 311.2 | 193.6 |
| | 7.0 | 177.6 | 23.7 | 10.3 |
| | 12.0 | | 1.0 | |
| | 15.0 | | 2.7 | 43.1 |
| 9/15/09 | 1.9 | 1362.8 | | |
| | 4.9 | 1484.5 | 1281.0 | |
| | 18.4 | | | |
| 10/1/09 | 2.0 | | | |
| | 4.8 | | | |
| | 7.2 | | | |
| | 24.0 | | | |
| 8/16/10 | 2.0 | 52.9 | 43.2 | 36.1 |
| | 9.3 | 59.6 | 48.0 | |
| | 14.0 | 54.5 | 53.1 | 34.9 |
| | 19.1 | 90.3 | 42.3 | 30.8 |
| 9/10/10 | 2.0 | 8.1 | 13.1 | |
| | 13.0 | 33.6 | | 71.4 |
| | 17.8 | 42.5 | | 13.8 |
| | 17.1 | | | 9.4 |

Table A2: Chemoautotrophy rates (presented early) and Nitrapyrin-inhibited chemoautotrophy rates from the 9 field sampling dates during the summers of 2009 and 2010 at station A4. The Nitrapyrin-inhibited rates were not used in the analysis because these rates were frequently greater than those measured for total chemoautotrophy.

| Date | Depth [m] | Total DDA [µgC $L^{-1}$ $d^{-1}$] | Nitrapyrin-inhibited DDA [µgC $L^{-1}$ $d^{-1}$] |
|---|---|---|---|
| 6/9/09 | 2.5 | 0.0 | |
| | 8.0 | 0.0 | |
| | 11.8 | 0.0 | |
| | 16.5 | 0.0 | |
| 6/23/09 | 3.0 | 10.2 | 12.9 |
| | 10.0 | 21.9 | 19.2 |
| | 15.0 | 1.7 | 7.4 |
| | 21.0 | 2.2 | 702.6 |
| 7/14/09 | 1.5 | 35.1 | 34.5 |
| | 9.0 | 8.2 | 16.5 |
| | 19.0 | 229.1 | 15.1 |
| 8/11/09 | 2.1 | 199.7 | 398.5 |
| | 5.0 | 0.0 | 409.6 |
| | 10.1 | 0.0 | 23.9 |
| | 22.2 | 18.5 | 0.0 |
| 8/28/09 | 2.0 | 42.2 | 45.7 |
| | 7.0 | 69.9 | 58.9 |
| | 12.0 | 20.1 | 15.3 |
| | 15.0 | 16.4 | 11.0 |
| 9/15/09 | 1.9 | 7.1 | 6.4 |
| | 4.9 | 4.5 | 4.7 |
| | 18.4 | 7.5 | 9.4 |
| 10/1/09 | 2.0 | 1.1 | 0.7 |
| | 4.8 | 3.2 | 2.7 |
| | 7.2 | 0.7 | 0.5 |
| | 24.0 | 0.6 | 0.5 |
| 8/16/10 | 2.0 | 6.3 | 54.7 |
| | 9.3 | 4.5 | 22.9 |
| | 14.0 | 5.8 | 27.0 |
| | 19.1 | 6.1 | 31.5 |
| 9/10/10 | 2.0 | 5.2 | 10.1 |
| | 13.0 | 4.4 | 4.6 |
| | 17.8 | 2.6 | 3.1 |
| | 17.1 | 5.3 | 6.2 |